Measuring Compensatory Eye Movements to Assess Sensory and Learning Properties

Marcella Spoor

Measuring Compensatory Eye Movements to Assess Sensory and Learning Properties

Metingen van Compensatoire Oogbewegingen om Sensorische Eigenschappen en Leervermogen te Bepalen

Proefschrift

ter verkrijging van de graad van doctor

aan de Erasmus Universiteit Rotterdam

op gezag van de

rector magnificus

Prof.dr. R.C.M.E. Engels

en volgens besluit van het College voor Promoties.

De openbare verdediging zal plaatsvinden op

woensdag 22 januari 2020 om 11:30 uur

door

Marcella Spoor

geboren te Rotterdam

Erasmus University Rotterdam

Promotiecommissie

Promotor:	Prof.dr. M.A. Frens
Overige leden:	Prof.dr. J.G. Borst
	dr. A. Maassen van den Brink
	Prof.dr. E.H.M. Sterck
Copromotor:	dr. J.N. van der Geest

Table of Contents

Chapter 1 - General Introduction

This thesis deals with measuring compensatory eye movements to assess sensory and learning properties of humans and mice.

In this first chapter a brief introduction is presented of the visual system, discussing visual acuity and contrast sensitivity. This is followed by an introduction of the compensatory eye movement system that deals with stabilising the visual image on the retina. Finally, the research questions that are addressed in the experimental chapters will be presented.

The visual system

Visual perception is the ability to interpret information and surroundings from the effects of visible light reaching the eye. The resulting perception is also known as eyesight, sight, or vision. Light that enters the eye passes through the cornea, the lens, the vitreous and several layers of the retina and eventually stimulates light sensitive cells of the retina, called photoreceptors. Photoreceptors come in two main varieties: rods and cones. Rods are responsible for vision in conditions with reduced light, cones for colour vision and for perceiving fine detail. When light strikes these photoreceptors the energy of light is converted into a neuro electrical signal (photo transduction) that is relayed to the brain via the optic nerve. The brain processes the electrical signals into a visual percept of the environment.

Humans are predominantly visual animals. We use vision to evaluate our surroundings and guide our behaviour. Humans, by nature, are active during daytime (diurnal) and have eyes evolved for fine detailed daytime vision. Approximately 5% of the human photoreceptors are cones (Wikler & Rakic, 1990) and 99% of theses cones reside in the fovea, a specialized region that occupies approximately 1% of the retinal area (Perry & Cowey, 1985). The fovea is responsible for sharp vision in the centre of the line of sight, i.e. the direction of gaze. The fovea covers only a small portion of the entire visual field. To have a sharp image of an object in the periphery, humans can shift their gaze to align the object with the fovea using saccades and smooth pursuit eye movements. Humans actively explore their environment by using these gaze shifts that allow successive images to fall upon the fovea (Chapman & Corneil, 2008).

Mice, on the other hand, are not predominantly visual animals. Being ‘prey’ animals who are adapted to a nocturnal dim light niche, they rely primarily on olfaction, audition and the use of their whiskers for sensing their environment (Pinto & Enroth-Cugell, 2000). However, mice do have a visual system and the primary use of vision is likely to be the detection of potential predators, identifying escape routes and positional hazards. The mouse retina is specialized for vision under low

light (scotopic) conditions using the rod-type photoreceptors. The distribution of rods across the mouse retina is relatively uniform. The retina is similar to the peripheral retina of a human. Approximately 3% of mouse photoreceptors are cones, which are equally distributed across the retina. In contrast to humans, mice therefore do not have a fovea and they cannot see objects in great detail. In other words, mice have a low visual acuity. They can detect large objects at a distance or small objects at closer range, especially objects that are moving (Huberman & Niell, 2011).

Visual acuity

An important aspect of visual functioning in humans is related to visual acuity. Visual acuity refers to the details that an observer can detect. Visual acuity can be measured using an eye chart, such as the commonly used Snellen chart, developed in 1862 by the Dutch ophthalmologist Herman Snellen (Snellen, 1868). Here, the participant has to read increasingly smaller letters on a chart from a certain distance (usually 6 meters; Figure 1.1). A person with 6/6 is considered to have standard ("normal") vision (1.0 acuity) and can identify letters on a Snellen chart that subtend a visual angle of 5 minutes of arc. Other similar tests used to measure visual acuity are the E-chart or the Landolt C chart, in which subjects are asked to report the orientation of a capital E or C that become increasingly smaller, similar to the letters in the Snellen chart. Nowadays many opthalmologists use the LogMAR chart, which standardizes visual acuity testing between non-standard viewing distances and letter sizes. With all these acuity tests the highest resolution that someone can perceive is measured. An acuity test provides a reasonable measure for the quantity of vision and is a useful method to determine refractive errors of the eye (Ginsburg, 2003).

Figure 1.1. Snellen chart. When printed at the right size, and displayed at 6m (20ft), the visual acuity can be derived from the smallest set of letters that the participants can read.

However, visual acuity alone does not provide an accurate measure of the overall quality of visual function. While everyday objects have a wide range of sizes and contrasts, the acuity measures mentioned above only measure a small subset of what the visual system is able to perceive, namely objects with high spatial frequency at very high contrast (Ginsburg, 2003). Visual spatial processing is organized as a series of parallel, but independent, channels in the nervous system; each tuned to targets of a different size (Campbell, Cooper, Robson, & Sachs, 1969). As a result of this parallel organisation, visual acuity measurements do not adequately describe the spatial visual abilities. The

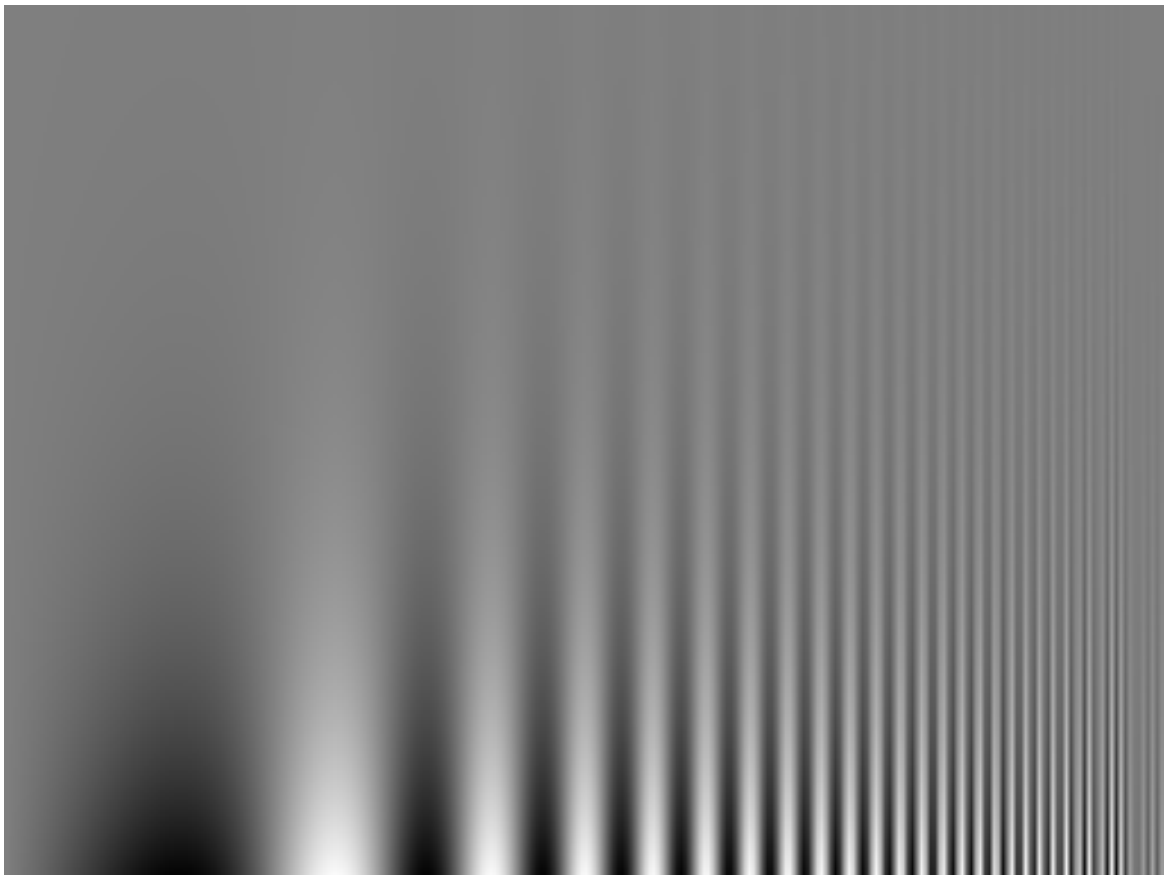

Figure 1.2. Spatial frequencies (horizontal) and contrast (vertical). Depending on the visual sensitivity of the readers, and their distance to the page, the threshold for detecting the image will vary with spatial frequency and has an optimum around the center of the image.

capacity to detect and identify spatial form varies widely as a function of size, contrast, and spatial orientation (Braddick, Campbell, & Atkinson, 1978; Olzak & Thomas, 1981).

Another limitation of acuity charts is that they measure visual acuity only in a very restricted contrast range. Contrast is defined as the amount of lightness and darkness an object has relative to its surroundings. Black letters on a white background (high contrast) are more readily perceived than dark grey letters on a light-grey background (low contrast). This means that the acuity tests

mentioned above are limited, in that they only measure the ability to see objects (or letters) of different sizes but only at very high contrast.

Contrast Sensitivity

A more thorough way to look at vision is by measuring the sensitivity of an observer for low contrast stimuli tested over a range of different sizes (spatial frequencies). This measure is known as Contrast Sensitivity and tests a broader spectrum of visual functioning, from high to low contrast and from low to high spatial frequency. Generally larger and smaller objects need more contrast to be seen (Figure 1.2).

Contrast Sensitivity is ideally tested by means of sine wave grating charts which have the same average luminance (i.e. brightness) but differ in the contrast between the light and dark bars and the spatial frequency (Figure 1.3). The spatial frequency is defined as the number of cycles (i.e. one dark and one light bar in the grid pattern) subtending one degree of visual angle. The lower the contrast that one is able to detect for any grating, the higher the contrast sensitivity. Approximately 60 cycles per degree (cpd) is the general upper limit of human vision.

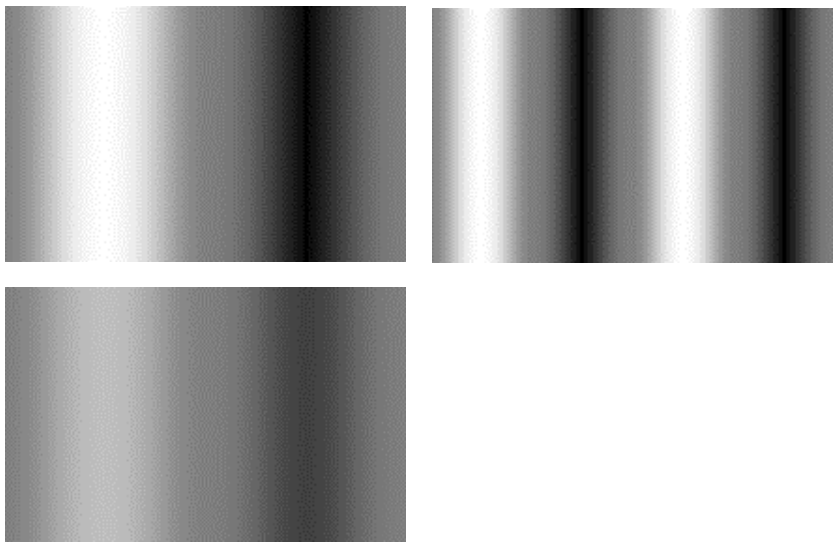

Figure 1.3. Sine gratings with different spatial frequencies. The upper left grating subtends one cycle within the image, the right grating subtends two cycles. Therefore, the spatial frequency of the latter is twice the spatial frequency of the left grating. The lower left grating has the same frequency, but lower contrast.

Thus, assessing the contrast sensitivity function in addition to foveal visual acuity might provide a better estimate of visual functioning. However, while we can ask human observers to trace the threshold in an image as presented in figure 1.2, this is not possible in mice. However, by measuring compensatory eye movements, we might be able to determine their visual thresholds for various contrasts and frequencies.

Compensatory eye movements

Stabilisation of the retinal image during image or self-motion is required for proper visual processing in both foveate and afoveate animals. Movement of the observer or the surroundings generates a slip of the image across the retina. This retinal slip will blur the perceived image of the outside world, reducing visual acuity (Collewijn, 1981). Image stabilisation is predominantly mediated by two types of oculomotor responses: the optokinetic reflex (OKR) that is driven by visual motion, and the vestibulo-ocular reflex (VOR) that responds to vestibular information due to head motion (Collewijn, 1981; Leigh & Zee, 2015). Both types of reflexes work in conjunction to enable stable retinal projections in everyday life.

The OKR is a visual reflex which stabilizes the retinal image by compensating for visual movement of the surroundings. The OKR is induced when the visual scene drifts across the retina (retinal slip). Retinal slip elicits eye movements in the same direction as the movement of the image and at a velocity that minimizes the motion of the image on the retina. The VOR is an analogous response to head movements which are detected by the vestibular system rather than from the retina (Frens & Donchin, 2009). The function of this reflex is to maintain a stable image on the retina during rapid head rotation. The VOR produces conjugate movements of the eyes in the direction opposite to head movement. The OKR and VOR work together to ensure image stabilisation on the retina. The OKR functions optimally for relatively slow image movements, whereas the VOR is optimally tuned for high frequency head movements.

Both the OKR and the VOR are largely controlled by subcortical circuits (Figure 1.4). Visual signals necessary for OKR are transmitted from the retina to the accessory optic system, via the vestibular nuclear complex, to the extra-ocular motor neurones which drive eye muscle activity (Leigh & Zee, 2015). This optomotor system is a closed loop that adjusts eye velocity according to a retinal slip signal. At the beginning of this loop are motion sensors. These motion sensors do not code for pure velocity but depend on textural properties such as the temporal (cycles per second) and spatial frequency (cycles per visual degree) contrast of the image.

The VOR is a compensatory ocular movement in response to stimulation of the vestibular organ. The vestibular organ contains specialized areas with receptor cells that translate head movement into neural signals. Head acceleration is mechanically integrated to a velocity signal. The connection between the vestibular organ and the extra ocular muscles of the eye ball is a three neurone reflex arc that functions as an open loop, in which signals are translated from the vestibular organ to the vestibular nucleus, and from there to the same oculomotor nuclei as the OKR pathway (Leigh & Zee,

2015). Attached to the three-neurone VOR arc is an inhibitory side loop that involves the cerebellum (Voogd & Barmack, 2006).

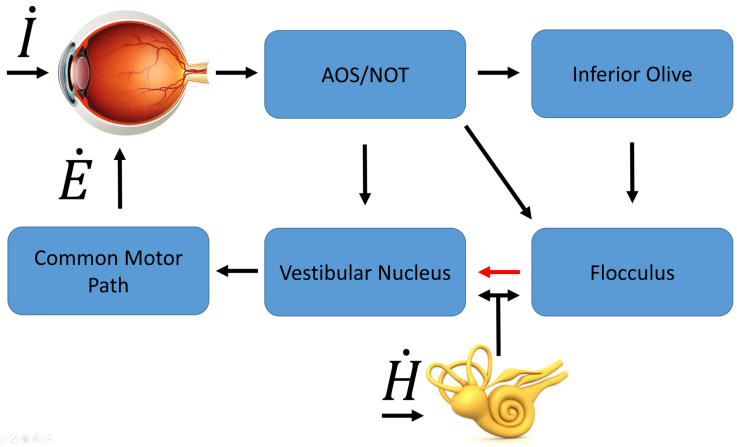

Figure 1.4. Compensatory eye movement pathways. Image motion ($\dot{I}$) and head motion ($\dot{H}$) are sensed by the retina and the semicircular canals respectively. Ideally the reflexes lead to an eye movement ($\dot{E}$) that opposes the image motion in amplitude and direction. See text for details.

The cerebellum or little brain plays a role in the fine tuning of movement. The part of the cerebellum involved in coordinating eye movements is the vestibulo-cerebellum. Visual and vestibular information related to the visual and vestibular information is relayed to the layered cortex of this part of the cerebellum, the flocculus, where the information is processed. Subsequently the output relayed by the cerebellar Purkinje cells is directed to the vestibular nuclei. The input comes from two different sources. Mossy fibres convey vestibular and visual information to the granule cell layer (input) that excites the Purkinje cells via parallel fibres. The second input, an error signal, i.e., the retinal slip, together with eye motor and vestibular information from the inferior olive, is conveyed via the climbing fibre directly to the Purkinje cells (Shin, Zhao, & Raymond, 2014a; Winkelman & Frens, 2006). When the information is processed and integrated in the Purkinje cells it leaves the cortex and inhibits the vestibular neurones which are part of the three neurone-arc to control motor output.

Compensatory ocular response as a tool to measure both visual and vestibular functioning as well as motor learning.

Stable images on the retina are maintained under various movement conditions by using both reflexes: OKR and VOR. The reflex systems can be easily and accurately investigated by measuring the eye movements. These reflexes are particular appropriate for examining motor behaviour because these reflexes are easy to elicit in a controlled manner. Moreover, they can also be manipulated simply by changing the input. Another advantage of the use of OKR and VOR is that these behaviours do not need training. Therefore, OKR and VOR measurements are frequently used

to examine the effects of mutations in mice, human brain lesions and other situations that disrupt processes in the brain.

In addition, another advantage of the use of gaze stabilisation reflexes to infer sensory and learning functionality, is that humans as well as mice both show robust gaze stabilisation eye movements.

By measuring the OKR in response to specific visual information, we can test visual functioning and, for instance, explore the contrast sensitivity function in both humans and mice. Similarly, recording the VOR allows for testing vestibular functioning. Combining visual and vestibular stimulation allows for studying oculomotor learning. Also, by means of compensatory eye movements we can measure the behavioural effects of cerebellar stimulation.

Scope of this thesis

The central theme of this thesis is the assessment of sensory functioning and learning in both mice and humans by measuring compensatory eye movement behaviour.

Assessing compensatory eye movements is a useful model to evaluate visual function. This is the topic of the first three experimental chapters. In chapter 2 we investigated how gaze following eye movements in humans are affected by stimulus contrast and spatial frequency. Moreover, we assess the effect of aberrations in central visual acuity due to refractive errors on these eye movements in humans. In chapter 3 eye movements are recorded in mice to assess whether DNA damage can cause age-related vision loss. We test vision in Ercc1δ/– mutant mice, which are deficient in DNA repair of distorting DNA lesions and interstrand DNA crosslinks. Eye movement behaviour of wild-type mice with varying pigmentation is presented in chapter 4. Here, mice are screened for oculomotor abnormalities in order to identify a possible mouse model for infantile nystagmus syndrome.

The next two chapters deal with learning new motor behaviour in which the cerebellum plays an important role. In chapter 5 we explore the effect of direct current stimulation (DCS) on the adaptation of the VOR system. DCS is a non-invasive brain stimulation technique, which showed to have a modulatory role in other cerebellar dependent motor learning tasks. In chapter 6 we explore the question to what extent the housing conditions of wildtype mice affect their capacities in terms of behaviour and learning. We compare mice kept in standard conventional housing and mice kept in an enriched environment, using various widely used paradigms in neuroscientific laboratory animal research, including oculomotor testing.

Finally, a general discussion of our findings, and recommendations for future studies, are presented in chapter 7. I hope you will have an enjoyable time reading my thesis.

Chapter 2 - Human Gaze Following Response Is Affected by Visual Acuity [1]

Marcella Spoor, Behdokht Hosseini, Bart van Alphen, Maarten A. Frens, and Jos N. van der Geest

Abstract

The present study investigated how gaze following eye movements are affected by stimulus contrast and spatial frequency and by aberrations in central visual acuity due to refractive errors. We measured 30 healthy subjects with a range of visual acuities but without any refractive correction. Visual acuity was tested using a Landolt-C chart. Subjects were divided into three groups with low, intermediate, or good visual acuity. Gaze following responses (GFR) to moving Gabor patches were recorded by video-oculography. In each trial, the subjects were presented with a single Gabor patch with a specific spatial frequency and luminance contrast that moved sinusoidally in the horizontal plane.

Introduction

Vision is the ability to observe the world by interpreting light that is reflected from the surroundings and reaches the retina. Loss of visual function can severely affect daily human activities and may effectively decrease the quality of life (Armbrecht, Aspinall, & Dhillon, 2004; Warrian, Altangerel, & Spaeth, 2010). Loss of vision can be caused by various ocular diseases, such as retinitis pigmentosa, macular degeneration (de Jong, 2006), or glaucoma. Loss of vision can also occur as a symptom of other disorders like multiple sclerosis (Compston & Coles, 2008) or diabetic retinopathy.

Visual acuity is one of the important aspects of visual function. Currently, visual acuity is mainly assessed by measuring central visual acuity using, for instance, a letter chart on which a subject has to read increasingly smaller letters while standing at a particular distance (Snellen acuity). Other acuity measures use the E-chart or the Landolt-C chart, in which subjects are asked to report the orientation of a capital E or C, respectively. A person with normal acuity (20/20 vision) can identify the standardized symbols on the chart at a distance of about 6 meters (20 feet). A person with 20/30 vision can identify symbols on the chart from 20 feet that a person with normal acuity could see from 30 feet. This method to assess acuity measures the highest resolution that the visual system can perceive and is useful to determine refractive errors of the eye.

However, several issues arise using such a measure. For instance, these acuity tests often yield highly variable results between examinations due to, for instance, observer based (i. e. , by clinicians

[1]Journal of Ophthalmology; Volume 2014; Article ID 543478; http://dx.doi.org/10.1155/2014/543478

or experimenters) variability (Gibson & Sanderson, 1980) and differences in recording settings, such as distances from chart and light conditions (Pandit, 1994). In addition, active cooperation of the observer is required: the observer has to actively report, for instance, the orientation of a C. This not only requires compliance of the observer, but also means that it is a subjective measure of visual function, in the sense that no strong conclusions can be drawn from an inability to read out the next line. Finally, with this type of acuity tests only a small subset of the sensitivity of the visual system is probed: objects with high spatial frequencies at very high contrast (Ginsburg, 2003).

Several studies related visual acuity to optokinetic eye movements (Wester, Rizzo, Balkwill, & Wall, 2007), or smooth pursuit eye movements (Schor & Levi, 1980), and did so by varying the spatial frequency of the stimulus. Optokinetic eye movements refer to the following of a moving pattern of dots or stripes in the full visual field. These studies used gaze and ocular following responses as a tool to assess visual function in visually impaired participants and reported that reduced visual acuities decreased the amplitude of the following response. However, these studies did not vary the contrast of the stimulus and, hence, did not determine the interaction between visual acuity and contrast sensitivity in more detail.

Contrast sensitivity is the ability to detect differences in contrast between shades of grey in a visual stimulus. This sensitivity varies with spatial frequency, that is, the level of visual detail of the stimulus. A contrast sensitivity test measures the smallest amount of contrast needed to detect a visual stimulus and provides a more complete quantification of a person's visual capabilities by taking two variables into account, spatial detail and contrast. Contrast sensitivity is measured by asking an observer to detect or discriminate gratings as targets instead of (Arundale, 1978; Kara-Junior et al., 2011). Sine-wave gratings possess useful mathematical properties and early stages of visual processing are optimally "tuned" to such targets (Maffei & Fiorentini, 1973; Watson & Robson, 1981). Each sine-wave grating consists of a given spatial frequency which is specified in terms of the size of the grating at the back of the eye considering the number of sinusoidal luminance cycles per degree (cpd) of visual angle. The contrast of the target grating at a specific spatial frequency is then varied while the observer's contrast detection threshold is determined.

The contrast sensitivity function has become a well-established tool to probe the functional integrity of the visual system (Leguire et al., 1991). Over the last decades many techniques, including psychophysics (Drover, Wyatt, Stager, & Birch, 2009) and the recording of optokinetic nystagmus (Schor & Levi, 1980; Wester et al., 2007), have been described to measure the contrast sensitivity function. Leguire et al. (1991) compared the contrast sensitivity function based on psychophysics with optokinetic measurements in a small group of healthy subjects and found a good association

between the two measures. Here we aim to determine the contrast sensitivity function in humans by measuring the gaze following response (GFR) in reaction to moving stimuli of varying contrasts and spatial frequencies. The GFR is an eye movement that drives the eye to follow stimuli in the visual field and may contain both voluntary and involuntary components. This technique was originally developed to determine contrast sensitivity in mice (van Alphen, Winkelman, & Frens, 2009a). The present study is for proof of principle only and shows how foveally induced gaze following responses to moving Gabor patches are affected by contrast and spatial frequency of the stimulus. In addition, we studied how these eye movement responses are affected by aberrations in central visual acuity due to uncorrected refractive errors.

Materials and Methods

Subjects.

We measured 30 healthy subjects (13 females) between 22 and 57 years of age (median of 27 years). One eye was measured per subject without any refractive correction, while the other eye was patched. The study followed the tenets of the Declaration of Helsinki and informed consent was obtained from all subjects before the experiment.

Visual Acuity.

Central visual acuity was assessed using a Landolt-C chart, which requires an observer to report the orientation of a gap in a ring. The size of the ring and gap is reduced every three rings. The visual acuity score of the observer was defined by the smallest visual angle of the ring for which the observer reported the orientation correctly at least two times. Variability was limited by using a fixed viewing distance of 6 meters (~20 feet) and by having one experimenter testing all subjects under identical light conditions. Subjects were divided into three groups based on these visual acuity scores: low (score of 20/200 and below), intermediate (scores between 20/200 and 20/20), and high (score of 20/20 and above) visual acuity.

Contrast Sensitivity Measurements

All experiments were performed in a darkened room. The gaze following response (GFR) was evoked by moving a visual stimulus horizontally. The stimulus was back-projected via computer-controlled movable mirrors (Laser2000, The Netherlands) on a transparent screen (135 by 99 cm) using a digital projector (Sanyo PLV-Z2) with a resolution of 1024 by 768 pixels (see Figure 2.1a). Viewing distance was 305 cm.

Each stimulus showed a circular Gabor patch with a standard deviation of 5 degrees of visual angle in diameter, thus covering the fovea and a substantial part of the parafoveal area when looked at. The

Gabor patches were generated in Matlab (The Mathworks, Natick, MA, USA). A Gabor patch consisted of vertically oriented lines with a particular luminance that was determined by a sinusoid having a specific frequency (0. 48, 0. 96, 1. 93, 3. 87, or 7. 74 cycles per degree) and a specific black and white contrast (1, 2, 4, 8, 16, 32, 48, 64, or 100%). Luminance of the bright (L_{max}) and dark stripes (L_{min}) in the centre of the patch was measured with a luminance meter (LS-100; Minolta Camera, Osaka, Japan), after which contrasts were calculated according to the Michelson formula:

$$Contrast = \frac{L_{max} - L_{min}}{L_{max} + L_{min}}$$

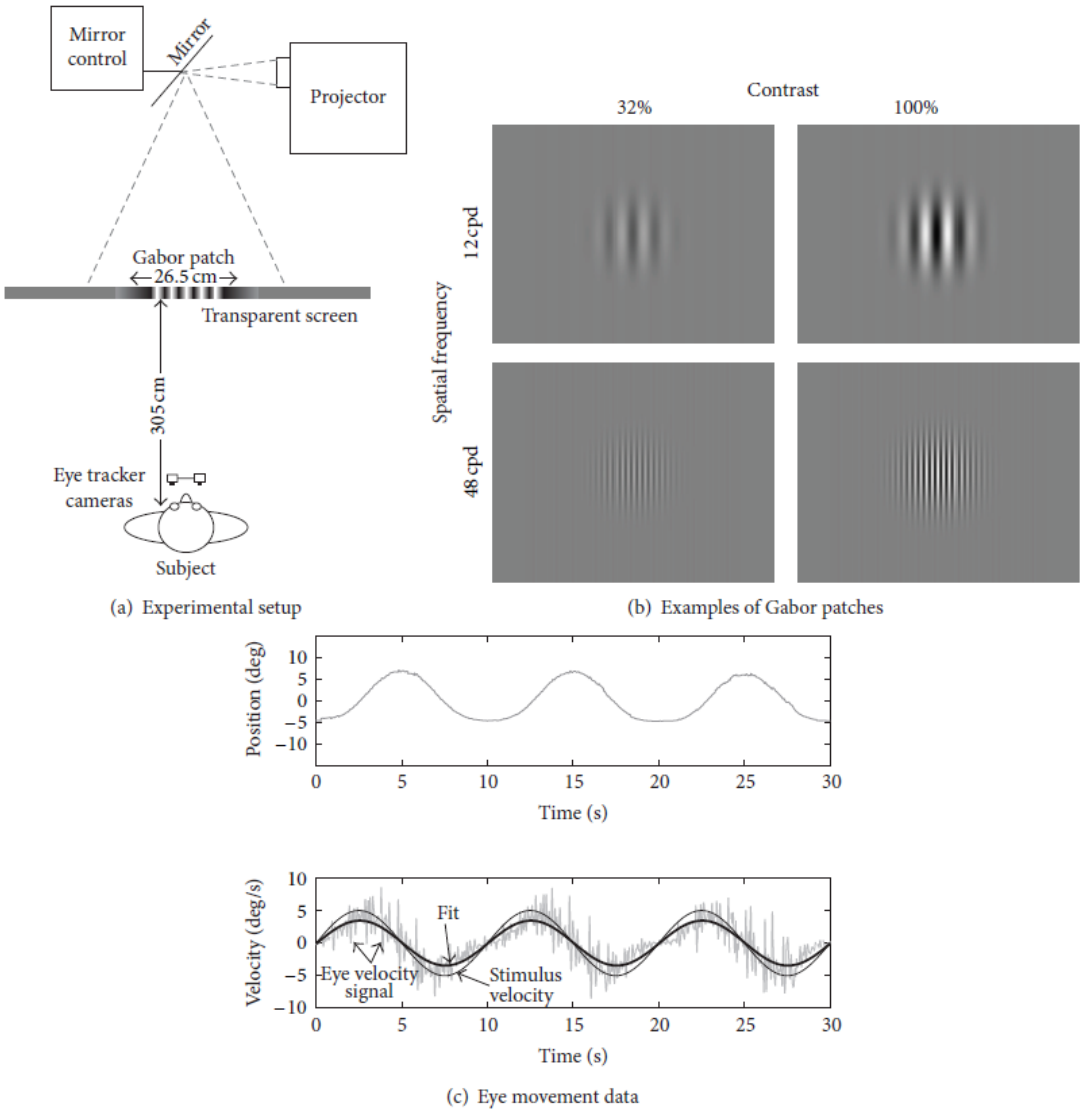

Figure 2.1: (a) shows a schematic drawing of the experimental setup. The stimulus, a Gabor patch, was back-projected via mirrors on a transparent screen. Movement of the mirrors induced a horizontal movement on the screen. (b) shows four examples of Gabor patches. Each stimulus contained a Gabor patch with a unique combination of spatial frequency and black-white contrast. (c) shows an example of the eye movements of an observer who explicitly followed the movement of the Gabor patch. This observer was not included in this experiment. The Gabor patch moved sinusoidally from left to right in the horizontal plane. The top plot of (c) shows the raw eye position trace. The bottom plot of (c) shows the corresponding eye velocity trace (grey line), the stimulus velocity trace (thin black line), and the fitted sinusoid through the eye velocity signal (thick black line).

Average luminance was 16 cd/m^2 in all stimulus conditions. For the stimuli with 100% contrast, the luminance of the dark stripes was 0. 15 cd/m^2 and the luminance of the white stripes was 32 cd/m^2.

Combining these two variables yielded 45 unique Gabor patches and each was presented once in a random order (see Figure 2.1b for stimulus examples).

The movements of the mirrors were controlled by a computer running Spike-2 (version 4. 20, Cambridge Electronic Design) in such a way that the stimulus moved sinusoidally in the horizontal plane (frequency of 0. 1Hz, peak velocity of 5 degrees per second, and peak to peak amplitude of 15. 9 degrees) for three full cycles. Hence, each stimulus presentation lasted for 30 seconds. Between stimulus presentations there was a random blank interval of 5–15 seconds. The experimenter told the subject when the next stimulus was about to be presented. Subjects were instructed to keep their eyes open and look at the stimulus, without specific instructions. The whole experiment lasted for about 40 minutes. Head movements were restrained using a bite board. Monocular eye movements were recorded using an EyeLink infrared camera system (EyeLink 1 Desktop, SensoMotoric Instruments GmbH, Teltow, Germany) at a 250Hz sampling rate (van der Geest & Frens, 2002a). Calibration and calibration-accuracy validation were performed prior to each experiment using the standard EyeLink routine.

Analysis

Eye movement recordings were analysed offline using custom-written software in Matlab. The first 3 seconds of data was discarded. Instantaneous eye velocity was calculated by taking the first derivative of horizontal eye position over time. Fast phases (saccades) were removed using a velocity threshold of 10 degrees per second (i. e. , twice the stimulus velocity). A sine-wave was fitted to the remaining velocity signal, yielding a fitted peak eye velocity (see Figure 2.1c for an example).

The eye velocity gain was calculated for each subject, contrast, and spatial frequency by dividing the fitted peak eye 4 Journal of Ophthalmology velocity by the peak stimulus velocity (fixed at 5 deg/s). Per subject, all gains were then normalized by setting the gain obtained in the highest contrast (100%) and lowest spatial frequency (0. 48 cpd) to 1. A multivariate repeated measures analysis (ANOVA) was carried out for the eye movement gains with three factors: “Group” (3 levels: low, intermediate, and high visual acuity), “Contrast” (9 levels), and “Spatial Frequency” (5 levels). Differences between groups were evaluated by subsequent planned comparisons (uncorrected). All statistical analyses were done in SPSS 20.

Results

In two subjects, not all responses could be reliably measured due to eye tracking failure; their data was discarded. Based on their visual score in the visual acuity test, the remaining 28 subjects were classified as having low (score of 20/200 and below, N = 11), intermediate (scores between 20/200 and 20/20, N = 10), or high (score of 20/20 and above, N = 7) visual acuity. Ages did not differ between the three groups (median test, p = 0. 75).

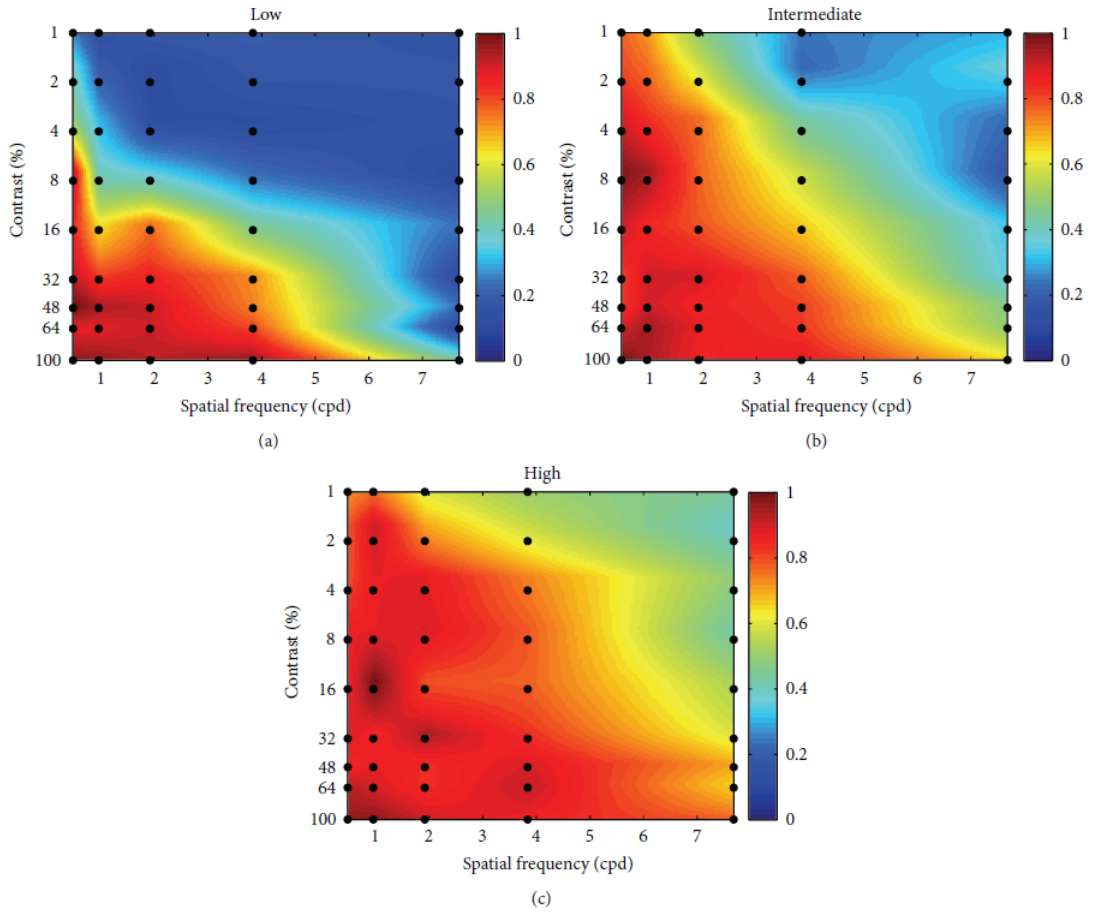

Figure 2.2: For each of the three groups (low, intermediate, or high visual acuity), the color reflects the averaged normalized GFR gains at 45 combinations of contrast and spatial frequency (indicated by black dots). The space between the measured points is linearly interpolated.

Before normalisation (see Methods), the gains across all 45 Gabor presentations and all 28 subjects ranged from 0. 0 to 0. 53 with a grand overall median of 0. 25. After normalisation, the GFR gains (averaged over the 45 Gabor presentations) ranged from 0. 40 to 0. 95 across subjects (median of 0. 65). There was a positive correlation between acuity scores and the average normalized GFR gains (Spearman correlation of 0. 78, $p < 0.001$).

Figure 2.2 shows the normalized GFR gain as a function of spatial frequency and contrast of the stimulus for the 3 groups separately. Differences can clearly be observed, most prominently at high spatial frequencies and low contrast.

In order to quantify these differences, the average normalized gains obtained for each contrast and each spatial frequency from each group are plotted in Figure 2.3A and B, respectively.

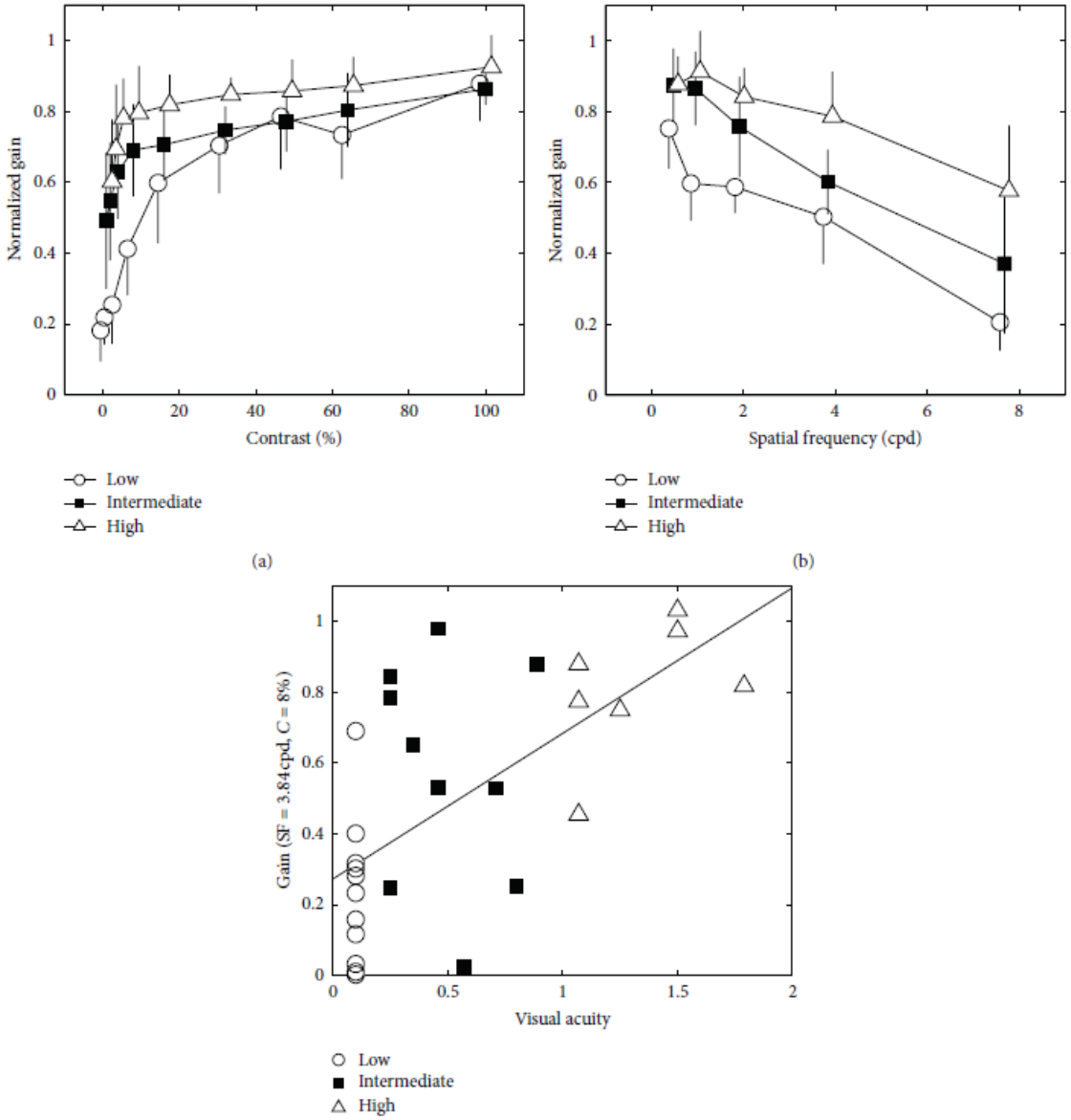

Figure 2.3: For each of the three groups (low, intermediate, or high visual acuity), the averaged normalized GFR gains are pooled over the 5 levels of spatial frequency and plotted against contrast in (a) and pooled over the 9 levels of contrast and plotted against spatial frequency in (b). The error bars represent standard error of the mean. The normalized GFR gain in response to a moving Gabor patch with a spatial frequency of 3. 84 cpd and a contrast of 8% is plotted against the visual acuity score in (c); each symbol represents a single subject.

Statistical analysis showed a significant main effect of "Group" ($F(2) = 21.4$, $p < 0.001$): high acuity subjects had on average higher GFR gains (0. 80 ± 0. 03 [Standard Error]) than the intermediate (0. 69 ± 0. 03, $p < 0.001$) and low acuity subjects (0. 53 ± 0. 03, $p < 0.001$). The difference in average gain between the low and intermediate acuity groups was also significant ($p = 0.024$).

The significant main effects of "Contrast" ($F(8) = 29.5$, $p < 0.001$) and "Spatial Frequency" ($F(4) = 48.4$, $p < 0.001$) showed that decreasing the contrast or increasing the spatial frequency of the visual stimulus reduced the GFR gain.

The interactions between "Group" and "Contrast" ($F(2, 8) = 3.62$, $p < 0.001$) and between "Group" and "Spatial Frequency" ($F(2, 4) = 3.79$, $p = 0.013$) were significant. Post hoc analyses showed that especially for lower contrasts (1%–8%) the low acuity group had significantly lower GFR gains than both the intermediate and high acuity groups (all $p < 0.01$; see Figure 2.3a). The average GFR gain was lowest in the low acuity group for all spatial frequencies. Furthermore, for low spatial frequencies (0.48 to 1.92 cpd) the intermediate acuity group differed from the low acuity group, whereas for higher frequencies (3.84 and 7.68 cpd) the intermediate group differed from the high acuity group (see Figure 2.3b).

From these analyses, we observed that our groups were best separated using a moving Gabor patch with a spatial frequency of about 4 cpd and a contrast of about 8%. We found a positive correlation between visual acuity scores and the normalized GFR gains for this particular Gabor patch (Spearman correlation of 0.64, $p = 0.002$, Figure 2.3c). We did not compute the correlations for the other 44 stimuli.

Discussion

We observed that the gaze following response (GFR) is influenced by both the spatial frequency and the contrast of a sinusoidally moving sine grating. In addition, this eye movement response was affected by central visual acuity, as it varied between three groups of subjects with varying visual acuity scores. Reduced central visual acuity related to uncorrected refractive errors induced lower GFR gains. This suggests that the GFR response can be used to estimate human contrast-sensitivity function and to determine how well a stimulus is seen.

The method of measuring the GFR has several advantages over a central visual acuity test using, for instance, a letter chart or a Landolt-C chart. For instance, the latter does not cover the whole visual spectrum but only the high spatial frequency and very high contrast ranges (Ginsburg, 2003), and, therefore, a 20/20 result in visual acuity will not always uncover loss of vision for other contrasts and spatial frequencies. Hence, tests in low vision patients (patients with impaired eye sight that cannot be corrected by conventional means) often depend on self-reported changes in visual function and acuity, which can be highly inaccurate (Skeel, Nagra, VanVoorst, & Olson, 2003; Warrian et al., 2010). The eye movement response can provide useful additional information, for instance, an extra dimension of data: that of response magnitude. The gaze following responses measured with the contrast sensitivity test are not bimodal ("I can see it" or "I cannot see it," as in the common acuity

test) but graded; the gain of the GFR decreases as stimuli become harder to see (Cahill & Nathans, 2008; van Alphen et al., 2009a). This response sensitivity makes the GFR method suitable to use when screening for small changes in contrast sensitivity, which can be caused by degenerative diseases or by treatment methods that aim to improve visual function in low vision patients. With stimuli covering the whole range of human vision, small changes in contrast sensitivity could be detected using this approach. In addition, using the GFR reflex to test contrast sensitivity provides us with an objective test and without user bias, which often occurs in perception tasks when the stimulus is close to the perceptual threshold.

We tested a small range of spatial frequencies, because there are some technical challenges to measure all the way up to the maximum visible spatial frequency [about 60cpd (Williams, 1985)] using a standard computer display. For instance, a 24- inch widescreen monitor is approximately 48 cm wide and has a horizontal resolution of 1920 pixels. This means that at most 20 black lines and 20 white lines, each being only 1 pixel wide, can be drawn per cm, resulting in a square wave grating of 20 cycles per cm. At a viewing distance of about 170 cm, this would yield a spatial frequency of 60 cpd. For sine gratings, requiring 4 (or even more) visible lines with different contrasts, the viewing distance has to be doubled (at least) to accommodate the entire stimulus. In our setup, the maximum spatial frequency of projected sine-wave grating was limited by viewing distance (305 cm), screen width (135 cm), and projector resolution (1204 pixels), resulting in a projection of about 41 pixels per degree, that is, a maximum spatial frequency of 10 degrees. However, we already observed a decrease in GFR gain for moderate spatial frequencies up to 10 degrees; higher frequencies would have most likely led to negligible eye movement responses. This observation can be exploited in future studies by modifying the experiment into an adaptive procedure which allegedly restricts the number of required trials, thereby reducing the total time of the test substantially. At present, measuring the GFR at all possible combinations of spatial frequencies and contrasts took about 40 minutes, whereas a regular visual acuity test takes only a few minutes to complete.

In the present study, the non-normalized GFR gains were rather low. This was probably related to the instruction given to the subject. We told them to look at the stimulus, without explicitly instructing them to fixate at the centre of the moving Gabor patch.

Our study suggests that measuring the GFR provides insight into the sensitivity of spatial frequency and contrast in healthy adult subjects. In addition to measuring central visual acuity (preferably by means of a logMAR chart) it may have several clinical applications. For instance, it is known that contrast sensitivity decreases with age (Greene & Madden, 1987; Sekuler, Hutman, & Owsley, 1980),

which is, however, generally not picked up with an acuity test. In elderly persons, decreased contrast sensitivity contributes to a poor postural stability which leads to a doubling of the already increased likelihood of falling (Turano, Rubin, Herdman, Chee, & Fried, 1994). As a note, the Landolt-C chart measures central visual acuity and we did not assess peripheral visual function. There are many complex ocular conditions; some conditions affect central visual function, like macular degeneration, whereas others result in macular sparing and induce tunnel vision. Moreover, there is a difference between peripheral and central contrast sensitivity. Future studies using the GFR as a measure for contrast sensitivity might use stimuli that target the peripheral retina in particular.

We conclude that measuring the gaze following response (GFR) for a wide range of stimulus contrasts and spatial frequencies is useful for observing changes in contrast sensitivity. We observed that worse central visual acuity affects this eye movement response. Measuring the GFR may contribute to a better estimate of changes in visual function as a result of ageing, disease, or treatments meant to improve visual function.

Acknowledgments

The authors would like to thank Junior Med School students Saskia van Grondelle and Simone Dijkland for their assistance in data collection. The authors would also like to thank the reviewers for providing valuable feedback on their work. This study was supported by HFSP (Marcella Spoor), NWO 813. 07. 002 (Bart van Alphen), the Prinses Beatrix Fund (Jos N. van der Geest),Marie Curie ITN Programme C7 (Maarten A. Frens) and the EUR Interreg Initiative TC2N (Maarten A. Frens and Jos N. van der Geest).

Chapter 3 - Accelerated Loss of Hearing and Vision in the DNA-repair deficient Ercc1δ/− Mouse [2]

Marcella Spoor, Paul Nagtegaal, Yanto Ridwan, Nils Z. Borgesius, Bart van Alphen, Ingrid van der Pluijm, Jan H.J. Hoeijmakers, Maarten A. Frens, J. Gerard G. Borst

Abstract

Age-related loss of hearing and vision are two very common disabling conditions, but the underlying mechanisms are still poorly understood. Damage by reactive oxygen species and other reactive cellular metabolites, which in turn may damage macromolecules such as DNA, has been implicated in both processes. To investigate whether DNA damage can contribute to age-related hearing and vision loss, we investigated hearing and vision in Ercc1δ/− mutant mice, which are deficient in DNA repair of helix-distorting DNA lesions and interstrand DNA crosslinks. Ercc1δ/− mice showed a progressive, accelerated increase of hearing level thresholds over time, most likely arising from deteriorating cochlear function. Ercc1δ/− mutants also displayed a progressive decrease in contrast sensitivity followed by thinning of the outer nuclear layer of the eyeball. The strong parallels with normal ageing suggest that unrepaired DNA damage can induce age-related decline of the auditory and visual system.

Introduction

Among the most common impairments associated with ageing are age-related loss of hearing (presbycusis) and vision. Presbycusis is characterized by increased hearing thresholds, especially at higher frequencies, accompanied by a progressive reduction of distortion product otoacoustic emissions (DPOAEs; Dorn, Piskorski, Keefe, Neely, & Gorga, 1998; Jens Oeken, Andreas Lenk, Friedrich, 2000; Uchida et al., 2008). This process results from a lifetime of insults to the auditory system to which the cochlear outer hair cells are probably most sensitive (Gates & Mills, 2005; Ohlemiller, 2006).

Senescent changes in visual performance include declines in visual acuity (the smallest detail that can be resolved at high contrast levels) and spatial contrast sensitivity (the ability to detect small increments in shades of grey on a uniform background;(Spear, 1993)). Studies on the effect of age on the spatial contrast sensitivity curve in humans have shown a fall in high frequency sensitivity at middle age (Arundale, 1978; Derefeldt, Lennerstrandt, & Lundh, 2009; Owsley, Sekuler, & Siemsen, 1983; Spear, 1993; Wright & Drasdo, 1985), leading to intermediate and high spatial frequency

[2] Mech Ageing Dev. 2012 Feb-Mar;133(2-3):59-67; https://doi.org/10.1016/j.mad.2011.12.003

attenuation above 60 years of age (Derefeldt et al., 2009; Owsley et al., 1983). Moreover, an age-related decline in contrast sensitivity was found across all spatial frequencies when measured under scotopic conditions (Schefrin, Tregear, Harvey, & Werner, 1999). Recently, an age-related decline in contrast sensitivity was also revealed in mice (van Alphen et al., 2009a). The major optic changes during ageing are insufficient accommodation ability due to hardening of the lens, decrease in pupil size and increase in density and yellowing of the lens. Within the retina, a loss of photoreceptors, bipolar cells, ganglion cells, or changes in their connections can contribute to impaired vision (Spear, 1993).

Natural compounds such as cyclopurines produced by free reactive oxygen species (ROS; Brooks, 2008), malondialdehyde (Niedernhofer et al., 2006; Weeda et al., 1997) or acetaldehyde (Abraham, Balbo, Crabb, & Brooks, 2011; Langevin, Crossan, Rosado, Arends, & Patel, 2011) can cause DNA damage. Indeed, damage caused by ROS has been suggested to be one of the driving mechanisms for age-related hearing and vision loss (Fletcher, 2010; Willott, Hnath Chisolm, & Lister, 2001). Even though it is not easy to establish a causal relationship, ROS-induced DNA damage has been suggested to be implicated in presbycusis in several studies (Darrat, Ahmad, Seidman, & Seidman, 2007; Jiang, Talaska, Schacht, & Sha, 2007; Pickles, 2004; Seidman, Khan, Tang, & Quirk, 2002). Indeed, mice lacking the Cu/Zn superoxide dismutase (SOD), a major radical scavenger, exhibit accelerated age-related hearing loss and cochlear hair cell loss (McFadden, Ding, Burkard, et al., 1999; McFadden, Ding, Reaume, Flood, & Salvi, 1999).

Further support for the idea that accumulating DNA damage contributes to presbycusis and age-related vision loss comes from patients suffering from the rare inherited DNA repair disorders xeroderma pigmentosum (XP) or Cockayne syndrome (CS). Already at an early age they can show signs of presbycusis, vision loss and degeneration of the retina (Iwasaki & Kaga, 1994; Kenyon, Booth, Prasher, & Rudge, 1985; Mimaki et al., 1986; Rapin et al., 2006; Robbins et al., 1991; Scaioli, D'Arrigo, & Pantaleoni, 2004). However, patients carrying these DNA repair deficiencies are genetically and phenotypically very heterogeneous, complicating deduction of cause–consequence relationships. A genetically more defined mouse model of Cockayne syndrome, which displays several features of the human syndrome, albeit in a relatively mild form (van der Horst et al., 1997), exhibits an age-dependent thinning of the outer nuclear layer (ONL) of the retina due to spontaneous loss of photoreceptors (Gorgels et al., 2007); loss of photoreceptors is also commonly observed in ageing humans (Aggarwal, Nag, & Wadhwa, 2007; Curcio, Millican, Allen KA, & Kalina, 1993; H. Gao & Hollyfield, 1992; Panda-Jonas, Jonas, & Jakobczyk-Zmija, 1995) and mice (Bravo-Nuevo, Walsh, & Stone, 2004; Sanyal & Hawkins, 1986). Mice with a deletion of the Ercc1 gene have a progressive neurological phenotype. Already at a young age, they display among others a reduced

optokinetic response (OKR), suggesting that vision is reduced (Lawrence, Sacco, Brownstein, Gillingwater, & Melton, 2008). The lifespan of this mouse is 2–3 months (Selfridge, 2001), and the main cause for the neurological phenotype, including the decreased OKR, is proposed to be a consequence of the prominent, progressive kidney failure (Lawrence et al., 2008).

Here, we investigate in detail the role of unrepaired DNA damage on the onset and progression of presbycusis and age-related vision loss in Ercc1δ/− mice of different ages. The Ercc1δ/− mouse mutant lacks one allele of the excision repair cross-complementing group 1 (Ercc1; ERCC1 in humans) gene. The protein derived from the other allele shows reduced activity owing to a seven amino-acid carboxy-terminal truncation (Weeda et al., 1997). This hypomorph mutation results in severely impaired nucleotide excision repair, interstrand cross-link repair (Weeda et al., 1997) and double-strand break repair (Seidman, Khan, et al., 2002). Consequently, spontaneously occurring DNA damage remains largely unrepaired. As a consequence the mutant mice display several features of accelerated segmental ageing, including early cessation of growth and nuclear abnormalities in liver and kidney, resulting in premature death (Weeda et al., 1997) and accelerated motor neurone degeneration (de Waard et al., 2010). The maximum lifespan of these mice in the homogenous F1 C57BL/6J-FVB/N genetic background used here is approximately 6 months (IvdP and JHJH, unpublished observations), a time frame which is convenient for analysis of development and progressive decline. Therefore we investigated hearing and vision in this mutant to assess whether DNA damage exerts any effect on the age-related functioning of these organs.

Materials and methods

In this study 60 Ercc1δ/− mutants and 53 wild type littermates in an F1 hybrid Fvb/N-C57Bl/6J background strain were used. All mice were housed on a 12 h light/12 h dark cycle with unrestricted access to food and water. Experiments were done during the light phase. All experiments were approved by the local ethics committee and were in accordance with the European Communities Council Directive (86/609/EEC). For the contrast sensitivity experiments 14 Ercc1δ/− mutants and 14 wild type littermates were used, which were measured longitudinally. For auditory-evoked brainstem response (ABR) recordings 11 Ercc1δ/− mutants and 10 wild type littermates were measured longitudinally. For DPOAE measurements, 2 groups of 6 Ercc1δ/− mutants and 6 littermates, were measured, one group at 4 and one group at 12 weeks of age. For histology 34 Ercc1δ/− mutants and 27 littermates were used.

Auditory experiments

ABR recordings

ABR recordings, which were used to obtain hearing level thresholds, were performed largely as described previously (van Looij et al., 2004). The mice were anesthetized with a mixture of ketamine/xylazine (60/10 mg/kg) i.p. and placed in a sound-attenuated box with the ears at a distance of 4 cm from a frontally placed tweeter loudspeaker (Radio Shack Super Tweeter 40-1310B). Active needle electrodes were positioned subdermally at the base of both pinnae. The reference electrode was placed at the vertex. In addition, a ground electrode was placed near the sacrum. Presentation of stimuli and averaging of responses was controlled by custom-made software (EUPHRA = Erasmus University Physiological Response Averager). Tone pip stimuli (1 ms duration, 0.5 ms cosine-squared ramps, alternating polarity, repetition rate 80 per second) were generated by a Hewlett Packard 33120A waveform generator. Responses were acquired and averaged by a 32 MHZ DSP Motorola 56002 board. The sound pressure level (SPL; re 20 µPa) of the stimuli ranged between −10 and 110 dB. For determining ABR thresholds, 500 responses with artefacts <30 µV were averaged. Stimuli were calibrated by comparing peak-to-peak values of the tone pip stimuli (measured with a 1/2" Bruel and Kjær microphone, type 4192) with a calibrated tone (Bruel and Kjær sound calibrator, type 4231, 94 dB) on an oscilloscope (Tektronix TDS 1002). Hearing level thresholds were measured at 4, 8, 16 and 32 kHz. Thresholds were defined as the lowest SPL (5 dB resolution) at which a reproducible peak (usually peak II or IV) was still present in either ear. After finishing recordings the mice were injected with atipamezole (25 µg s.c.) to facilitate recovery from anesthesia.

DPOAE

We used the DP 2000, Starkey system to measure 2f1 − f2 DPOAEs, with f2/f1 = 1.2. The intensity of f1 and f2 was set at 65 and 55 dB SPL, respectively. Recordings were done at f2 = 4, 6, 8, 10, 12 and 16 kHz. First the speaker was calibrated, followed by three measurements in both ears. The maximum DPOAE amplitude per frequency in each mouse was included in the analysis. Noise floor values were obtained from recordings in a dead animal. DPOAEs of wild type animals were not above baseline between 4 and 8 kHz and therefore only results obtained at 10, 12 and 16 kHz are presented.

Visual experiments

Mouse contrast sensitivity function was determined as described previously (van Alphen et al., 2009a). This method infers contrast sensitivity by measuring how the magnitude (gain) of compensatory eye movements varies with different combinations of contrast and spatial frequency.

Animals were prepared for head fixation by attaching two metal nuts to the skull using a construct made of a micro glass composite.

Stimulus setup

Optokinetic stimuli were created using a modified Electrohome Marquee 9000 CRT projector (Christie Digital Systems, Cypress CA, USA), which projected stimuli via mirrors onto three transparent anthracite-coloured screens (156 cm × 125 cm) that were placed in a triangular formation around the recording setup (see van Alphen et al., 2009, for more details). This created a green monochrome panoramic stimulus fully surrounding the animal. The stimuli were programmed in C++ and rendered in openGL and consisted of a virtual, vertically oriented cylinder with a dotted pattern or vertically oriented sine grating on its wall. Each pixel subtended 4.5 × 4.5 arcminutes. Contrast (C) in the projected sine gratings was calculated using the Michelson formula: $C = (L_{max} - L_{min})/(L_{max} + L_{min})$, where L_{max} and L_{min} are the maximum and minimum luminance in a grating, respectively. The average luminance was kept constant at 17.5 cd/m^2 in all stimulus conditions. At maximum contrast, the minimum and maximum luminance of the stimulus were 0.05 cd/m^2 and 35.0 cd/m^2, respectively.

Eye movement recordings

Mice were immobilized by placing them in a plastic tube, with the head pedestal bolted to a restrainer that allowed placing the eye of the mouse in the centre of the visual stimulus, in front of the eye position recording apparatus.

Eye movements were recorded with an infrared video system (Iscan ETL-200). Images of the eye were captured at 120 Hz with an infrared sensitive CCD camera (see van Alphen et al., 2009, for more details). To keep the field of view as free from obstacles as possible, the camera and lens were mounted under the table surface, and recordings were made with a hot mirror that was transparent to visible light and reflective to infrared light. The eye was illuminated with two infrared LEDs at the base of the hot mirror. The camera, mirror and LEDs were all mounted on an arm that could rotate about the vertical axis over a range of 26.12° (peak to peak). Eye movement recordings and calibration procedures were similar to those described by Stahl, van Alphen, & De Zeeuw (2000). Trials were randomized, mice were assigned a number and the data analysis scripts were automated. All data were analysed after the experiment.

Contrast sensitivity function

Afoveate mammals (like mice) show robust gaze-stabilising eye movements, such as the optokinetic reflex (OKR). The OKR prevents the image of the surroundings to slip across the retina during movement of the visual scene. Contrast sensitivity was tested by presenting moving visual stimuli to

the mice and recording eye movements evoked by those stimuli (van Alphen et al., 2009a). Each stimulus was a vertical sine wave grating made up of a combination of one of seven spatial frequencies (0.03, 0.05, 0.08, 0.17, 0.25, 0.33, or 0.42 c/°) and one of six contrast values (100%, 75%, 50%, 25%, 10%, 1%). The 42 stimulus combinations were presented in random order. A stimulus was first projected and kept stationary for one minute, allowing the animal to adjust to changes in the stimulus. Subsequently, the stimulus started to move with a constant velocity of 1.5°/s. After moving to one direction for 2 s, it changed direction and moved in the opposite direction for 2 s. This was repeated six times, yielding 10 changes in direction. While the stimulus was moving, motion of the left eye was recorded.

Recorded eye positions were transformed offline into a velocity signal. Fast phases and saccades were removed from the eye movement recordings using a velocity threshold of 3°/s, i.e. twice the stimulus velocity. The first 200 ms after stimulus onset and after each change in direction were removed as well. Because the stimulus velocity was constant and eye data in the first 200 ms after the stimulus direction changes were ignored, average absolute eye velocity could be divided directly by the stimulus velocity to calculate a gain value for each combination of spatial frequency and contrast. An eye movement that perfectly follows the visual stimulus has a gain of 1 (Collewijn, 1969).

Saccade analysis

Since changes in the optokinetic reflex may be due to impaired vision, impaired motor system or a combination of both, we analysed a second type of eye movement, saccades, in order to rule out an impaired motor system in the mutant mice. Saccades are rapid eye movements that are clearly distinct from the optokinetic reflex. Saccades are made spontaneously and are not directly related to the optokinetic stimulation. The kinematics of saccades are extremely stereotyped; there is a fixed relation between the amplitude of a saccade and its peak velocity. This relation is known as the main sequence (Bahill, Bahill, Clark, & Stark, 1975). Peak velocity increases with amplitude. At larger amplitudes this relation saturates, but the oculomotor range of the mouse is too small to reach these values. Age-related changes in the oculomotor system predict that the slope of the main sequence relation decreases over time. Possible saccade on- and offsets were marked automatically, using a velocity threshold of 3 times the stimulus peak velocity. The exact on- and offsets were subsequently marked by hand. To compare the main sequences, regression lines were fitted for each age and the slope values were used for statistical purposes.

Immunohistochemistry

For isolation of the eyes, animals were euthanized by CO2 inhalation. Eyes were marked on the nasal side with Alcian blue (5% Alcian blue in 96% ethanol), dissected and subsequently fixed in 4% paraformaldehyde in 0.1 M phosphate buffer and embedded in paraffin. Five µm thick, transverse paraffin sections were cut. For determination of retinal surface area, digital images of the whole retina were taken using a microscope equipped with a high-resolution camera (BX40 microscope, ColorViewIIIu camera and the CellA program). The CellA program was used to make digital images of the same sections used for quantification of the apoptotic cells in the outer nuclear layer (ONL). The program Sigmascan Pro5 was used to measure the surface area of the ONL. Apoptotic cells were visualized using the TdT-mediated dUTP Nick-End Labeling (TUNEL) method according to the specifications of the manufacturer of the kit (Apoptag Plus Peroxidase In Situ Apoptosis Detection Kit, Chemicon). For quantification, the number of TUNEL-positive cells in the ONL was counted using a BX40 microscope with a minimum of 5 transverse cut sections per mouse. To standardize the chosen area of the retina, the sections closest to the eye nerve were selected for immunohistochemistry and quantification. The number of apoptotic cells and retinal surface area in 5 sections per animal were averaged and animals were averaged per group accordingly.

Statistics

The effect of the Ercc1δ/− mutation on contrast sensitivity, hearing thresholds and DPOAEs was analysed using a repeated measures ANOVA with three factors. For contrast sensitivity we used genotype as between-subjects factor and contrast and spatial frequency as within subject factor. Post hoc, groups were compared at each contrast by averaging OKR gains over spatial frequencies. Differences between groups were analysed for significance with Student's t-test. For the effect of the Ercc1δ/− mutation on hearing thresholds and DPOAEs we used genotype and age as between and frequency as within-subjects factors. Post hoc, groups were compared with two-way ANOVAs and Bonferroni tests. Comparison of main sequence slopes was done by Monte Carlo bootstrapping each main sequence (N = 1000), and comparing them by two-tailed Student's t-tests.

Results

Progressive hearing loss in Ercc1δ/− mice

To objectively assess whether presbycusis develops in Ercc1δ/− mice, hearing level thresholds were measured longitudinally using the auditory brainstem response (ABR). Auditory thresholds in Ercc1δ/− mice were already elevated at 5 weeks of age, the first measurement point. Importantly, auditory function further deteriorated in the following 9 weeks (Figure 3.1A), suggesting that the defect at 5 weeks of age is part of a progressive degenerative process. We performed a three-way

repeated measures ANOVA with genotype and age as between, and frequency as within-subjects factors. All three main effects and their pair-wise interactions had a significant effect on hearing level thresholds (all $p < 0.001$). To clarify the origin of these significant changes, we performed a two-way repeated measures ANOVA. The Ercc1δ/− mice showed a significant effect of age ($p < 0.001$) and a significant interaction of age and frequency ($p < 0.001$). In contrast, there was no effect of age in the wild type mice ($p = 0.30$; Figure 3.1A). This shows that only the Ercc1δ/− mice have an age-dependent increase in hearing thresholds and, importantly, that this increase is not the same for all frequencies. Age had a significant effect for 8 kHz ($p < 0.05$), 16 kHz and 32 kHz (both $p < 0.001$) but not for 4 kHz ($p > 0.05$; Bonferroni post hoc test). Taken together, these findings show that the Ercc1δ/− mice have an age-dependent increase in hearing thresholds especially at higher frequencies, while their wild type littermates are not affected.

Progressive hearing loss in Ercc1δ/− mice is caused by hair cell loss

Further studies were performed to determine the site of origin of the hearing loss within the auditory pathway. The conduction speed of the auditory response was used as a test for possible retrocochlear pathology. We identified peaks I–V in the ABR and compared the inter-peak latencies of the most prominent peaks, II and IV, at ages 4 and 12 weeks between wild type and Ercc1δ/− mice

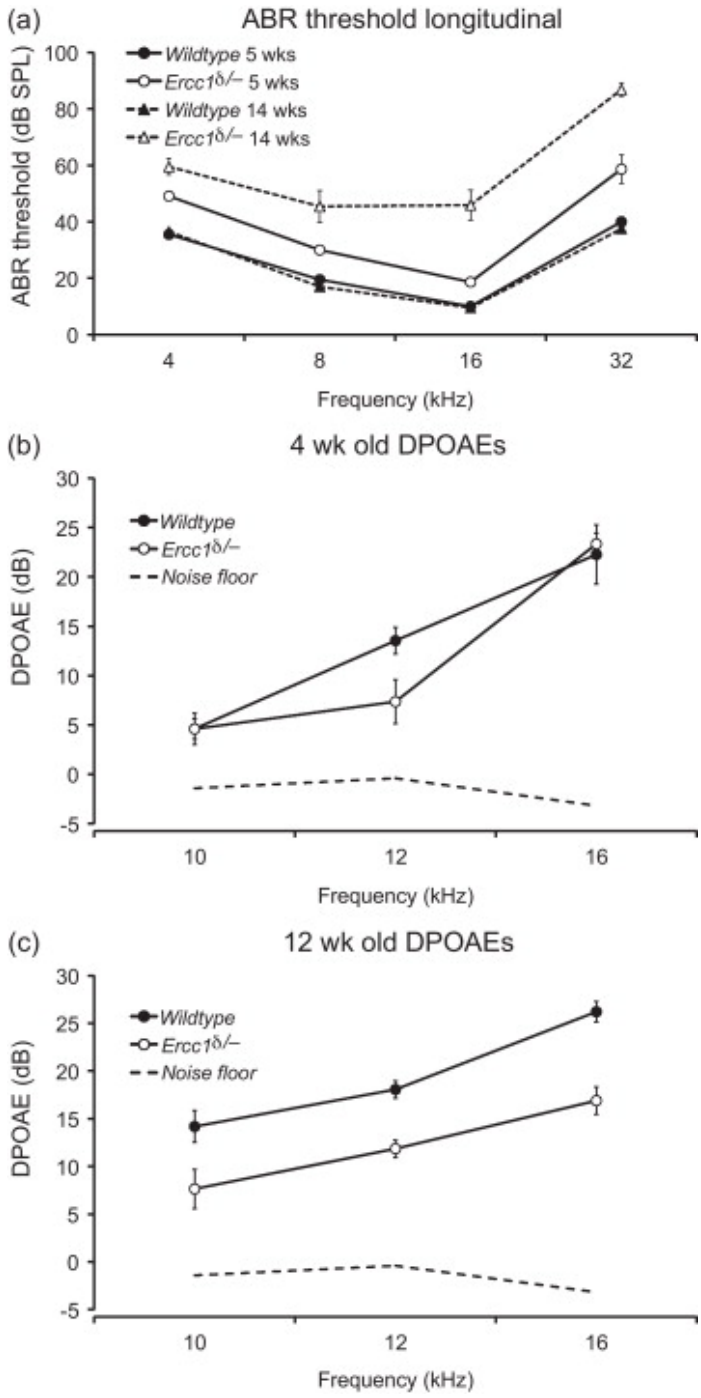

Figure 3.1. The combination of increased ABR hearing thresholds and reduced DPOAE suggests outer hair cell loss in the cochlea of Ercc1δ/− mice. (A) Ercc1δ/− mice show hearing loss, especially at higher frequencies, from 5 to 14 weeks of age. Filled symbols represent wild type and open symbols Ercc1δ/− mice. Circles and triangles represent 5 and 14 week old animals, respectively. (B) 4 week old Ercc1δ/− mice have similar DPOAEs as their wild type littermates. (C) 12 week old Ercc1δ/− mice have reduced DPOAEs at higher frequencies compared to their littermates, suggesting outer hair cell loss. Data are shown as mean ± SEM.

at 4 and 16 kHz. No statistically significant latency differences were observed between wild type and Ercc1δ/− mice both with and without correction for difference in minimum hearing level threshold

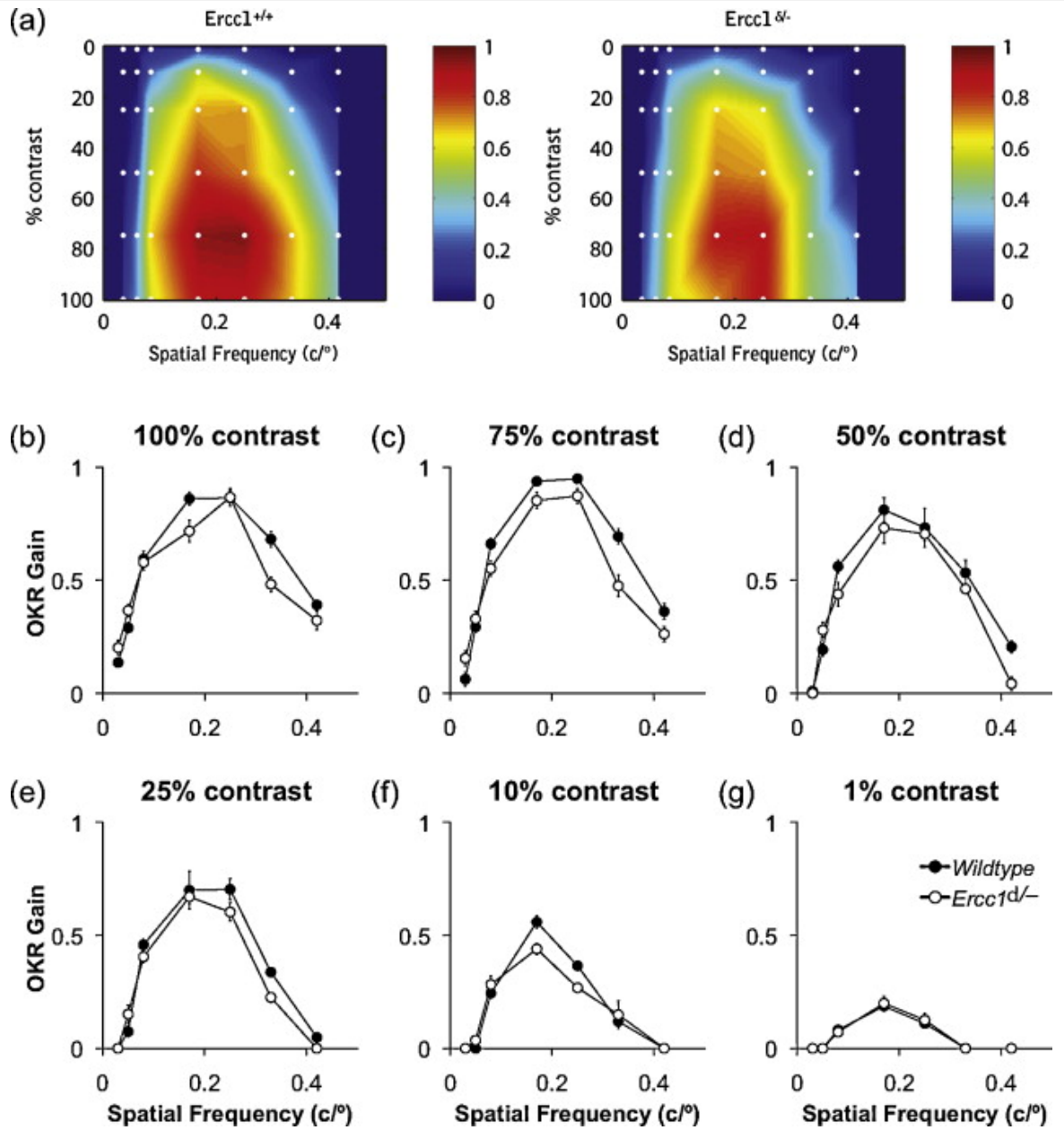

Figure 3.2. Normal contrast sensitivity in Ercc1δ/− mice and their littermates at 6 weeks of age. (A) The colour reflects the OKR gains at 42 different combinations of spatial frequency and contrast. Measured points are connected through linear interpolation. (B–G) Six cross sections of (A) and (B) are plotted, one for each contrast. Even at low contrast values, Ercc1δ/− mice have similar OKR gains as their wild type littermates, indicating normal vision. All data represented as means ± SEM. Filled circles represent wild type and open circles Ercc1δ/− mice.

($p > 0.05$). II–IV inter-peak latencies at 4 kHz were 1.89 ± 0.06 (mean ± SEM) and 1.82 ± 0.11 ms for wild type and 1.91 ± 0.03 and 1.71 ± 0.08 ms for Ercc1δ/− mice at 4 and 12 weeks, respectively. At 16 kHz, II–IV intervals were 1.99 ± 0.04 and 1.83 ± 0.10 ms for wild type and 2.03 ± 0.08 and 1.82 ± 0.09 ms for Ercc1δ/− mice at 4 and 12 weeks, respectively (results not shown). This suggests that the observed differences in hearing level thresholds are not due to retrocochlear deficits in the mutants.

Otoacoustic emissions are a sensitive assay of cochlear function, especially of the outer hair cells. We evoked DPOAEs at 4 and 12 weeks of age in Ercc1δ/− mice and their age-matched littermates (Figure 3.1B and C). We performed a three-way repeated measures ANOVA with genotype and age as between, and frequency as within-subjects factors, which revealed that all main effects and their interactions were significant (all $p < 0.05$). Two-way ANOVA testing indicated no effect of genotype ($p = 0.27$) at 4 weeks (Figure 3.1B), while a highly significant effect size ($p < 0.0001$) was observed at 12 weeks (Figure 3.1C).

Together, the lack of a significant difference in ABR inter-peak latencies and the decreased DPOAEs in 12-week-old Ercc1δ/− mice indicate a cochlear origin of the hearing loss, probably including outer hair cell damage.

Progressive decline of vision in Ercc1δ/− mice

To assess visual performance of Ercc1δ/− mice over their life span we measured in a longitudinal study the optokinetic reflex (OKR) gains at several different spatial frequencies and contrast values. At 6 weeks of age, all stimuli evoked OKR gains that were similar in both genotypes (Figure 3.2). The only exception was at 75% contrast, where the gain was slightly lower in Ercc1δ/− ($p < 0.05$). Both groups showed a similar optimum for all contrasts, which was reached at 0.17–0.25 c/°. At 10 weeks of age, OKR gains were lower in Ercc1δ/− mutants (Figure 3.3). Ercc1δ/− mice performed worse than their wild type littermates at all contrast levels ($p < 0.05$), except at 100% contrast. Gains were lower and the window in which responses occurred narrowed, i.e. the highest (0.42 c/°) and lowest (0.03 c/°) spatial frequencies did not elicit any response in mutant mice at contrasts below 100%. At 14 weeks of age, all OKR gains were strongly reduced in Ercc1δ/− mutants ($p < 0.001$) (Figure 3.4). The response window narrowed further, i.e. there was almost no response below 0.08 c/° or above 0.25 c/°. Below 50% contrast, hardly any response was observed. Moreover, even within the optimal stimulus window, i.e. 100% contrast and 0.17–0.25 c/°, the evoked OKR gain was lower in the Ercc1δ/− mice.

At all ages, the mutant mice made smaller saccades compared to the wild type mice (Figure 3.5), probably due to a smaller oculomotor range. However, the main sequence was not different

between mutants and wild types, nor did it change over time in either group, indicating an intact oculomotor system (all $p > 0.05$).

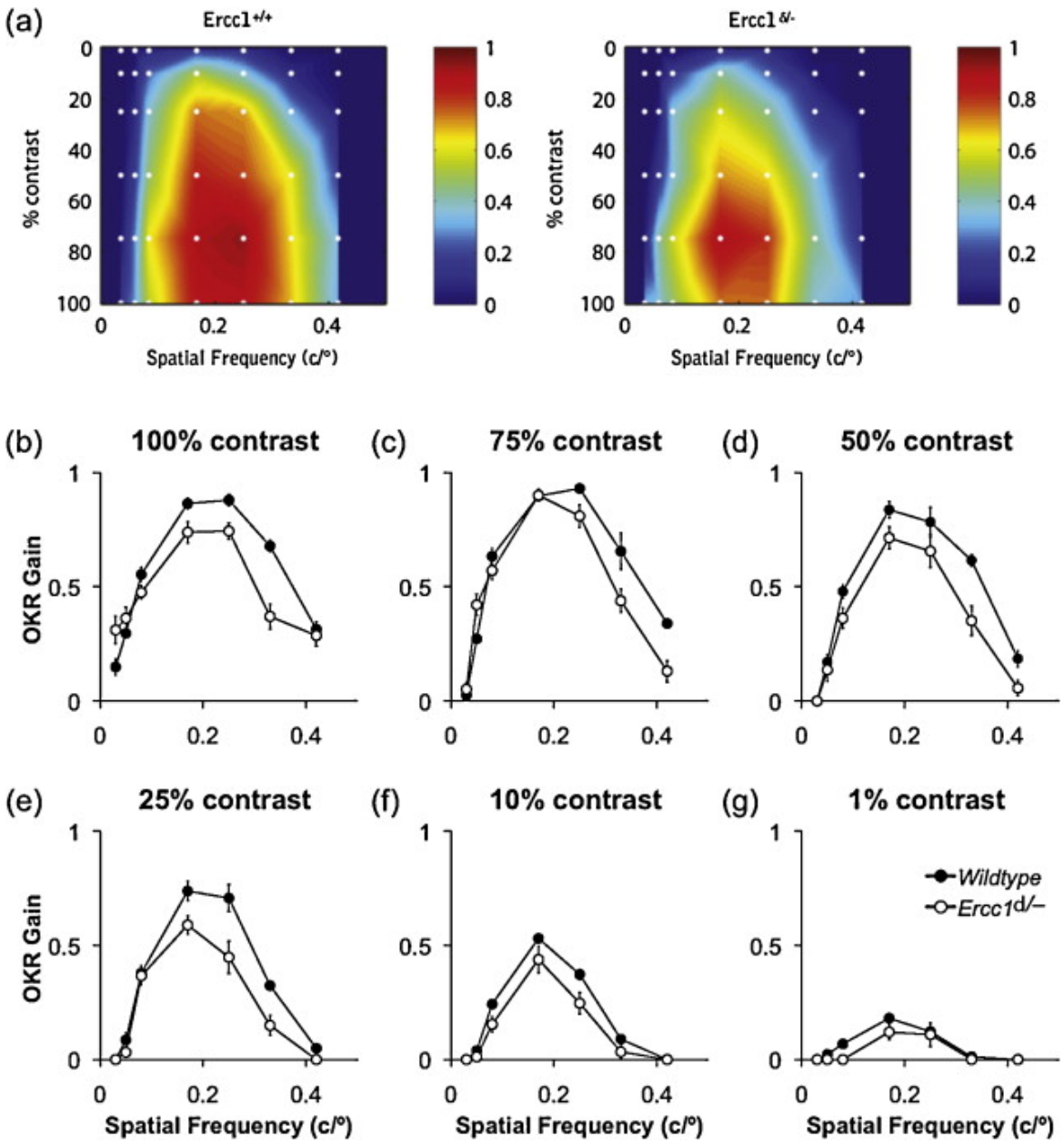

Figure 3.3. Reduced contrast sensitivity in Ercc1δ/− mice and their littermates at 10 weeks of age. (A) The colour reflects the OKR gains at 42 different combinations of spatial frequency and contrast. Measured points are connected through linear interpolation. (B–G) Six cross sections of (A) and (B) are plotted, one for each contrast. Compared to 6 week old animals, Ercc1δ/− mice show slightly reduced OKR gains at all contrast values. All data represented as means ± SEM. Filled circles represent wild type and open circles Ercc1δ/− mice.

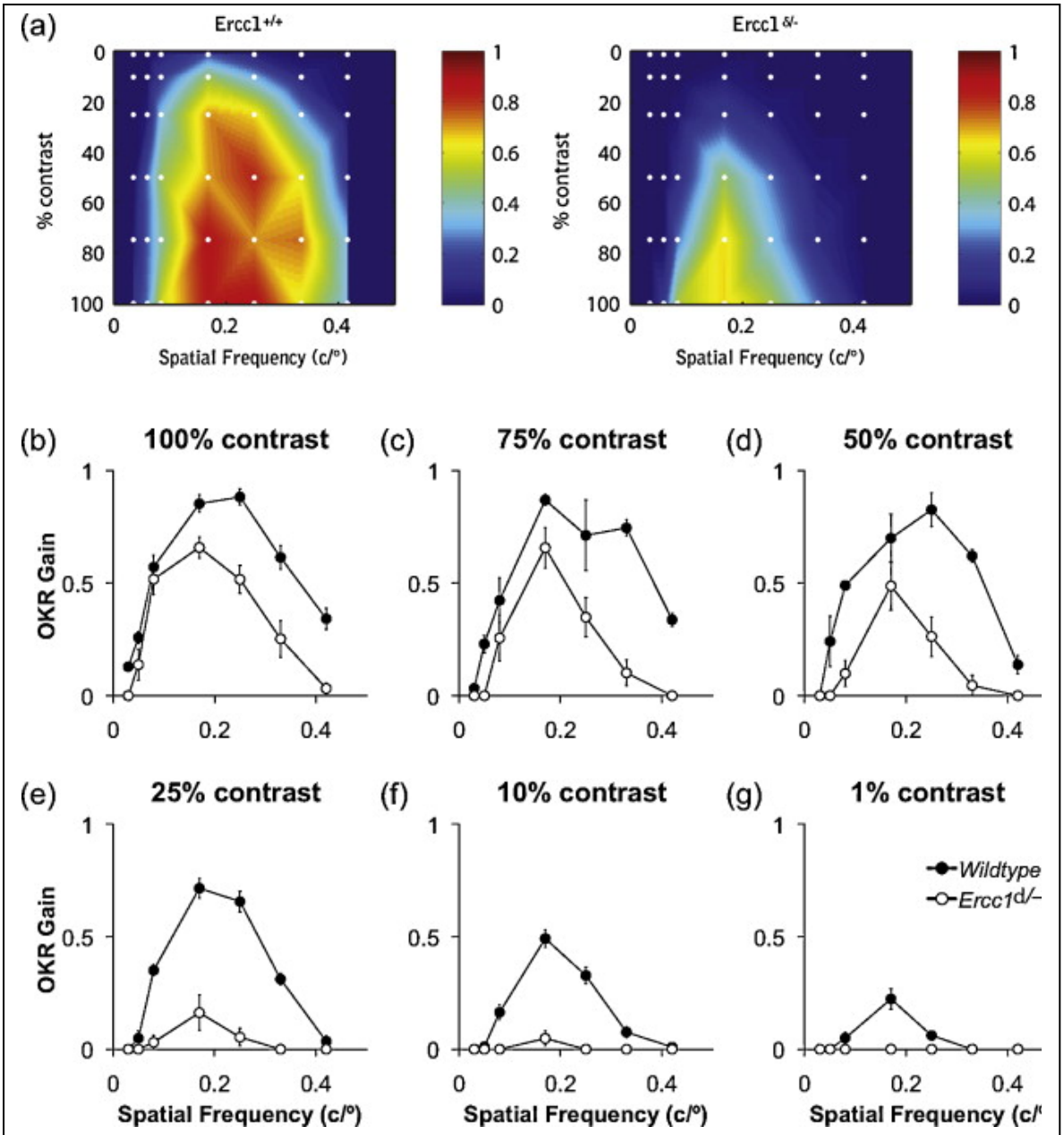

Figure. 3.4. Severely reduced contrast sensitivity in Ercc1δ/− mice and their littermates at 14 weeks of age. (A) The colour reflects the OKR gains at 42 different combinations of spatial frequency and contrast. Measured points are connected through linear interpolation. (B–G) Six cross sections of (A) and (B) are plotted, one for each contrast. Visual performance is severely reduced in Ercc1δ/− mice, even at 100% contrast. All data represented as means ± SEM. Filled circles represent wild type mice and open circles Ercc1δ/− mice.

Progressive reduction of outer nuclear layer in Ercc1δ/− mice

One explanation of the loss of visual performance could be loss of photoreceptor cells in the retina. Therefore, we determined the surface area of the outer nuclear layer (ONL) in cross sections of the eye at 4, 9, 18 and 25 weeks of age in Ercc1δ/− mice and their age-matched littermates (Figure 3.6A). We performed a two-way ANOVA and found a significant effect for both age and genotype (p

< 0.0001) and for their interaction ($p < 0.005$). Bonferroni post hoc tests revealed that only at 25 weeks of age there was a significant genotype effect ($p < 0.001$). This shows an age-dependent reduction of the ONL in Ercc1δ/− mice suggestive of loss of cells, most likely photoreceptors. To further investigate the cause of the reduction of the ONL we determined the number of TUNEL-positive cells, i.e. cells in apoptosis, in the ONL at 4, 9, 18 and 25 weeks of age (Figure 3.6B). Two-way ANOVA analyses revealed a significant effect of age, genotype and their interaction ($p < 0.0001$). These results strongly suggest that the progressive reduction of the ONL was caused by loss of cells through apoptosis.

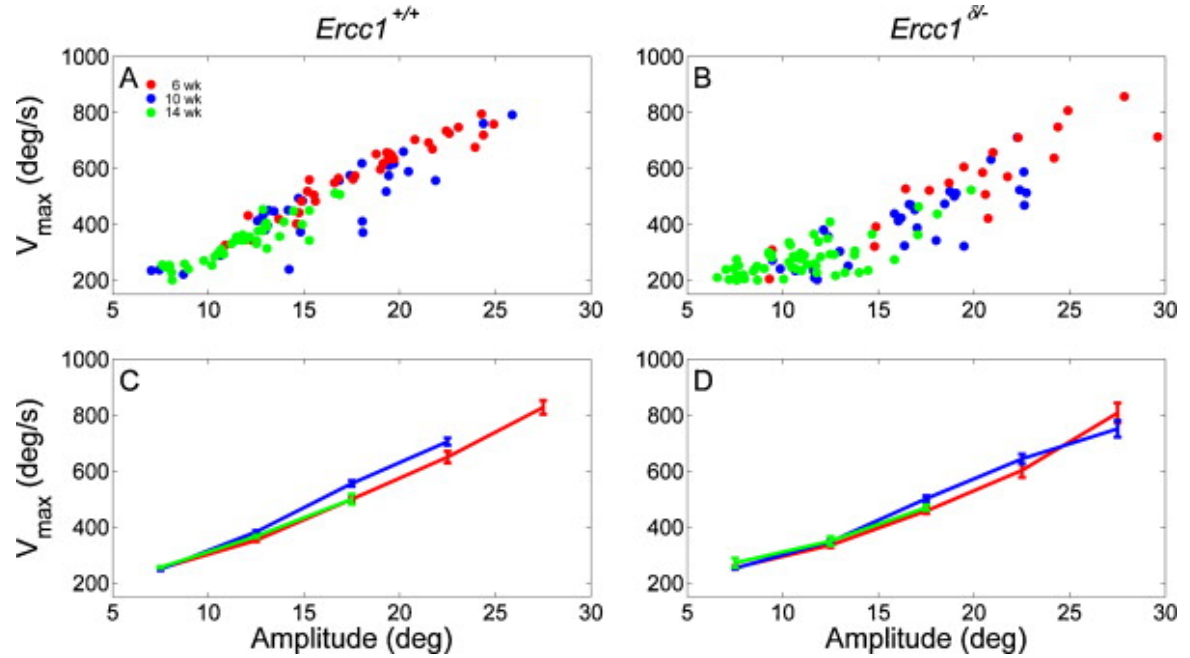

Figure. 3.5. Saccade peak velocity as function of amplitude. Representative examples of saccade peak velocity recorded from a wild type (A) and a mutant mouse (B) at three different ages. Each dot represents a single saccade. Average peak velocity of saccades recorded from 14 wild type (C) and 12 mutant mice (D) at three different ages. There is no evidence for degeneration of the oculomotor system, as the slope remains unaltered with increasing age. Data represented as means ± SEM.

Discussion

Our findings demonstrate that the DNA repair defect in Ercc1δ/− mouse results in accelerated age-related decline of both vision and hearing compared to wild type littermates. This indicates that accumulation of spontaneous DNA damage, which normally would have been repaired by nucleotide excision and cross link repair, triggers accelerated loss of hearing and vision abilities. The most likely cause for these deficits is that helix-distorting and interstrand crosslink DNA damage within the cochlea and retina is responsible for the observed age-dependent deterioration. However, cochlea-

and retina-specific mutants would be needed to fully exclude a possible contributing role of for example liver or kidney failure (Borgesius et al., 2011; McWhir, Selfridge, Harrison, Squires, & Melton, 1993; Pinto & Enroth-Cugell, 2000; Selfridge, 2001; Selfridge, Song, Brownstein, & Melton, 2010; Weeda et al., 1997).

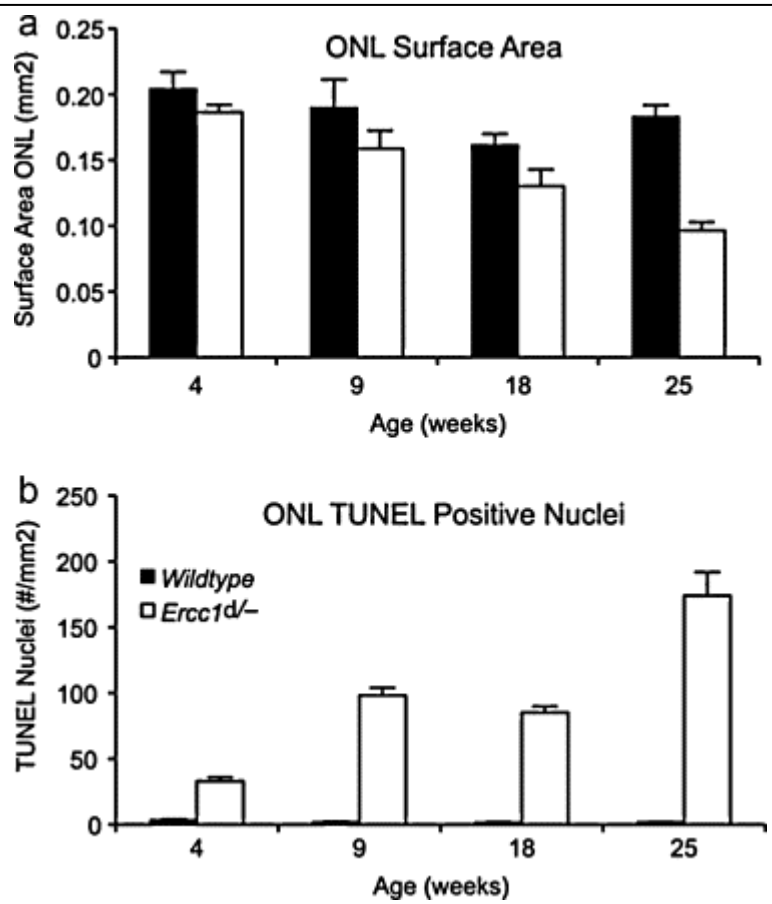

Figure. 3.6. Age-dependent loss of cells through apoptosis in the ONL in Ercc1δ/− mice. (A) Age-dependent reduction of ONL surface in cross sections of Ercc1δ/− eyes compared to those of their littermates. (B) Age-dependent increase of TUNEL-positive cells normalized to ONL surface in Ercc1δ/− mice. Black columns represent wild type mice and open columns Ercc1δ/− mice. All data represented as means ± SEM.

Presbycusis

We found that Ercc1δ/− mice display a progressive increase of hearing thresholds in combination with reduced DPOAEs. Thresholds were already elevated at the youngest age we tested. This might be due to very rapid deterioration or due to abnormal development, a distinction which is not always easily made for the neurological abnormalities that are associated with DNA repair disorders (Kraemer et al., 2007). The unchanged ABR inter-peak latencies suggest a lack of major changes in the central auditory pathway, even though more subtle changes cannot be excluded (Walton, 2010). These findings thus indicate a cochlear origin of the hearing loss. The hearing loss is unlikely to be an

indirect consequence of renal or liver failure (Lawrence et al., 2008; McWhir et al., 1993; Selfridge, 2001; Weeda et al., 1997), since encephalopathy following renal or liver failure is generally not associated with hearing loss (Bismuth, Funakoshi, Cadranel, & Blanc, 2011; Seifter & Samuels, 2011), 2011), whereas high bilirubin resulting from liver failure targets central auditory structures, but spares the cochlea (Shaia, Shapiro, & Spencer, 2005; Shapiro, 2003). The phenotype of the Ercc1δ/− mice, i.e. increased hearing threshold, reduced DPOAE and normal ABR inter peak latencies, is similar to what is seen in human presbycusis (Dorn et al., 1998; Gates & Mills, 2005; Heman-Ackah, Juhn, Huang, & Wiedmann, 2010; Howarth, 2006; Oeken, Lenk & Bootz, 2000; Ohlemiller, 2006; Uchida et al., 2008).

Considerable evidence for a causative role of mitochondrial DNA (mtDNA) damage in presbycusis has been presented (Kujoth et al., 2005, Niu et al., 2007, Someya et al., 2007). However, the complex nucleotide excision repair pathway involving at least 30 proteins (Gillet & Schärer, 2006) is restricted to the nucleus and the Ercc1δ/− mutations are not expected to directly affect mtDNA repair. Hence, our results indicate that, in addition to mtDNA damage, nuclear DNA damage can also play a causative role in presbycusis. Moreover, since nuclear DNA encodes the vast majority of mitochondrial proteins, an indirect effect on mitochondrial function can be anticipated.

One of the options emerging from the above scenario for the etiology of presbycusis is the possibility for prevention of hearing loss by antioxidants to reduce ROS levels which may be one of the causative factors for DNA damage. Several such studies have been reported in mice (Davis, Kuo, Stanton, Krieg, & Alagramam, 2007; Derin et al., 2004; Heman-Ackah et al., 2010; Le & Keithley, 2007; Seidman, Ahmad, & Bai, 2002), rats (Derin et al., 2004) and humans (Durga, Verhoef, Anteunis, Schouten, & Kok, 2007; Takumida & Anniko, 2009) with overall promising results. Our findings lend support to the idea that a possible preventive effect of antioxidants in presbycusis would act by preventing cochlear DNA damage.

Age-related vision loss

We measured OKR gains to infer the contrast sensitivity and visual acuity of mice. To this end we presented visual stimuli with different spatial frequencies and contrasts. In 6-week-old mice there were only subtle differences in contrast sensitivity between wild types and mutants, as similar OKR gains were recorded for all stimuli in our study. However, at 14 weeks of age, contrast sensitivity had decreased to the point where mutant mice were only able to observe a small set of contrast–spatial frequency combinations. The overall decrease in contrast sensitivity occurring in the Ercc1δ/− during a period of only 8 weeks followed a similar pattern as was reported for normal ageing in C57Bl/6J mice (van Alphen et al., 2009a), for which the ability to perceive low contrasts and high spatial

frequencies disappeared first. A much more severe phenotype was previously observed in an Ercc1 null mutant, in which the very severe, lifespan-limiting liver degeneration of Ercc1 null mice was rescued by an Ercc1-liver-specific transgene. In this model the OKR response was already very poor at 4 weeks, with little change at 8 weeks (Lawrence et al., 2008). These mice have a life span of only 2–3 months (Selfridge, 2001) as compared to 4–6 months for the milder Ercc1δ/− mice, suggesting that the more severe phenotype of the null mutant is most likely caused by the more complete genetic deletion.

Apart from confirming the contrast sensitivity in another Ercc1-deficient mouse model, our study used a different contrast sensitivity measurement than Lawrence et al. (2008) and recorded the actual eye movements instead of observing head tracking. This enables measurement of the optokinetic response and therefore vision more accurately (van Alphen et al., 2009a). In any behavioural response, pathology of the motor system can play a role, as was also suggested by Lawrence et al. (2008). However, also by analysing saccadic eye movements, and showing that their dynamics were intact (Figure 3.5) we demonstrated that both the neural and the muscle parts of the oculomotor system were unaffected by the mutation. We conclude that the decrease in OKR gain most likely resulted from age-related deterioration of the visual system.

In humans, OKR gains decline with age, at high frequencies as well as at high velocities, owing to an impaired sensorimotor system (Leigh & Zee, 2015; Paige, 1994). In contrast, this effect was not found in mice (Stahl, 2004; Stahl, James, Oommen, Hoebeek, & De Zeeuw, 2006). However, it could be that the mice were still too young (about 15 months) to reveal an age-dependent effect. Studies in humans on the effect of age on the spatial contrast sensitivity function curve have shown a decline in high frequency sensitivity at middle age, leading to intermediate and high spatial frequency attenuation with increasing age due to optical and neural degeneration (Arundale, 1978; Derefeldt et al., 2009; McGrath & Morrison, 1981; Nameda, Kawara, & Ohzu, 1989; Nomura, Ando, Niino, Shimokata, & Miyake, 2003; Owsley et al., 1983; Wang, 2001).

Our histology data showed increased, age-related loss of photoreceptors in the mutants. However, it is unlikely that this fully explains the observed vision loss, as the effects of age on vision were already apparent at 10 weeks while the reduction of the ONL did not reach significance until 25 weeks. Indeed, Samuel, Zhang, Meister, & Sanes (2011) showed recently that other, more subtle factors in the mouse retina are mainly responsible for the deterioration of vision in ageing mice, and similar mechanisms may play a role in the Erccδ/− mutant. Our data thus agree with and extend previous experiments on an Ercc1 null mutant, for which the loss of contrast sensitivity was not matched by histological abnormalities in the retina (Lawrence et al., 2008).

Although photoreceptor loss or thinning of the ONL is commonly seen in ageing in humans (Aggarwal et al., 2007; Curcio et al., 1993; H. Gao & Hollyfield, 1992; Panda-Jonas et al., 1995), mice (Bravo-Nuevo et al., 2004; Sanyal & Hawkins, 1986) and mouse models of accelerated ageing (Gorgels et al., 2007; Shoji et al., 1998; van der Pluijm et al., 2006), it is not clear how relevant this phenomenon is to age-related vision loss. Nevertheless, since optic changes cannot fully explain age-related vision loss, it is likely that loss or reduced function of photoreceptors does contribute to age-related vision loss (Spear, 1993).

In conclusion, the Ercc1δ/− mutant shows accelerated age-related loss of hearing and vision with characteristics very similar to human presbycusis and age-related vision loss. This suggests a causative role of DNA damage in the etiology of presbycusis and age-related vision loss. Our results also suggest a possible causative role for (functional) loss of outer hair cells and photoreceptors, although a contribution of other cell types cannot be excluded. Additional research using conditional knockouts will help resolve the relative contribution of different cell types to these processes.

Acknowledgments

We thank Dr. Efstathios B. Papachristos for help with statistical analysis and Dr. Ype Elgersma for helpful comments on an earlier version of this manuscript. MS was supported by a HFSP grant. BvA was supported by a NWO-ALW grant. APN was supported by the Heinsius-Houbolt fund. JHJH and YR were supported by a Top Instititute Pharma grant, Markage (FP7-Health-2008-200880), LifeSpan (LSHG-CT-2007-036894), National Institute of Health (NIH)/National Institute of Ageing (NIA) (1PO1 AG-17242-02) and the European Research Council (ERC advanced scientist grant to JHJH).

Chapter 4 - Albino Mice as an Animal Model for Infantile Nystagmus Syndrome [3]

Ghislaine L. Traber; Chien-Cheng Chen; Ying-Yu Huang; Marcella Spoor; Jeanine Roos; Maarten A. Frens; Dominik Straumann; Christian Grimm

Abstract

Individuals with oculocutaneous albinism are predisposed to visual system abnormalities affecting the retina and retinofugal projections, which may lead to reduced visual acuity and Infantile Nystagmus Syndrome (INS). Due to absence of an established mammalian animal model, mechanisms underlying INS remain elusive. In this study, we screened wild-type mice of varying pigmentation for ocular motor abnormalities in order to identify a possible mouse model for INS.

Three albino mouse strains (CD1, BALB/c, DBA/1), and two normally pigmented strains (129S6, C57BL/6) were screened using infrared oculography. Varying visual stimuli (black or white background, stationary pattern, optokinetic, i.e., horizontally rotating pattern) were displayed to the full (fVF) or anterior visual field (aVF) of the restrained mouse.

We found spontaneous nystagmus, specifically jerks and oscillations, in albino mice under all experimental conditions. Median eye velocity was between 0.8 and 3.4 ˚/s, depending on the strain. In contrast, the eyes in pigmented mice were nearly stable with a median absolute eye velocity of below 0.4 ˚/s. In albino mice, fVF optokinetic stimuli elicited an optokinetic response (OKR) in the correct direction, albeit with superimposed oscillations. However, aVF optokinetic stimuli evoked reversed OKR in these strains, a well-known feature of INS.

Based on our results, we endorse the investigated albino mouse strains as new animal models for INS.

Introduction

Infantile Nystagmus Syndrome (INS) is a relatively common ocular motor (Forssman & Ringnér, 1971; Sarvananthan et al., 2009) characterized by involuntary, predominantly horizontal conjugate oscillations of both eyes. The syndrome usually manifests itself within the first six months after birth (Gresty, Page, & Barratt, 1984; Maybodi, 2003) and remains throughout life. Distinctive features of INS in humans include specific waveforms of eye movement (which is usually a jerk with an

[3] Investigative Ophthalmology & Visual Science August 2012, Vol.53, 5737-5747. doi:10.1167/iovs.12-10137

increasing slow phase velocity, but which may also be pendular or both), foveation periods (Dell'osso & Daroff, 1975), and inversion of the optokinetic reflex (OKR; Halmagyi, Gresty, & Leech, 1980; Thurtell & Leigh, 2011). Although INS can be idiopathic, a majority of patients have associated visual system abnormalities like albinism, retinal dystrophies, aniridia, optic nerve hypoplasia, or congenital cataracts. (Lorenz & Gampe, 2001; Sarvananthan et al., 2009; Weiss & Biersdorf, 1989). Due to absence of an appropriate mammalian animal model, the mechanisms underlying INS remain incompletely understood. The known association between albinism and INS prompted us to screen wild-type mice of varying pigmentation for ocular motor abnormalities in order to identify a possible new animal model for INS.

Methods

All experiments were performed in accordance with the animal welfare guidelines of the Federal Veterinary Office of Switzerland, and experimental procedures were approved by the local authorities (Cantonal Veterinary Office Zurich). Experiments adhered to the ARVO Statement for the Use of Animals in Ophthalmic and Vision Research.

Animals

CD1 [Crl:CD1(ICR), unpigmented, white; Charles River, Sulzfeld, Germany], BALB/c (BALB/cAnNTac, unpigmented, white; Taconics, Ejby, Denmark), DBA/1 (DBA/1JbomTac, hypopigmented, grey; Taconics), 129S6 (129S6/SvEvTac, pigmented, brown; Taconics), and C57BL/6 (C57BL/6NTac, pigmented, black; Taconics) were purchased from commercial suppliers. In this paper, the three mouse strains with oculocutaneous albinism, CD1, BALB/c, and DBA/1, will be referred to as albino mice. 129S6 and C57BL/6 will be referred to as pigmented mice. At least five 12- to 25-week-old male mice (van Alphen et al., 2009a) of each strain were recorded and screened for ocular motor abnormalities. Some CD1 strains are known to show retinal degeneration. Even though this has not been reported for Crl:CD1(ICR) mice (Serfilippi, Pallman, Gruebbel, Kern, & Spainhour, 2004), we ruled out a possible Rd1 mutation by genotyping according to published procedures (Samardzija et al., 2006).

Surgery

Reproducible recording of eye movements required restraint of the mouse heads by an aluminium plate attached to the skull. Animals were surgically prepared as described previously (Lütcke et al., 2010; van Alphen et al., 2009a). Briefly, mice were anesthetized with a subcutaneous injection of ketamine (1.7 µL/g)/xylazine (0.2 µL/g). After a sagittal incision of the scalp was made, connective tissue was removed from the skull and the exposed bone was air dried for at least 1 minute. A light curing, one component adhesive (iBond Total Etch; Heraeus Kulzer GmbH, Hanau, Germany) was

applied to allow bonding between skull and dental cement (Charisma A1; Heraeus Kulzer GmbH). The latter formed the basis into which the aluminium plate was imbedded. It was then covered with a fluid composite (Tetric EvoFlow; Ivoclar Vivadent, Schaan, Lichtenstein) to ensure firm adhesion of the aluminium plate to the cement. All respective layers needed to be light cured with blue light (400–500 nm) in order to form a hard layer (bluephase; Ivoclar Vivadent). Mice were allowed to recover from surgery for at least one week before eye movement recordings.

Stimulus Setup

A commercially available optomotor system (OptoMotry VR 1.7.7; CerebralMechanics Inc., Lethbridge, Alberta, Canada) was used to project different visual stimuli (Figure 4.1). The system consists of four 20’ monitors creating a nearly cubic arena. Between the monitors, there are 5-cm large edges without image in the corners (Figure 4.1B). The restrained mouse was placed on an elevated platform (Figure 4.1B) with the forehead in the centre of that arena. The mouse faced the middle of one monitor with the body axis perpendicular to the front and back monitor, and parallel to the monitors on each side. The distance of the forehead to each monitor is 23.5 cm. The OptoMotry stimulus system is designed such that the projected sine gratings get larger towards the corners of the arena as they compensate for the increasing viewing distance. This creates the illusion of a virtual cylinder around the mouse instead of the cubic geometry of the four screens. The presented visual stimuli were a projected black background, a projected white background, a stationary pattern of vertical sine gratings (spatial frequency 0.17 cyc/˚, contrast 100%), and a rotating sine grating eliciting an optokinetic response in temporonasal (tn) and nasotemporal (nt) direction relative to the recorded eye. The rotating visual stimulus had a velocity of 6.1 ˚/s. All visual stimuli were presented binocularly, however, eye movements were only recorded from the right eye. During recordings, the room was otherwise always dark.

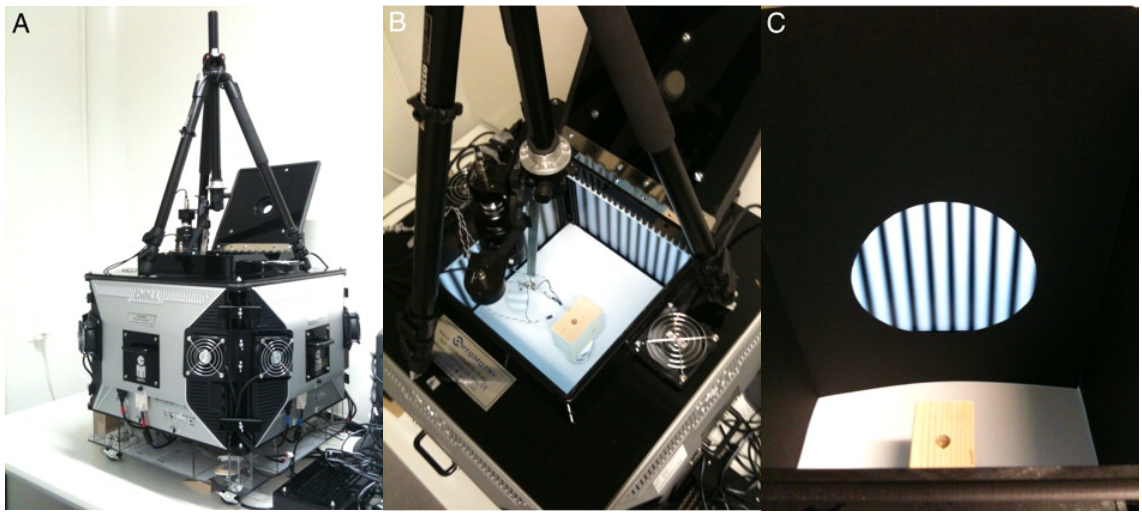

Figure 4.1 The experimental setup consisted of a commercially available optomotor system that allowed projection of visual stimuli on four monitors (A), and an infrared camera for eye tracking. The camera was placed on top of the OptoMotry system (A), with a hot mirror deviating the reflected infrared light from the eye to the camera (B). Visual stimuli were presented binocularly. However, only the right eye was tracked. The eye was illuminated with three infrared LEDs (B). For aVF stimulation, monitors were masked with black cardboard except for a round window in front of the mouse (C). The window allowed binocular viewing of the stimuli in the aVF, 30° to each side of the midline.

Albino mice are known to have a chiasmatic projection error with retinal ganglion cells (RGC) from the inferotemporal retina being misdirected to the contralateral hemisphere (Grant W. Balkema & Dräger, 1990; Dräger & Olsen, 1980). To selectively activate the temporal RGCs, which are misrouted in albino mice, visual stimuli were also displayed in the anterior visual field (aVF) only. For this purpose the monitors were masked with black cardboard except for a round window in front of the mouse (Figure 4.1C). The window allowed binocular viewing of the stimuli in the aVF, 30° to each side of the midline. (Window diameter 17.3 cm in 15-cm distance from the mouse.) Except for the dark background, the exact same visual stimuli were presented in the full visual field (fVF) and aVF. The dark situation was not repeated with VF restriction, since it would again result in fVF darkness.

Illuminance of the white [L_{max} = 283 lux (lx)] and dark (L_{min} = 1.4 lx) monitor was measured using a lux-meter (T-10; Konica Minolta Sensing, Inc., Osaka, Japan), which allowed calculation of sine grating contrast according to the Michelson formula [$C = (L_{max} - L_{min})/(L_{max} + L_{min})$]. The calculated contrast was 99% and, for better readability, will be referred to as 100% in this paper. Average illuminance was 155 lx at the level of the mouse eye for both the stationary pattern and the optokinetic stimulus (OKS).

Eye Position Recording

Eye position of the right eye, illuminated with three infrared LEDs, was recorded with infrared oculography at 120 Hz (ELT-200; ISCAN, Inc., Woburn, MA). The camera was placed on top of the OptoMotry system, with a hot mirror deviating the reflected infrared light from the eye to the camera (Figure 4.1). The fact that albino mice have translucent irides made pupil tracking impossible in CD1 and BALB/c mice. Instead, an infrared absorbing marker (black iron oxide; H. Schmincke & Co., Erkrath, Germany) was applied to the cornea after local anaesthesia with oxybuprocaine. The infrared camera would then automatically track the marker. This method could not be applied to the other three strains since the marker would not sufficiently stand out from the pigmented iris to be recognized by the tracking function and software. This even applied to the DBA/1 mouse with its intermediate iris pigmentation. However, pupil and marker tracking has been compared earlier (van Alphen, Winkelman, & Frens, 2010), and did not show significant differences with regard to recorded eye velocities. On the computer screen connected to the camera, the tracked eye was visualized by a zoomed live image.

While optimising the experimental setup, all mice had gone through one or two training sessions before acquisition of the experimental quantitative data. During training sessions, ocular motor responses of up to 2 minutes per stimulus were observed. However, due to decreasing cooperation in some mice and the heating up of the OptoMotry system, the recording sessions were shortened for the experiment. A record of at least 10 seconds per stimulus in good tracking quality was considered sufficient. Usually 15 to 30 seconds, and for the stationary pattern, 30 to 60 seconds, were recorded, though. When a considerable build-up of the ocular motor response was noted, the record was prolonged or restarted. The complete protocol of visual stimuli was recorded in one session for better comparability of ocular motor responses to various stimuli within one animal. If a session had to be stopped for some reason, the complete data set was repeated later. Loss of the corneal marker was one of the major reasons for postponing a session in CD1 and BALB/c mice. Some mice started to fight their restraint or to clean the whiskers, the latter especially being the case for DBA/1 mice. Often the attention of the mouse could be re-established with noise (by clapping hands). Even though blinking was not a general problem, it was still a reason for prolonged recording sessions in some of the mice. Depending on the cooperation of the mouse, the duration of each recording session was, thus, variable. Mice were, however, restrained for a maximum of approximately 30 minutes. In sum, pigmented mice had one to two training sessions, and one to two

recording trials. Albino mice had two training sessions, and one to four recording trials. No more than one recording trial was done on one particular day.

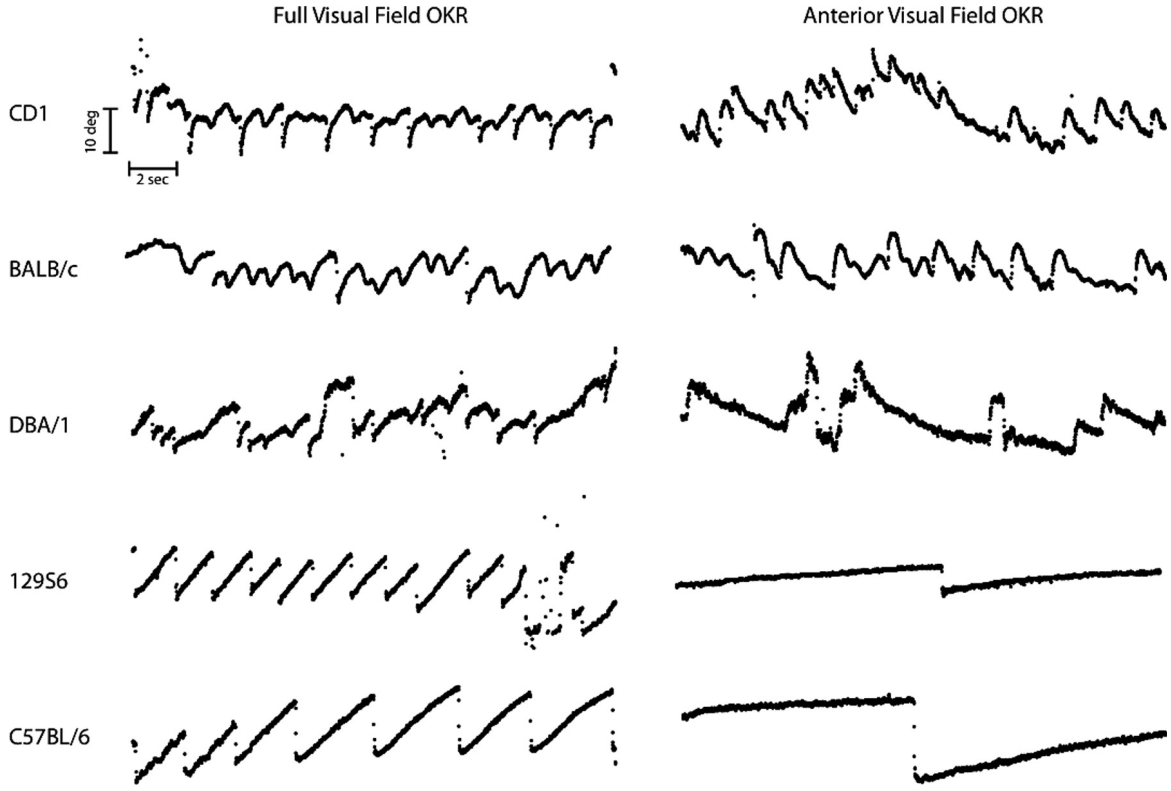

Figure 4.2 Optokinetic response. An OKS (direction: nasal to temporal with respect to the recorded right eye; velocity: 6.1 ˚/s; spatial frequency: 0.17 cyc/˚; contrast: 100%) was presented to the fVF (left column) or the aVF (right column). Eye movements were recorded from right eyes of the five mouse strains and presented as horizontal pupil position (y-axis) over time (x-axis). A lower position on the y-axis indicates a more nasal pupil position, whereas a higher position on the y-axis indicates a more temporal pupil position. Scaling is identical for all traces shown and indicated for CD1 after stimulation of the fVF. With a fVF OKS, the slow phase followed the direction of the rotating grating in all strains. Albino strains showed some superimposed oscillations. aVF stimulation resulted in reversal of the OKR in albino mice (i.e., the slow phase direction was opposite to the stimulus direction). In pigmented mice, the OKR was reduced with VF restriction, but the direction remained unchanged. Representative recordings of single mice are shown. Note, that in albino mice the degree of the nystagmus and the waveforms varied considerably over time.

Data Analysis

The horizontal pixel position (512 × 256 pixel matrix) of the corneal marker or pupil was transformed into a velocity signal by taking the first derivative (MATLAB; The MathWorks, Natick, MA). Measurement of the eye lid width (distance from medial to lateral canthus) in pixels on the screen and in millimetres in vivo (3.3–3.7 mm, depending on the strain) as well as assumption of an eye radius of 1.67 mm (Chalupa & Williams, 2008; Remtulla & Hallett, 1985; Schmucker & Schaeffel, 2004; Shupe, Kristan, Austad, & Stenkamp, 2006) allowed calibration of the system and calculation of velocities by a trigonometric function. Outliers with a change of greater than or equal to 0.5°

between two recorded pixel positions (0.008 second interval at 120 Hz) were filtered applying a customized MATLAB function, and the remaining curve was smoothed with a Gaussian filter (low pass cut-off of 2.5 Hz).

Recordings of 10 seconds duration were selected for quantitative analysis. The strongest responses with the least noise or blinking artefacts were chosen. Slow phase velocities in response to different visual stimuli were computed by ranking eye velocities of a single recording and calculating the median. This allowed computation of slow phase velocities without explicitly removing fast phases/saccades, which are not easily recognized in oscillating eye movements. Median eye velocities (MEV) in response to non-moving visual stimuli were calculated as absolute values (statistical analysis on logarithmic data), whereas MEV in response to optokinetic visual stimuli were calculated in real numbers in order to preserve the information on slow phase direction. Eye movements in tn direction were assigned a negative value, eye movements in nt direction were assigned a positive value. OKR velocities of both directions were subtracted from each other ([−MEV] − [+MEV]) resulting in a sum of the responses in both OKR directions. They were, thus, analysed in one statistical test that was based on repeated measure ANOVA. Strain was the between-subject contrast, VF and visual stimulus were the within-subject contrasts. Differences between strains were analysed by post hoc analysis with Bonferroni correction. All effects were considered as significant at P less than or equal to 0.05. Additional paired t-tests (level of significance adjusted for multiple testing) allowed comparisons of ocular motor responses to different visual stimuli within one strain. Significant t-test results are highlighted by asterisks (*) in the figures.

Results

VF ($p < 0.001$) and strain ($p < 0.001$) significantly influenced MEV and slow phase direction in OKR.

In the fVF situation, all strains had a slow phase direction following the direction of the OKS. Pigmented mice had smooth slow phases between fast phases, whereas albino strains showed oscillating slow phases, making it difficult to discern the slow phase direction. However, the slow

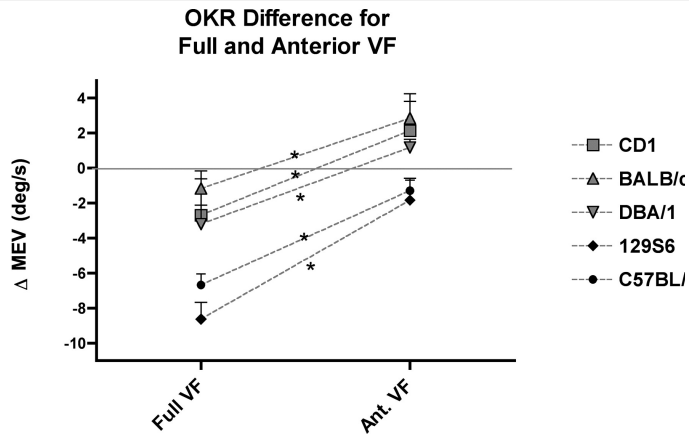

*Figure 4.3 Optokinetic response. The difference of the OKR MEV (Δ MEV) between tn direction (assigned a negative value) and nt direction (assigned a positive value) was calculated and plotted (mean ± SD; N = 5–6 per strain) for fVF and aVF stimulation. All strains had a significantly changing OKR response with VF restriction (*P ≤ 0.05). Note that Δ MEVs in albino strains were negative for fVF stimulation and positive for aVF stimulation indicating a reversal of the OKR direction after presentation of the stimulus to the aVF.*

phase direction can be deduced from the more easily recognizable fast phase direction (Figure 4.2). Albino mice had a significantly lower MEV as compared with pigmented mice when the moving stimulus was presented to the fVF (Figure 4.3, Table 4.1; univariate analysis, $p < 0.001$). Accordingly, their calculated mean gain values defined as slow phase velocity divided by stimulus velocity were only 0.1 to 0.4 [CD1: 0.4 ± 0.1 (tn direction) and 0.1 ± 0.2 (nt direction); BALB/c: 0.1 ± 0.1 (both tn and nt); DBA/1: 0.3 ± 0.2 (tn) and 0.2 ± 0.03 (nt)], whereas pigmented strains reached gain values of 0.5 to 0.7 [129S6: 0.7 ± 0.1 (both tn and nt); C57BL/6: 0.6 ± 0.03 (tn) and 0.5 ± 0.1 (nt)]. The reason for the strongly asymmetric OKR response in CD1 mice is not clear and might warrant further investigation.

When the OKS was restricted to the aVF, all albino mice showed a significant change in their MEVs and a reversed OKR (i.e., an inversion of the slow phase direction). In contrast, pigmented mice showed only a reduction of MEV, but no change of direction (Figures 4.2, 4.3, Table 4.1; univariate analysis, $p < 0.001$). As mentioned before, slow phase direction can be deduced from the more easily

Table 4.1. Median Eye Velocity of the Optokinetic Response

Strain (*n*)	OKStn (fVF)	OKSnt (fVF)	ΔMEV (fVF)	OKStn (aVF)	OKSnt (aVF)	ΔMEV (aVF)
CD1 (6)	–2.2 ± 0.8	0.5 ± 1.3	–2.7 ± 2.1	0.7 ± 0.4	–1.4 ± 1.9	2.1 ± 2.1
BALB/c (6)	–0.5 ± 0.5	0.7 ± 0.8	–1.2 ± 1.0	1.7 ± 0.7	–1.2 ± 0.5	2.8 ± 1.0
DBA/1 (5)	–1.9 ± 1.0	1.3 ± 0.2	–3.2 ± 1.1	0.3 ± 0.1	–0.9 ± 0.4	1.2 ± 0.5
129S6 (6)	–4.1 ± 0.6	4.5 ± 0.4	–8.6 ± 1.0	–1.2 ± 1.1	0.6 ± 0.3	–1.8 ± 1.3
C57BL/6 (6)	–3.4 ± 0.2	3.3 ± 0.8	–6.7 ± 0.6	–0.8 ± 0.7	0.5 ± 0.3	–1.3 ± 0.6
Statistics			$p < 0.001$			$p < 0.001$

MEV (˚/s; mean ± SD; *N* = 5–6 per strain as indicated) of the OKR to an OKS in the fVF or aVF moving in a tn or nt direction. ΔMEV corresponds to the difference between the MEV in the two directions [ΔMEV = MEV(OKStn) − MEV(OKSnt)]. Statistical analysis is based on the latter. Univariate analysis indicated significant MEV differences between strains. MEV of all albino strains were significantly different from MEV of pigmented strains (post hoc analysis).

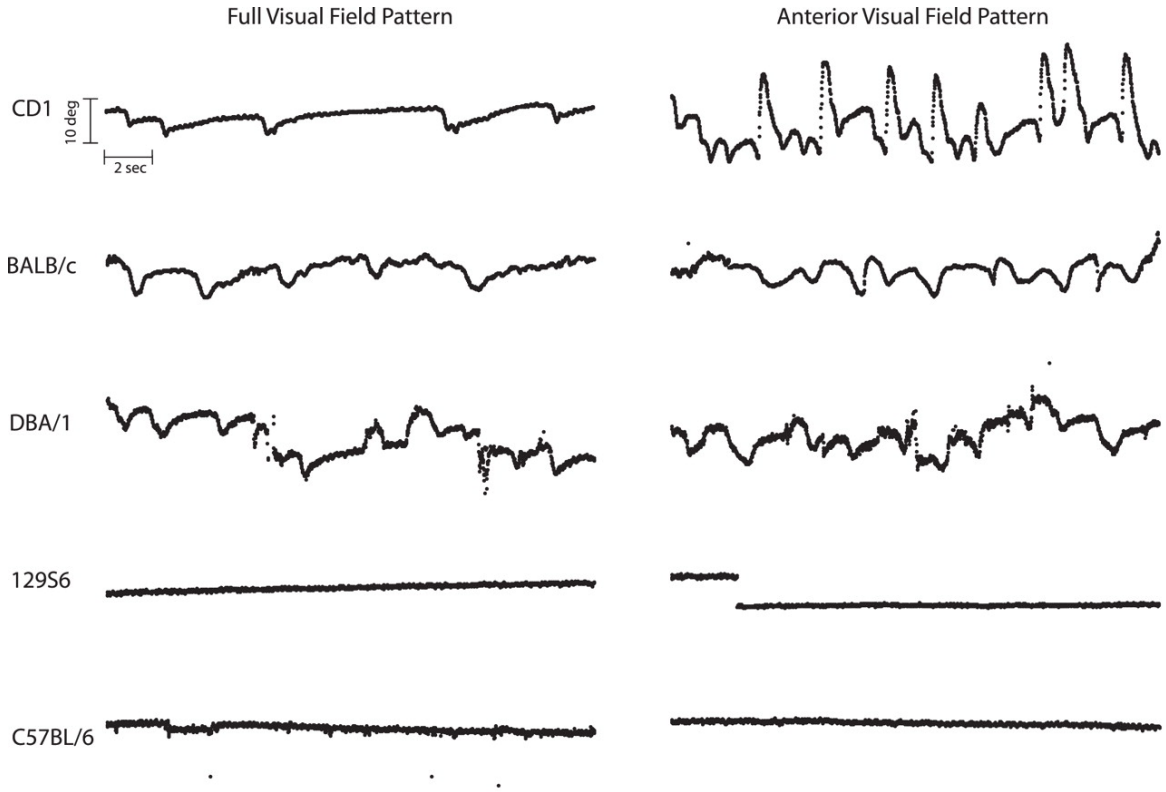

Figure 4.4 Spontaneous eye movements. A stationary pattern stimulus (spatial frequency: 0.17 cyc/°; contrast: 100%) was presented to the fVF (left column) or the aVF (right column). Spontaneous eye movements were recorded from right eyes of the five mouse strains and presented as horizontal pupil position (y-axis) over time (x-axis). A lower position on the y-axis indicates a more nasal pupil position whereas a higher position on the y-axis indicates a more temporal pupil position. Scaling is identical for all traces as shown and indicated for CD1 after stimulation of the fVF. With a pattern stimulus, albino mice showed vigorous spontaneous oscillations, which further increased with VF restriction. In pigmented mice, only slowly drifting eye movements were present for both fVF and aVF stimulation.

recognizable fast phase direction by visual inspection. Looking at the traces in Figure 4.2, interpretation of slow phase reversal in albino strains with VF restriction still seems challenging. However, slow phase reversal could be confirmed quantitatively. Figure 4.3 summarizes the OKR responses to both directions in the fVF situation (left side of the graph) and the aVF situation (right side of the graph). To allow inclusion of both OKR directions within one graph and, more importantly, within one statistical analysis, the MEV responses to both directions were combined to one ΔMEV value per strain. Individual MEVs and the ΔMEV for each strain and stimulus are given in Table 4.1. MEV values of the second column (OKSnt, fVF) were subtracted from MEV values of the first column (OKStn, fVF), resulting in a negative ΔMEV for all strains, which is represented in the third column (ΔMEV, fVF) and in Figure 4.3 (left side). In the aVF situation, albino mice had an inversion of the slow phase direction (in both tested stimulus directions). Thus, the algebraic signs of the MEV in the fourth (OKStn, aVF) and fifth column (OKSnt, aVF) are opposite between pigmented

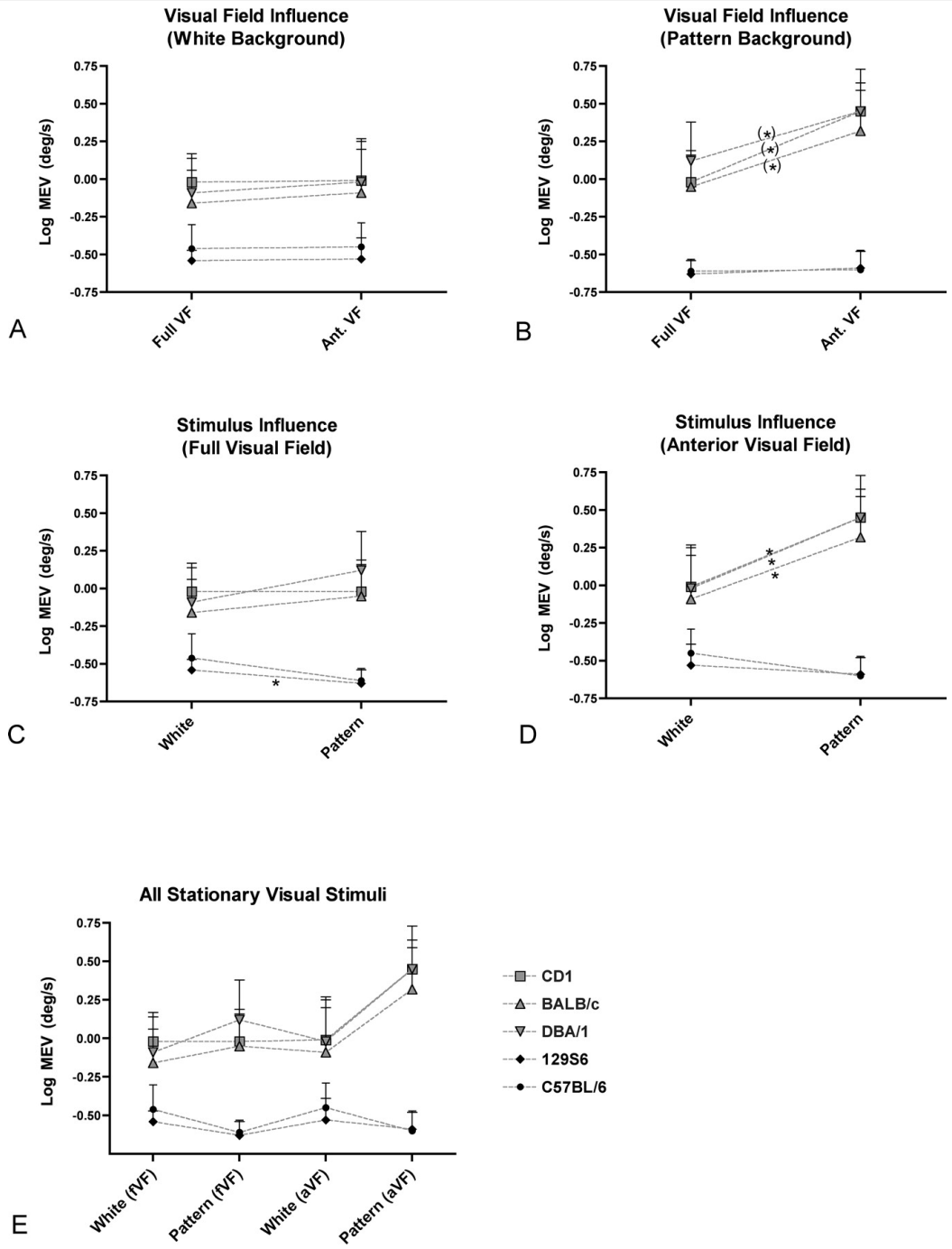

Figure 4.5 Spontaneous eye movements. Logarithmic MEV (mean ± SD; N = 5–6 per strain) of spontaneous eye movements with varying stationary visual stimuli in the fVF or aVF. Asterisks (*) indicate significant MEV changes within one strain. (A) VF restriction of an unstructured white background induced no significant change in MEVs. (B) VF restriction of a structured background induced a higher ocular motor instability in albino mice (VF dependency of ocular motor stability). However, significance was lost with correction for multiple testing, indicated with asterisks in brackets (0.05 ≥ P ≥ 0.0125). In pigmented mice, VF restriction had no effect on ocular motor stability. (C) The 129S6 strain showed a significant MEV reduction with a pattern stimulus in the aVF as compared with a white background stimulus (stabilizing effect of a structured background). (D) In albino mice, ocular motor instability significantly (P ≤ 0.0125) increased with pattern stimulation of the aVF (destabilizing effect). The stabilizing effect of the pattern was non-significant in pigmented mice. (E) Albino strains had significantly higher MEVs under all experimental conditions.

when subtracting the fifth column from the fourth column. This is represented in the sixth column (ΔMEV, aVF) and in Figure 4.3 (right side).

For both the fVF and restricted VF situation, no significant differences of the OKR response were recorded between strains within the albino or within the pigmented group.

Table 4.2 Median Eye Velocity of Spontaneous Eye Movements

Strain (*n*)	White (fVF)	Pattern (fVF)	White (aVF)	Pattern (aVF)
CD1 (6)	1.0 ± 0.4	1.0 ± 0.4	1.2 ± 1.1	3.4 ± 2.4
BALB/c (6)	0.8 ± 0.4	1.0 ± 0.6	1.1 ± 1.3	2.6 ± 1.6
DBA/1 (5)	0.9 ± 0.6	1.5 ± 1.1	1.1 ± 0.5	2.9 ± 0.9
129S6 (6)	0.3 ± 0.0	0.2 ± 0.0	0.3 ± 0.1	0.3 ± 0.1
C57BL/6 (6)	0.4 ± 0.1	0.2 ± 0.0	0.4 ± 0.2	0.3 ± 0.1
Statistics	$p < 0.001$ (BALB/c − BL/6: ns)	$p < 0.001$	$p = 0.001$ (BALB/c − BL/6: ns) (DBA/1 − BL/6: ns)	$p < 0.001$

Median eye velocities MEV (deg/s; mean ± SD; N = 5–6 per strain as indicated) of spontaneous eye movements for varying stationary visual stimuli in the fVF or aVF. Univariate analysis indicated significant MEV differences between strains. Apart from the exceptions mentioned in the table (ns = non-significant), MEV of all albino strains were significantly different from MEV in pigmented strains (post hoc analysis).

Stationary visual stimuli (uniformly white or sine gratings) were used to record spontaneous eye movements. Here, VF ($p < 0.003$), visual stimulus ($p < 0.001$), and strain ($p < 0.001$) had a significant effect on MEV (Figures 4.4, 4.5, Table 4.2). In addition, the data revealed a significant interaction between visual stimulus and strain ($p < 0.001$) indicating strain specific differences of the ocular motor response to stimulus changes.

Generally, albino mice had significantly higher MEVs (or greater ocular motor instability) compared with pigmented mice under stationary experimental conditions (Figures 4.4, 4.5, Table 4.2) except for the following: with a white background, the difference in MEV between C57BL/6 and BALB/c in the full field situation, and between C57BL/6 and BALB/c or DBA/1 in the restricted field situation were not significant (Table 4.2).

To analyse the influence of a VF change on ocular motor stability, the MEV in response to visual stimuli in the fVF and the aVF were compared. Whereas eye velocities did not change in any strain when a white stimulus was presented (Figure 4.5A), ocular motor instability significantly increased in albino strains in response to a pattern background when the VF was restricted ($p < 0.001$ with

significant interaction of VF and strain, $p < 0.001$) (Figure 4.5B). In individual strains, the changing ocular motor response with regard to pattern stimulation in the fVF and aVF was further analysed using paired t-tests with correction of the significance level for multiple testing (four t-tests per strain, i.e., one t-test per panel A–D in Figure 4.4). As a consequence of this correction, only a P value of greater than or equal to 0.0125 (0.05/4) could be considered significant. This 4-fold reduction of the significance level resulted in loss of significance of the observed VF influence in albino strains.

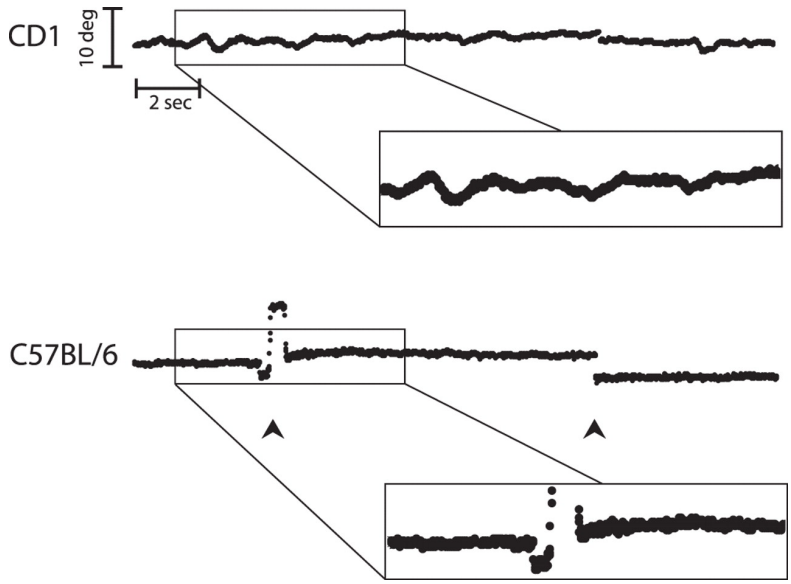

Figure 4.6 Spontaneous eye movements in the dark. Spontaneous eye movements were recorded from right eyes and presented as horizontal pupil position (y-axis) over time (x-axis). A lower position on the y-axis indicates a more nasal pupil position, whereas a higher position on the y-axis indicates a more temporal pupil position. Scaling is identical for both strains and as indicated for CD1. For better comparison with other stimulus conditions, scaling is identical for Figures 4.2, 4.4, and 4.6. Albino mice had subtle spontaneous oscillations in the dark indicating that the efferent visual system might be involved in the pathogenesis of spontaneous nystagmus as well. Pigmented mice seemed to have stable eye positions apart from occasional spontaneous saccades (arrowheads). Zoomed insets show those subtle spontaneous oscillations in a CD1 mouse as compared with stable eye positions with a saccade in a C57BL/6 mouse at higher resolution. Since physiologic pupil dilation in darkness generally caused increased background noise during pupil tracking, results for the three pupil tracked strains (DBA/1, 129S6, C57BL/6) were generally unreliable for statistic evaluation. An exceptionally good recording of a C57BL/6 mouse is shown as an example.

To analyse stimulus dependency of the ocular motor stability, MEVs in response to a white background were compared with a pattern background in the same VF (Figure 4.5CD). In albino mice, MEV and, thus, ocular motor instability tended to increase with the addition of a pattern to the background, while in pigmented mice, MEV remained stable or even decreased. The effect of the stimulus on the ocular motor response in albino mice reached statistical significance only in the restricted VF situation (Figure 4.5D; $p < 0.001$; with significant interaction of stimulus and strain, $p < 0.001$). This interaction and the destabilising effect of a stationary pattern in the aVF were confirmed in albino mice using paired t-tests ($P \leq 0.0125$). Our results suggested an opposite, stabilising effect of the pattern stimulus in pigmented strains. However, this was only

significant for the 129S6 strain in the fVF situation (Figure 4.5C). A summary of the MEVs for all strains in response to all stationary stimuli is given in Figure 4.5E.

To determine whether spontaneous nystagmus depends on visual input, we measured eye movements in darkness. With projection of a black background, albino mice had subtle spontaneous oscillations, whereas pigmented mice seemed to have stable eye positions apart from occasional saccades (arrowheads, Figure 4.6). However, these measurements were not included in the analysis because the physiologic pupil dilation in darkness created too much noise for pupil tracking and resulted in unreliable data in the three pupil tracked strains (DBA/1, 129S6, C57BL/6). An exceptionally good recording of a C57BL/6 mouse is shown in Figure 4.6.

Discussion

Melanin synthesis disorders, such as oculocutaneous albinism, predispose to visual system abnormalities affecting the retina (foveal hypoplasia; Elschnig, 1913; Kelly & Weiss, 2006; Naumann, Lerche, & Schroeder, 1976) and retinofugal projections (Creel, Witkop, & King, 1974; Guillery, Okoro, & Witkop, 1975; Hoffmann, Lorenz, Morland, & Schmidtborn, 2005; Morland, Hoffmann, Neveu, & Holder, 2002; Pott, Jansonius, & Kooijman, 2003; Schmitz, Krick, & Käsmann-Kellner, 2007; von dem Hagen, Hoffmann, & Morland, 2008; von dem Hagen, Houston, Hoffmann, & Morland, 2007), which lead to reduced visual acuity, loss of binocular vision, and INS in humans (Oetting & King, 1999). Melanin is mainly expressed in melanocytes (skin, iris, choroid) and in the retinal pigment epithelium (RPE; Ray, Chaki, & Sengupta, 2007). Reduced melanin content in the RPE of albinotic mice was correlated to a roughly 30% reduction in the number of rod photoreceptors (Jeffery, Brem, & Montoliu, 1997), to a prolonged cell cycle of RGCs in rats during neurogenesis (Ilia & Jeffery, 1996), to an underdeveloped central retina in several mammals (Donatien, Aigner, & Jeffery, 2002; Guillery et al., 1984; Jeffery & Kinsella, 1992; Stone, Rowe, & Campion, 1978), and to a reduction of uncrossed retinofugal projections in mouse (G W Balkema, Pinto, Dräger, & Vanable, 1981; Grant W. Balkema & Dräger, 1990; Dräger, 1974; Dräger & Olsen, 1980; Guillery, Scott, Cattanach, & Deol, 1973; Jeffery, Schütz, & Montoliu, 1994; Lavado, Jeffery, Tovar, Villa, & Montoliu, 2006; Lavail, Nixon, & Sidman, 1978; Pak et al., 1987; Rice, Williams, & Goldowitz, 1995), rat (Giolli & Creel, 1974; Lund, 1965), rabbit (Sanderson, 1975), cat (Guillery, 1969), ferret (Cucchiaro & Guillery, 1984; Guillery, 1971), and tiger (Guillery & Kaas, 1973). The percentage of ipsilateral projections in BALB/c and CD1 mice has been quantified to 1.8% as compared with the normal 2.8% in BL/6 mice (Rice et al., 1995).

CD1 and BALB/c mice carry a missense mutation in Tyr (tyrosinase), which leads to a cysteine to serine exchange at position 103 of the protein [TYR, C103S, c (albino) locus (Yokoyama et al., 1990)],

a key enzyme in melanin synthesis. 33 DBA/1 mice express a mutant form of the tyrosinase associated protein (TYRP1b) involved in a downstream enzymatic step during melanin synthesis (Jiménez-Cervantes et al., 1994) and in stabilisation of the tyrosinase (Kobayashi et al., 1994). The functional connection of these two proteins may explain the similarities we found in the ocular motor phenotype among the three albino mouse strains.

While recordings were straightforward in pigmented strains, especially in 129S6, data acquisition was much more challenging in albino strains due to eventual loss of the corneal marker, on the one hand, and behavioural differences with increased agitation of the albino mice on the other hand. Nevertheless, recordings finally resulted in analysable data for all animals. The fraction of usable data per session in pigmented mice was approximately 90%, while it was only approximately 40% in the albino strains, which generally had longer sessions and more session break offs. Alertness was difficult to judge in all five strains. Still, we are confident that the results reflect the response to the different testing paradigms, since our findings were consistent among the individual mice of a particular strain.

Assuming that spontaneous oscillations are related to the anomalous optokinetic performance in albino mice, OKR results will be discussed first, followed by discussion of spontaneous oscillations.

Optokinetic Response

Pigmented strains had a robust OKR to a fVF stimulus. The significantly weakened OKR in response to a restricted VF stimulus (anterior field) is in line with earlier findings (Mangini, Vanable, Williams, & Pinto, 1985; Shimizu et al., 2010). Despite superimposed oscillations increasing the calculated velocity signal, the median OKR velocities of albino mice were significantly lower during fVF stimulation as compared with pigmented mice. This may point either to an afferent or efferent visual system dysfunction (Optican & Zee, 1984), or to a combination of both. The visual gain might be reduced due to an altered retinal anatomy affecting visual acuity or due to the projection error inducing a conflicting visual input (Collewijn, Winterson, & Dubois, 1978). On the other hand, a miscalibrated efferent ocular motor system itself might limit the ocular motor response as well (Jacobs & Dell'Osso, 2004).

When albino mice were presented with an OKS in the aVF only, the OKR response was reversed as it has been reported earlier (Mangini et al., 1985). OKR data reported by Mangini et al., as well as our own OKR data, were tested at a stimulus velocity of 6.0 ˚/s and 6.1 ˚/s, respectively. Reversal of the OKR might, however, depend on stimulus velocity. This possible velocity relationship on the OKR response might warrant further investigation. In contrast to Mangini and co-workers (Mangini et al., 1985), we additionally detected a clear OKR in response to a stimulus in the fVF in a majority of

albino mice (Figures 4.2, 4.3), and report spontaneous oscillations (Figures 4.4, 4.5) in these mice. Since Mangini manually analysed videotaped eye recordings, the sensitivity of the system may not have been sufficient to reliably discover these movements. The automated eye tracking system used here might provide superior sensitivity and allow better quantification of oscillations.

The reversed OKR response may be based on the projection error in albinos (Collewijn et al., 1978), resulting in destabilising positive feedback in response to retinal slip. This hypothesis is supported by mathematical models (Huang, Rinner, Hedinger, Liu, & Neuhauss, 2006; Optican & Zee, 1984) and by recent experimental findings in belladonna (bel) zebrafish mutants, which display a reversed OKR that perfectly correlates with purely ipsilateral retinotectal projections, instead of the normal complete crossing of RGCs in wild type zebrafish (Huang et al., 2006; Rick, Horschke, & Neuhauss, 2000; Huang, Chen, Huber-Reggi, Neuhauss, & Straumann, 2011).

Due to differing views on eye movement analysis, Jacobs and Dell'Osso (2004)doubt the true nature of reversed OKR. Nevertheless, it has been described by several authors (Collewijn, Apkarian, & Spekreijse, 1985; Halmagyi et al., 1980; Mehdorn & Schade, 1988; St John, Fisk, Timney, & Goodale, 1984). Even though it is not present in all patients with INS, reversed OKR is considered a common pathognomonic finding in INS (Thurtell & Leigh, 2011). Except for one study (Collewijn et al., 1985), reversed OKR was mainly investigated with fVF stimulation (Halmagyi et al., 1980; Mehdorn & Schade, 1988; St John et al., 1984). Collewijn et al. (1985) additionally analysed the OKR response with VF restriction (to the temporal or nasal VF) in subjects with OKR inversion, but did not find any influence of the VF on the OKR response. These findings in humans contrast with our own OKR data in albino mice. Mice normally have 2.8% ipsilateral retinofugal projections 45 compared with 47% ipsilateral projections in humans (Kline, Arnold, & Eggenberger, 2008). Since mice have a rather small amount of normal ipsilateral projections, the misrouted fibres in albino mice only represent a very small proportion of the total projections. This might explain the fact that specific stimulation of the temporal retina is necessary to induce reversed OKR in mice.

Spontaneous Oscillations

Spontaneous oscillations have been analysed in the albino rabbit (Collewijn et al., 1978). They have also been observed in the albino mouse (G W Balkema, Mangini, Pinto, & Vanable, 1984) and the albino rat (Kolpakov, Alekhina, Barykina, Chugui, & Popova, 2001; Sirkin, Hess, & Precht, 1985); however, such oscillations have not been properly investigated in rodents.

Here, we present data clearly showing spontaneous nystagmus, specifically jerks and oscillations, in three albino mouse strains. In contrast, ocular positions were nearly stable in pigmented mice. Spontaneous MEVs were significantly greater in albino mice and showed a significant stimulus

dependency for ocular motor instability in the aVF. The fact that MEV markedly increased with a pattern background compared with a white background supports the positive feedback hypothesis in albinos, since spontaneous eye movements induce retinal slip in a structured environment, whereas in a uniform environment they do not. Conversely, the negative feedback system of pigmented mice seemed to induce a stabilisation of gaze, which was, however, only significant in one strain (129S6, fVF stimulation). There was a trend for VF dependency of ocular motor stability in albino strains (with pattern background). This might reach significance with the analysis of more animals per group and could be explained by the projection error of the corresponding retina. There was no indication of a similar effect of VF restriction in pigmented mice. The increasingly slow phase velocity of jerk waveforms was not a predominant feature in our albino mice, which might also relate to the fact that mice are afoveate species. In sum, our data support the idea of a dominant problem in the afferent pathways in the context of INS. However, the fact that spontaneous nystagmus was also detected in darkness, albeit with a smaller amplitude (Figure 4.6), may implicate the efferent visual system in the pathogenesis of INS as well, possibly as a result of central motor adaptation to the aberrant visual input.

The effect of ocular motor instability on visual performance may be tested in behavioural studies. Strong differences have been reported for albino mice in such tests (Puk, Dalke, Hrabé de Angelis, & Graw, 2008; Redfern et al., 2011; Wong & Brown, 2006), with BALB/c mice generally performing poorly. However, our results suggest that even BALB/c mice do have considerable vision, and, like CD1 and DBA/1 mice, react to stimuli in a consistent, albeit abnormal way. Variable performances in behavioural vision tests have also been reported in DBA/2J mice (Barabas et al., 2011; Puk et al., 2008; Rangarajan et al., 2011; Wong & Brown, 2006), a commonly used glaucoma mouse model. DBA/2J mice carry a digenic mutation in Tyrp1b and Gpnmb (Glycoprotein nonmetastatic melanoma protein B) causing pigmentary dispersion syndrome and pigmentary glaucoma leading to RGC degeneration (M. G. Anderson et al., 2002; Lu et al., 2011). When interpreting optomotor test results, it has to be kept in mind that the Tyrp1b mutation might influence ocular motor phenotype in the same way as it likely influences the investigated DBA/1 strain. Hence, more detailed studies are needed to quantify the visual capacities of this strain and how they are affected by nystagmus.

Current hypotheses on the etiology of INS include structural defects (i.e., misprojection 65) motor defects (Dell'Osso, 2006), impaired sensorimotor integration (Harris & Berry, 2006), and miscalibration of the visual system during development due to sensory disorders (J. R. Anderson, 1953; Jacobs & Dell'Osso, 2004).Interestingly, dark rearing has been shown to affect ocular motor function (reduced gain) in mice, suggesting that visual input might be needed for normal development of the ocular motor system (McMullen, Andrade, & Stahl, 2004).

Recently, mutations in the FERM domain containing 7 (FRMD7) gene have been identified in X-linked INS (Tarpey et al., 2006; Watkins, Thomas, Talbot, Gottlob, & Shackleton, 2012), which offers a completely new approach to INS related research. The function of FRMD7 is still unclear, but seems related to neuronal development (Betts-Henderson et al., 2010; Tarpey et al., 2006).

Still, mechanisms underlying INS remain incompletely understood, partly due to the absence of an easily accessible and established mammalian animal model. Although INS has already been reported in the achiasmatic mutant Belgian sheepdog (Dell'Osso & Williams, 1995; Dell'Osso, Williams, Jacobs, & Erchul, 1998), and RPE65-deficient canines (Acland et al., 2001), investigations in these animals are limited due to high costs and the unfeasibility of high throughput experiments. Other proposed animal models appeared to have induced latent (M X Repka & Tusa, 1995; Tusa, Mustari, Das, & Boothe, 2002), or acquired nystagmus (Waespe, Cohen, & Raphan, 1985), which may not be comparable to INS. More recently, the achiasmatic zebrafish belladonna mutant, a teleost, has been established as a valuable animal model for INS (Huang et al., 2011). Whereas the use of zebrafish has many advantages, like high throughput experiments and faster genetic manipulations, it seems necessary to establish a mammalian model for evaluation of generalizability of zebrafish data. Modern eye tracking systems now provide considerably enhanced research possibilities in the field (van Alphen et al., 2010; van der Geest & Frens, 2002b). Based on our results, we clearly demonstrate that albino mice show ocular motor abnormalities and spontaneous nystagmus. Thus, they could complement the zebrafish as a promising new mammalian model to study mechanisms of INS. As an intermediate species between the lower vertebrate zebrafish and humans, mice not only provide us with the power of mouse genetics, but also may enable us to investigate the role of the cortical visual pathways in INS, and to find a common mechanism for INS across species. In addition, mice might also provide the opportunity to test pharmacological approaches to developing non-invasive therapies for INS.

Acknowledgments

The authors thank Klara Landau, MD, David Margolis, PhD, Marijana Samardzija, PhD, Sarah Willcox, MD, Marco Penner, technician, and Konrad Weber, MD, for their contribution to this work.

Chapter 5 - Impairment of Long-Term Plasticity of Cerebellar Purkinje Cells Eliminates the Effect of Anodal Direct Current Stimulation on Vestibulo-Ocular Reflex Habituation[4]

Suman Das, Marcella Spoor, Tafadzwa M. Sibindi, Peter Holland, Martijn Schonewille, Chris de Zeeuw, Maarten A. Frens and Opher Donchin

Abstract

Anodal direct current stimulation (DCS) of the cerebellum facilitates adaptation tasks, but the mechanism underlying this effect is poorly understood. We have evaluated whether the effects of DCS effects depend on plasticity of cerebellar Purkinje cells (PCs). Here, we have successfully developed a mouse model of cerebellar DCS, allowing us to present the first demonstration of cerebellar DCS driven behavioural changes in rodents. We have utilized a simple gain down vestibulo-ocular reflex (VOR) adaptation paradigm that stabilizes a visual image on the retina during brief head movements, as behavioural tool. Our results provide evidence that anodal stimulation has an acute post-stimulation effect on baseline gain reduction of VOR (VOR gain in sham, anodal and cathodal groups are 0.75 ± 0.12, 0.68 ± 0.1, and 0.78 ± 0.05, respectively). Moreover, this anodal induced decrease in VOR gain is directly dependent on the PP2B medicated synaptic long-term potentiation (LTP) and intrinsic plasticity pathways of PCs.

Introduction

Transcranial direct current stimulation (tDCS) modulates cerebellar dependent motor learning tasks (Avila et al., 2015; Hardwick & Celnik, 2014; Herzfeld et al., 2014; Jayaram et al., 2012) by applying a weak constant electrical current (amplitude <2 mA) through scalp electrodes. This technique allows us to stimulate the target region by the positive (anodal) or negative (cathodal) current (Das, Holland, Frens, & Donchin, 2016). Data collected in humans suggests that polarity specific effects of tDCS may be obtained by changing cerebellar cortical excitability (Galea, Jayaram, Ajagbe, & Celnik, 2009). However, the mechanism behind tDCS dependent modulation of motor learning is unclear (Das et al., 2016). To optimally use tDCS in various cerebellar dependent motor learning disorders, a better understanding of mechanisms is vital (Bastian, 2011; Benussi, Koch, Cotelli, Padovani, & Borroni, 2015; Hardwick & Celnik, 2014; Ivry & Spencer, 2004; Xu-Wilson, Chen-Harris, Zee, & Shadmehr, 2009).

[4] Front. Neurosci. 11:444 (2017). doi: 10.3389/fnins.2017.00444

Various animal models of DCS (direct current stimulation that is not transcranial) serve in exploration of the mechanism of tDCS (Bindman, Lippold, & Redfearn, 1964; Creutzfeldt, Fromm, & Kapp, 1962; Purpura & McMurtry, 1965). In these models, a small part of the skull is removed at the site of stimulation in order to reduce the inter-subject variability of transcranial-conductance.

Our current study aims to explore the mechanism of action of DCS on cerebellar learning. To probe polarity specific effects of DCS on cerebellar learning, we employed a gain-down vestibulo-ocular reflex (VOR) adaptation task. The VOR aims to compensate for head movement by making an eye movement in the opposite direction, in order to stabilize the image on the retina (Probst, Brandt, & Degner, 1986). This compensatory eye movement can be adapted based on mismatched visual input, a process that requires the cerebellum (Kawato & Gomi, 1992). Here we presented a sinusoidal optokinetic stimulation by using a 360° virtual environment and vestibular stimulus by using a turntable in phase, resulting in a decrease of the response to the same vestibular stimulus in the dark (Tempia, Dieringer, & Strata, 1991). The turntable mimics the head movement while the movement direction of the virtual environment demands orientation specific compensation of the eye movement (similar to the natural environment).

The gain-down adaptation of the VOR (Tiliket, Shelhamer, Tan, & Zee, 1993) may depend partly on both the cerebellar flocculus and the downstream vestibular nuclei (VN; Ito, 1982; Lisberger & Fuchs, 1974). To test the importance of Purkinje cell (PC) plasticity in polarity-specific DCS modulation, we investigated L7-PP2B mice, lacking postsynaptic and intrinsic plasticity of PC (M. Schonewille et al., 2010). Our prediction is that at least some DCS effects (caused either by anodal or cathodal stimulation) would be compromised in this mutant because DCS has an extensive modulatory role on PC dendrites (Chan, Hounsgaard, & Nicholson, 1988; Chan & Nicholson, 1986).

A rodent model of DCS has been validated in cortical spreading depression (Liebetanz, Fregni, et al., 2006) and epilepsy (Liebetanz, Klinker, et al., 2006). Anodal stimulation of frontal cortex enhances the Blood-oxygen-level dependent (BOLD) signal, an indication of higher neuronal activity (Takano et al., 2011). Furthermore, DCS alters neocortical plasticity not only by altering pre-synaptic sensitivity (Marquez-Ruiz et al., 2012) but also by promoting brain-derived neurotrophic factor (BDNF) dependent long-term potentiation (LTP) (Fritsch et al., 2010). As the plasticity mechanisms of the cerebellar cortex are different from those in neocortex (Hansel, 2005; Lamont & Weber, 2012) there is ample justification for an animal model of cerebellar DCS. Moreover, the cerebellum is ideal to identify the mechanism(s) of DCS because—(i) the structure of rodent cerebellum is clear and accessible, (ii) the plasticity mechanisms are well studied, and (iii) there is a wide range of mutant mouse models available to test which pathways are functionally relevant (De Zeeuw et al., 2011).

Therefore, the present study focuses not only on developing an animal model of cerebellar DCS but also utilizes one of the most important mutant mouse models to unravel the role of PC plasticity in mediating DCS effects on VOR adaptation.

Methods

Summary of Methodology

C57BL/6 (wild type, N = 24) and L7-PP2B (LTP deficient mutants, N = 22) mice were implanted with a DCS-implant for administration of DCS over the cerebellum. DCS was applied to separate groups of mice as anodal, cathodal or sham-stimulation. Eye movements were recorded using an infrared-sensitive CCD camera during horizontal VOR gain-down adaptation learning. In testing sessions, the eye response to vestibular stimulation, i.e., the motion of the table, (amplitude of 5° at 1 Hz frequency) in the dark was recorded. In training sessions, vestibular and visual stimulation (amplitude of 5° at 1 Hz frequency) were coupled so as to cause reduction of the VOR gain. Two baseline test sessions were followed by 10 min of DC stimulation and then by an additional baseline test session. There were then 5 training sessions of 5 min each, each followed by a test session. We subsequently compared the reduction of VOR gain in the different stimulation groups and across strains.

Experimental Paradigm

Mice were habituated to the experimental apparatus for a minimum of 2 days to reduce the novelty-induced anxiety and restrain-stress after they recovered from the surgery.

Each experiment consisted of 8 test (T) and 5 training (Tr) sessions. The duration of each test session was 1 min, and the duration of each training session was 5 min. In test sessions, a sinusoidal vestibular stimulation which was generated by moving the table with a 5° amplitude at 1 Hz frequency, was applied in the dark. Eye movements were recorded simultaneously. In training

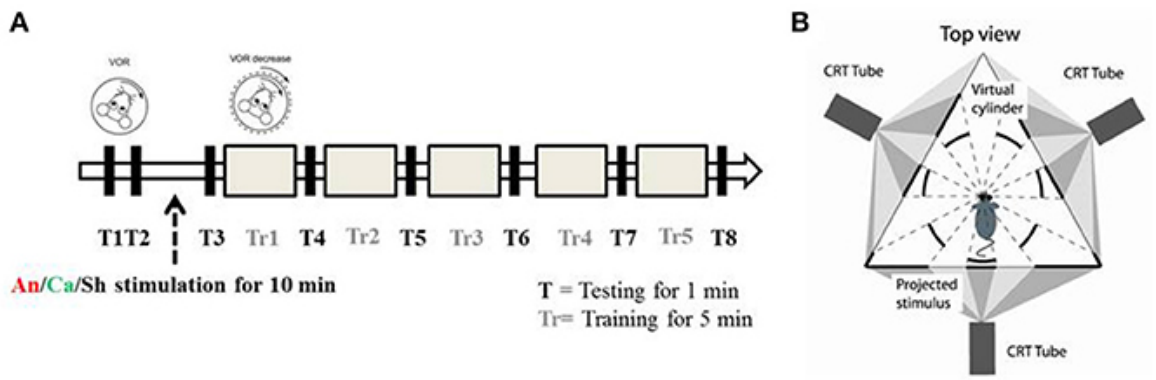

Figure 5.1. Experimental paradigm and set up (A) Schematic diagram of the experimental paradigm. T represents a testing session during which the animal is exposed to VOR in the dark by moving the turntable in a sinusoidal manner (5° amplitude at 1 Hz). Tr represents the training session during which the animal is presented with a sinusoidal visual cue which is in phase with the table movement. After two testing sessions (T1 and T2) the animals were randomly assigned to the anodal (An), cathodal (Ca) or sham (Sh) stimulation group. (B) Schematic diagram of the experimental apparatus. Top down view describes the position of the mouse in relation to the virtual environment created by three projectors.

sessions, in phase vestibular and optokinetic sinusoidal stimuli (5° amplitude at 1 Hz frequency) were given (Figure 5.1A), in order to reduce the VOR gain. Eye movements were continuously recorded.

Every experiment was initiated by two baseline measurements of VOR (T1 and T2). Then the mice were randomly divided into 3 groups, and received anodal, cathodal or sham DC stimulation. The current amplitude was ramped up over 30 s to 113.2 µA and kept constant for 10 min (positive polarity for the anodal group, negative polarity for the cathodal group). For the sham group, amplitude was then immediately ramped down (over 30 s) while for the anodal and cathodal groups current was maintained for 10 min of stimulation. After the stimulation, another session of testing (T3) was conducted and then gain-down adaptation learning training was initiated. A testing session was conducted to calculate the learning rate after every training session (Figure 5.1A).

Experimental Procedure

Animals

C57BL/6 (N = 24) mice were acquired from Charles River laboratories, Inc. (Wilmington, MA, USA). L7-PP2B mutants (N = 22) were bred in Erasmus MC, Rotterdam. Mouse lines used in this study have been described previously (Schonewille et al., 2010). Three to four mice were caged together in temperature-regulated (22 ± 1°C) housing with a 12:12 light-day cycle. Behavioural experiments were performed in the light cycle. Food and water was provided ad libitum. All experiments were reviewed and approved by the Erasmus animal ethics committee and conducted in accordance with Animal Welfare Committee of the Erasmus University and the European Communities Council Directive (86/609/EEC).

Surgery

Mice, aged 10–12 weeks, were handled for 2 days before the surgery to reduce the effect of handling-induced stress. The surgical procedure was performed under sterile conditions. Isoflurane (5% induction, 1.5% in 0.5 L/min O2, and 0.2 L/min air) was administered as an anaesthetic drug while body temperature was regulated around 36.5 ± 0.5° via a feedback-controlled heating pad. Breathing profile was continuously monitored. After shaving the head, a 1 cm long mid-sagittal incision was given. The bone was etched (37.5% phosphoric acid, Kerr, CA, USA) and a primer (Optibond, Kerr, CA, USA) was applied. To immobilize the animal during eye tracking, a pedestal containing two M1.4 nuts was glued to the skull using dental acrylic (Charisma, Flowline, Hereaus Kulzer GmBH, Germany).

In order to place a DCS implant, a circular craniectomy (approximately 2 mm in diameter) on the left occipital bone was performed after careful removal of the neck-muscles (vertical and horizontal) (Figure 5.2AB). The placement was on the centre of the left parietal bone (by keeping the superior cerebellar artery at the centre of the implant). A lubricating ointment (Duratears, Alcon Nederland BV, NL) was applied epidurally to protect the exposed area of brain from drying. The DCS implant (Figure 5.2C) was placed identically in all animals using an anatomical marker (Figure 5.2AB) and then glued to the skull using cyanoacrylate gel (Plastic One Inc., VA, USA).

The mice were given an analgesic (0.1 ml/mg of body weight Buprenorphine/Temgesic) and placed under an infrared heating lamp until the animals started to move. Mice were allowed at least 4–5 days to recover before recordings were performed.

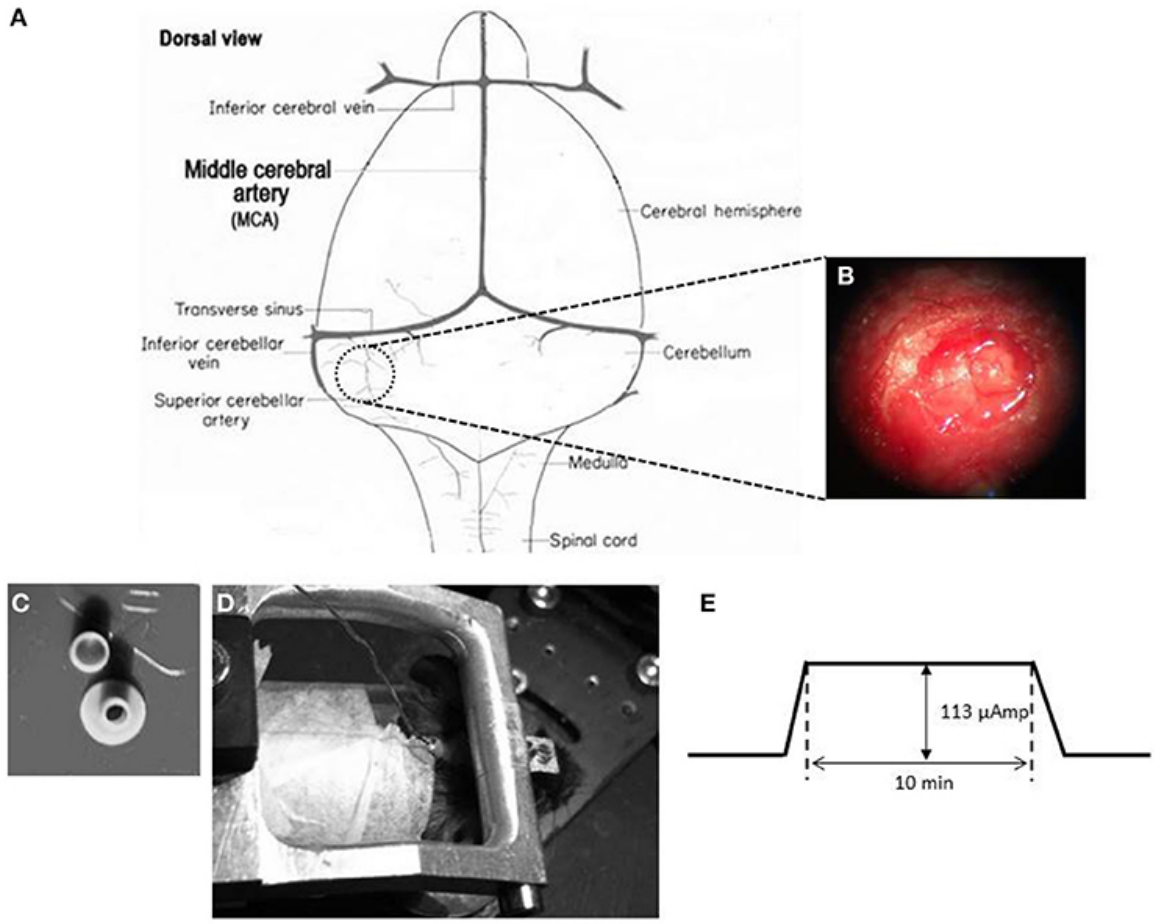

Figure 5.2. DCS location and procedure (A) Schematic representation of craniotomy for placement of implant over the cerebellum of a mouse brain. (B) Craniotomy. Anatomical location for the DCS-implant placement. (C) DCS implant. The DCS chamber serves as a bridge between the stimulating electrode and the brain. Above the chamber is the cap that serves to protect the brain from infection. (D) Stimulating the mouse cerebellum. The DCS chamber is filled with saline (0.9% NaCl) solution. A silver wire that touches the saline solution but not the dura directly is connected to the current generator (SUI-91, Isolated current source). During stimulation the mouse is awake but head restrained. (E) Stimulation paradigm. DCS is ramped up to 113 µAmp. The current is maintained at its peak value for 10 min. After the stimulation the current is ramped down.

Apparatus

Visual and Vestibular Stimulation

Mice were head-fixed in a restrainer, which was fixed onto the centre of a turntable, placed at the centre of an isolateral triangle made by three projector-screens. A panoramic virtual reality display with 360° field of view was created by projecting monochrome green dots on to those screens (Figure 5.1B). Horizontal rotation of the turntable was driven by a servomotor (Mavilor-DC motor 80, Infranor, Spain). Visual stimuli and movement of the turntable were under control of in-house software written in C++. Training and testing sessions were evoked by rotating the dots and/or the

turntable sinusoidally. During each session, stimuli were ramped up to their peak velocity in 5 s for a smooth transition from static to dynamic state. They were also ramped down at the end.

Eye Movement Recordings

Eye movements were recorded with an infrared video system (ETL-200 with marker tracking modifications; ISCAN, Burlington, MA). The camera and lens were mounted under the table surface to reduce hindrance of the mouse vision. A hot mirror which was transparent to visible light and reflective to infrared light was used. The eye was illuminated with three infrared LEDs. The camera, mirror and LEDs were all mounted on an arm that could rotate about the vertical axis over a range of 26.12° (peak to peak). Eye movement recordings and calibration procedures were similar to those described by Stahl et al. (J.S Stahl et al., 2000). Images of the eye were captured at 120 Hz with an infrared-sensitive CCD camera. The eye image contained a bright corneal reflection and a dark pupil reflection. The image was focused by manipulating the offset and the gain of the detectors through the ISCAN software. From this image, x and y positions of each of the three markers were recorded in real time giving their location on a 512 × 256-pixel grid, with a resolution of one-third pixel horizontally and one-tenth pixel vertically (van Alphen et al., 2010). These x and y translational positions of eye on the grid were converted into the angular rotation of the eyeball by the ISCAN system (resolution of 0.2° over a ±25° horizontal and ±20° vertical range using the pupil/corneal reflection difference). The horizontal and vertical pupil position data from the ISCAN were output as ±5 VDC signals. A delay of 30 ms in the eye movement signal was introduced by the video system. Furthermore, this output signal was low-pass filtered with a cut-off frequency of 300 Hz (Cyberamp 380; Axon Instruments, CA, USA), sampled at 1 kHz and stored for offline analysis.

Direct Current Stimulation

A low amplitude (113 µA) of continuous DCS was applied using a constant current stimulator (SUI-91, Isolated current source, Cygnus Technology Inc., NC, USA; range = 0.1 µA—10 mA). This intensity corresponded to a current density of 3.6 mA/cm^2 (Liebetanz et al., 2009). Currents were applied to the epidural surface of the cerebellar cortex through a circular DCS implant with a defined contact area (2 mm inner diameter). Prior to stimulation, the electrode was filled with saline solution (0.9% NaCl). A silver wire electrode connected to the stimulation device was attached to the DCS implant such that the tip of the silver wire touched the top level of the saline solution but did not touch the brain directly. This circular active electrode (Figure 5.2C) was chosen to create a symmetric current density without any edge effects (Ambrus, Antal, & Paulus, 2011). A disposable foam electrode (Kendall Medi-Trace mini resting ECG electrode, Davis medical products Inc., CA, USA), was placed onto the ventral thorax of the animal to complete the circuit. The entire circuit was connected through a multimeter to check online current amplitude. Mice were awake during DCS to prevent

possible interactions between DCS effects and anaesthetic drugs. In addition, mice were introduced to the adaptation task right after the stimulation to quantify acute effects of stimulation. To avoid stimulation break effects (Liebetanz et al., 2009), the current intensity was ramped up and down gradually over 30 s.

Data Analysis

Custom routines written in MATLAB (The MathWorks Inc., Natick, MA, USA) were designed and employed for automated offline data analysis. The position signal was shifted 30 ms back in time to correct for the camera delay. A median filter (width 50 ms) with a low-pass cut-off of 10 Hz was applied to smooth the position data before transforming to velocity domain by a Savitski-Golay differentiating filter (frequency 50 Hz with a 3° polynomial). Rapid eye movements were detected and removed via a velocity threshold (150°/s). Then a 3 Hz FIR Butterworth low pass filter of 50 ms width was applied.

The processed data was divided into non-overlapping epochs of 2 s (corresponding to two cycles of the stimulus). Amplitude data was obtained by fitting sine waves to the eye movement data in custom-made Matlab curve fitting routines using the least-squares method. Median amplitude values of the eye movement were calculated from the fitted sine waves. Gain was calculated for each testing session as the ratio between the fit eye velocity amplitude and stimulus velocity amplitude,

$$G_T = \frac{E_{Tn}}{S} \quad (1)$$

where E is the fitted eye amplitude of testing session n=1 through 8, and S is the stimulus amplitude.

Mice were excluded when the absolute difference between baseline gains (G_{T1}–G_{T2}) was > 0.2. The baseline gain (G_B) was set as the mean of gains in G_{T1} and G_{T2}. Normalized gain (G_N) was also calculated for every test session.

$$G_n = \frac{G_B - G}{G_B + G} \quad (2)$$

Statistical Analysis

Statistical analysis of the data was performed using SPSS 20.0 (SPSS, Chicago, IL). A three way mixed-ANOVA with repeated measures was used to compare interaction and group effects, as the data showed a normal distribution. Significance levels were set to 0.05. Later on, a Bonferroni corrected post-hoc analysis was applied to find intra-/inter-group interactions. Values are represented here as mean ± SEM.

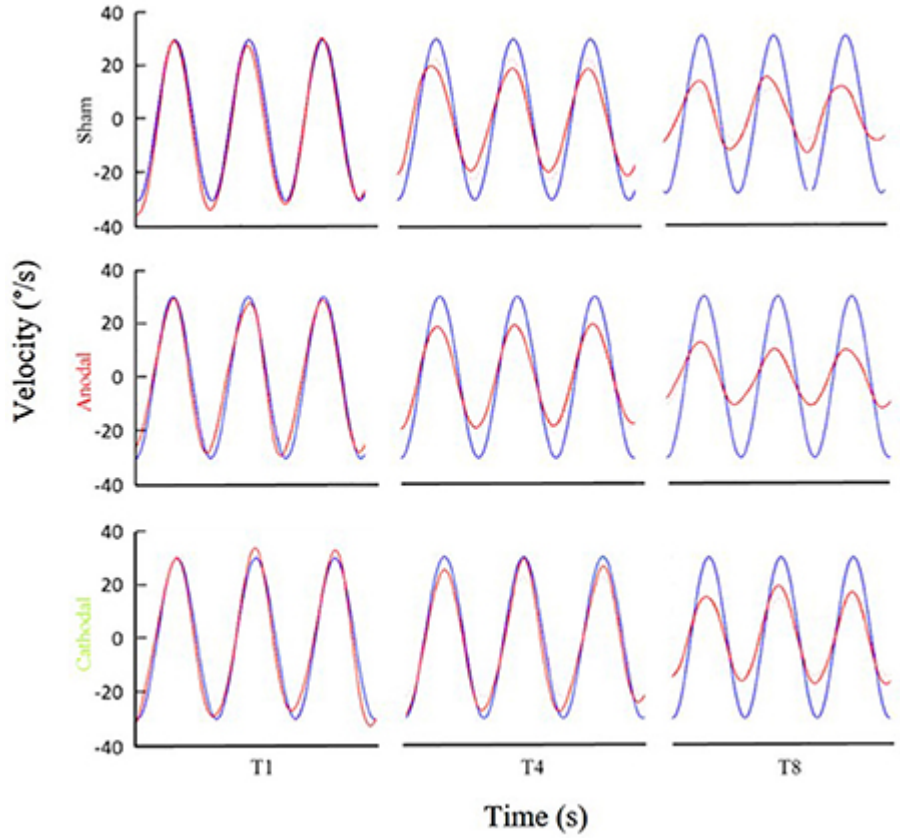

Figure 5.3. Examples of eye movement in different stimulation conditions. Examples of filtered eye velocity illustrate results from mice that exhibited a decrease in the VOR after training with sham (top panels), anodal (middle panels) and cathodal (bottom panels) stimulation. Blue is vestibular stimulus and red is eye amplitude (solid red line is filtered eye-velocity, dotted red line fitted sine wave). Eye-trace of each stimulus condition has been presented during pre-training (T1), after first-training (T4) and after final-training (T8) in the left, middle and right panels, respectively.

Results

Degree of Adaptation at the End of Training Session

The VOR gain-down adaptation paradigm caused a gradual reduction in VOR-amplitude in all mice (Figures 5.3–5.6). Initially, the amplitude of the eye movement was similar to the stimulus amplitude; i.e., the gain at T1 for C57BL/6 and L7-PP2B mice was 0.88 ± 0.03 and 1.03 ± 0.03, respectively (Figures 5.4, 5.6). The baseline VOR gain in L7-PP2B of more than 1 indicated that the eye amplitude overshot the head amplitude in these mice. After being subjected for 25 min to the gain-down training, the amplitude of VOR at T8 was reduced for both C57BL/6 (raw T8 gain = 0.33 ± 0.03) and L7-PP2B (raw T8 gain = 0.70 ± 0.03) group. In our multivariate ANOVA on the non-normalized data, the main effect of training over the time course was highly significant, F(7, 34) =

46.20, $p < 0.001$. However, comparison of the sham stimulation data showed that the degree of adaptation was significantly higher in C57BL/6 than L7-PP2B mice, $F(5, 40) = 14.94$, $p < 0.001$.

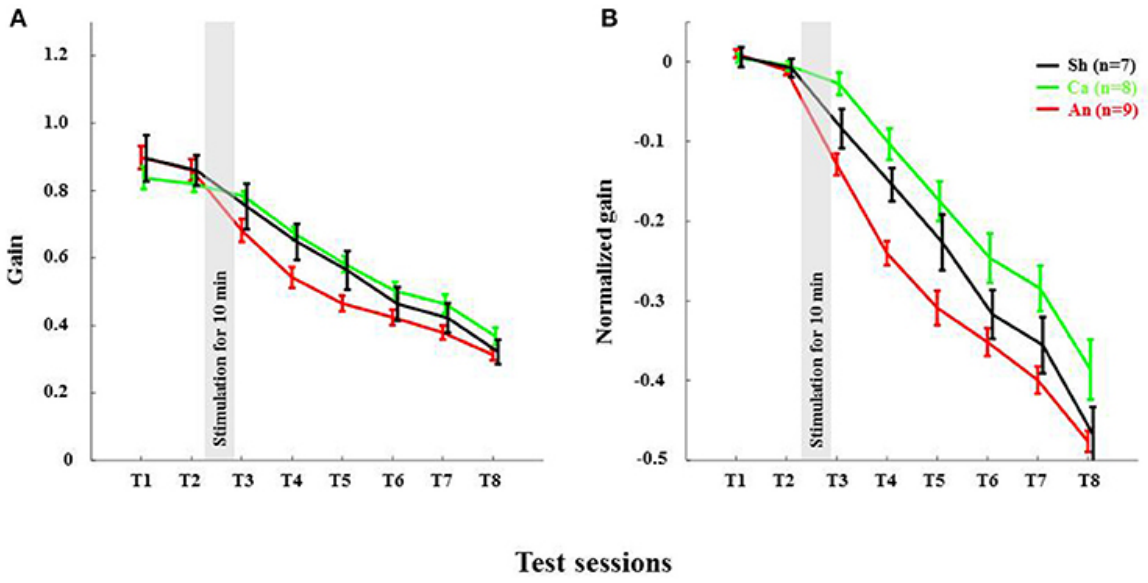

Figure 5.4. Anodal stimulation reduces VOR gain acutely in wild type C57BL/6 mice. (A) Time course of gain reduction due to adaptation: Changes in mean VOR gain during VOR-decrease training. The VOR was tested pre- and post-training by measuring the eye movement response to the vestibular stimulus. (B) Time course of normalized gain reduction due to adaptation: Trial-to-trial changes in mean normalized VOR gain during VOR-decrease training. Black, Green and Red lines are for sham, cathodal and anodal stimulation conditions, respectively. The gray bar indicates the stimulation period. Error bars represent SEM.

Reduction of Gain in C57BL/6 and L7-PP2B Mice

The reduction in gain made across the eight test sessions was strongly dependent upon the genetic composition of mice, $F(7, 38) = 4.98$, $p < 0.001$. We sought to find out at which steps the gain was maximally reduced between C57BL/6 and L7-PP2B mice. To do that, we checked the gain difference between two successive test sessions and then compared that across the mouse types. The tests of within-subjects contrasts illustrated that the gain reduction from T5 to T6 [$F(5, 40) = 2.48$, $p < 0.05$] and from T7 to T8 [$F(5, 40) = 2.66$, $p < 0.05$] was significantly greater for C57BL mice compared to the L7-PP2B mice.

Effects of DCS on VOR Adaptation

ANOVA further indicated that DCS polarity had a significant modulatory role on the gain reduction, $F(14, 70) = 2.07$, $p < 0.05$, suggesting that the amplitude of gain decrease across the eight tests (from T1 to T8) was dependent upon stimulus polarity. Moreover, the gain decrease across eight test sessions yielded a significant interaction between stimulus polarity and genetic background of the mice (C57BL/6 and L7-PP2B mice, [$F(7, 35) = 2.52$, $p < 0.05$]. In the following sections, we discuss how the modulatory role of DCS was altered depending on the mouse type.

Anodal Stimulation Reduced VOR Gain in C57BL/6 Acutely

The anodal stimulation triggered faster initial VOR gain reduction compared to the cathodal stimulation [$F(2, 21) = 9.56$, $p < 0.001$, Figure 5.4A] in wild type mice. There was a significant post-stimulation reduction of gain at T3 (pre-training reduction of gain) in the anodal group compared to the cathodal group. The contrast analysis, T2 vs. T3, comparing the raw gain at T2 with that made in T3, was statistically significant [$F(2, 21) = 6.01$, $p < 0.01$]. Interestingly, the anodal, sham and cathodal groups finished at the same degree of adaptation (T8), although the anodal group showed significant initial reduction in VOR gain.

Next, we normalized the gain of every mouse to its own baseline to provide a comparable measure of gain for all animals. Normalized gain (Figure 5.4B) depicted a clear polarity-dependent divergence. The initial post-stimulation period showed that the cathodal stimulation significantly decelerated gain reduction compared to the anodal stimulation. The reduction of gain in the sham condition—as expected—remained between the rate in the anodal and the cathodal conditions (Figure 5.4B).

Anodal stimulation lost its modulatory role when potentiation was eliminated from PCs (Figure 5.6A,B). Anodal stimulation failed to improve learning in L7-PP2B mice (T8 gain = 0.74 ± 0.04), compared to the sham group (T8 gain = 0.65 ± 0.08; Figure 5.5). Moreover, anodal stimulation could not reduce the baseline gain in these mutants (T2 gain = 1.06 ± 0.04, T3 gain = 0.99 ± 0.04). The large error bars in the sham condition is due to low sampling numbers (N = 3). Moreover, we think that chronic mutation (deletion of LTP in PCs) leads to the adoption of various adaptation mechanisms in the network. Therefore, when an external current stimulus was applied the network showed varied responses to cope with the situation. This could be the cause for finding a large variability in the stimulation groups.

Deletion of PP2B in PC Abolished Anodal Effect

An hour long sinusoidal oscillatory stimulus led to decrease in VOR gain (approximately to 28%) across various species (Tempia et al., 1991; Dow and Anastasio, 1998; Clément et al., 2002). The cause of this VOR gain reduction in rodents has been pointed out as habituation rather than learning (Tempia et al., 1991). Therefore, we think that the gain reduction (27 ± 2%) in L7-PP2B mice (similar to Schonewille et al., 2010) across all three stimulation-conditions is due to the habituation.

Discussion

Our study demonstrates three major findings of the polarity specific effects of DCS on VOR gain-down adaptation. First, anodal stimulation of cerebellar cortex decreases VOR gain acutely compared to the cathodal stimulation condition in C57BL/6 control mice. Second, despite differences in initial post-stimulation reduction in gain amplitude, the final gain reduction is similar

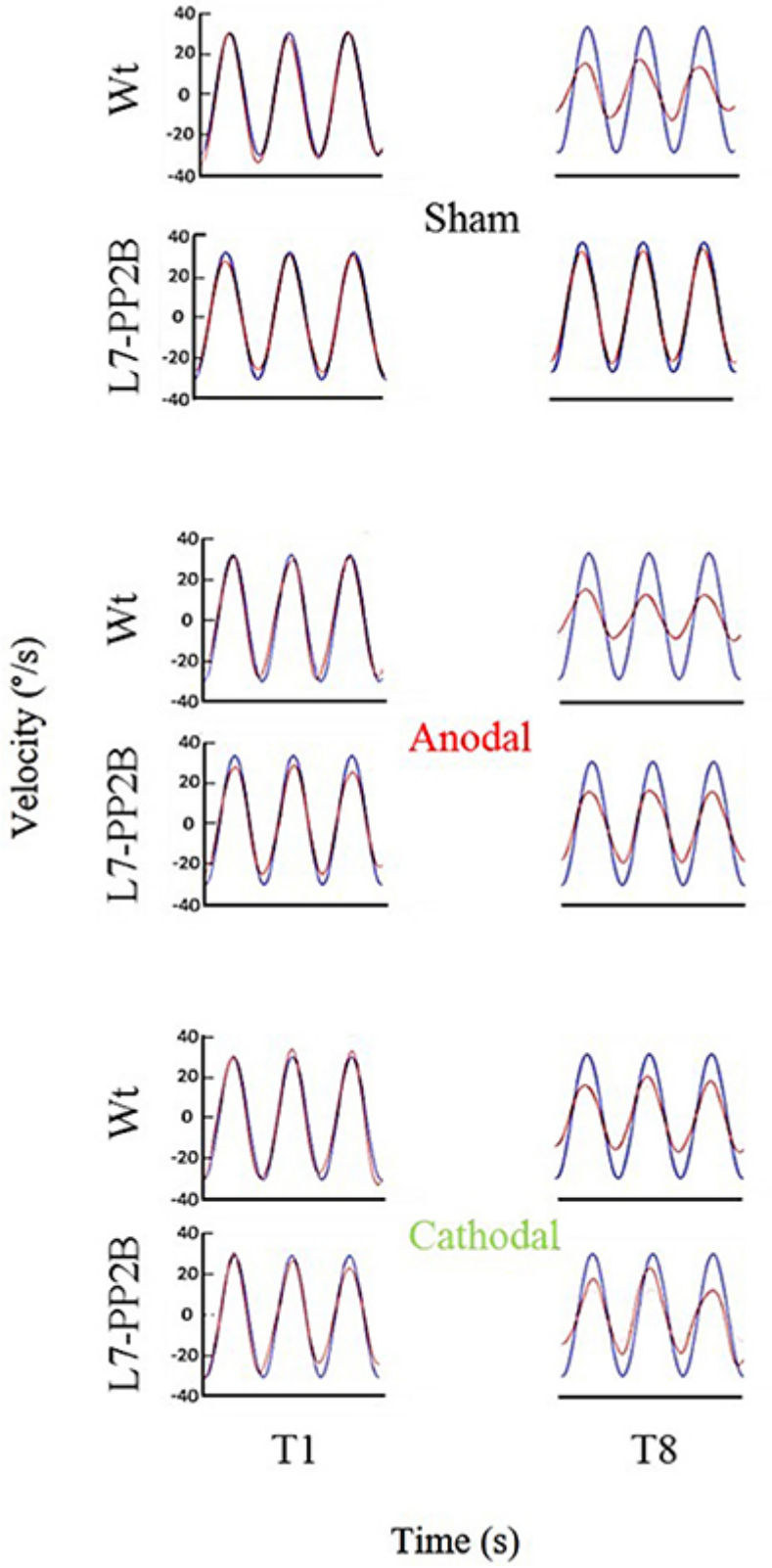

Figure 5.5. Eye amplitude show clear deficit in learning of L7-PP2B mice in all three stimulus conditions. Example filtered eye velocity traces illustrate typical results from mice of both genetic backgrounds before (T1) and after (T8) adaptation. Blue is vestibular stimulus and red is eye velocity (solid red line is filtered eye-signal, dotted red line is the fitted sine wave). Eye amplitude decreases from pre- to post-training sessions (T1 and T8, respectively) in wild type mice. In contrast, L7-PP2B undergoes little change between T1 and T8 sessions.

remarkably, shows when potentiation of the PCs is genetically ablated in L7-PP2B mice, anodal stimulation no longer led to VOR gain reduction. Hence, our interpretation is that anodal stimulation driven VOR gain reduction depends on a PP2B-dependent PC potentiation pathway, either at the upstream dendritic level or at the downstream axonal level where PCs innervate VN neurones (M. Schonewille et al., 2010).

We found that anodal stimulation of the cerebellum decreases VOR gain acutely (Figure 5.4A,B), though we don't see an effect on adaptation-rate like in other studies (Avila et al., 2015; Herzfeld et al., 2014; Jayaram et al., 2012; Zuchowski, Timmann, & Gerwig, 2014). We see that VOR gain is reduced prior to the training. Perhaps anodal stimulation induced an acute increase in inhibition by enhancing PC activity. Indeed, others have also reported that artificial activation of PCs may contribute to the induction of VOR gain-down adaptation (Nguyen-Vu et al., 2013). Moreover, a low amplitude external electric field (EEF) is sufficient to modulate PC activity (Chan et al., 1988; Chan & Nicholson, 1986). Together these results suggest that anodal DCS may induce higher PC activity, which in turn could lead to inhibition of its downstream structures.

The possibility that the effects of DCS on plasticity are in part secondary effects on downstream structures comports with there being at least two sites of VOR plasticity (Hansel, 2005): one in the floccular region of cerebellar cortex and one in the VN (Z. Gao, van Beugen, & De Zeeuw, 2012). Physiological studies would be necessary to elucidate the relative effects, and these studies would need to include direct measurements from both regions.

We also found that the total gain reduction was similar in the anodal and the cathodal stimulation conditions although the gain reduction at the early phase is clearly different (Figure 5.4A). In our study, training and testing are assessed post DCS, whereas most of the reports available today are based on stimulation applied during learning. For instance, anodal stimulation facilitates learning in locomotor (Jayaram et al., 2012), force field (Herzfeld et al., 2014), and saccade (Avila et al., 2015) adaptation as well as eye-blink conditioning tasks (Zuchowski et al., 2014), while cathodal stimulation hinders leaning in all these tasks. Surprisingly, the post-stimulation deadaptation curve (Herzfeld et al., 2014; Jayaram et al., 2012) or extinction rate (Zuchowski et al., 2014) shows no difference across various stimulation groups. The later finding is notable because irrespective of altered rate and total amount of learning, polarity has no effect on post-stimulation de-adaptation/ learning processes. In our study, we find that DCS has no post-stimulation effect on the learning phase. Therefore, our study clearly depicts both anodal and cathodal stimulation have short-lasting effects on the habituation phase of the gain-down VOR adaptation task. The de-adaptation experiment (like other studies) is redundant, as we have done all the adaptation training sessions in

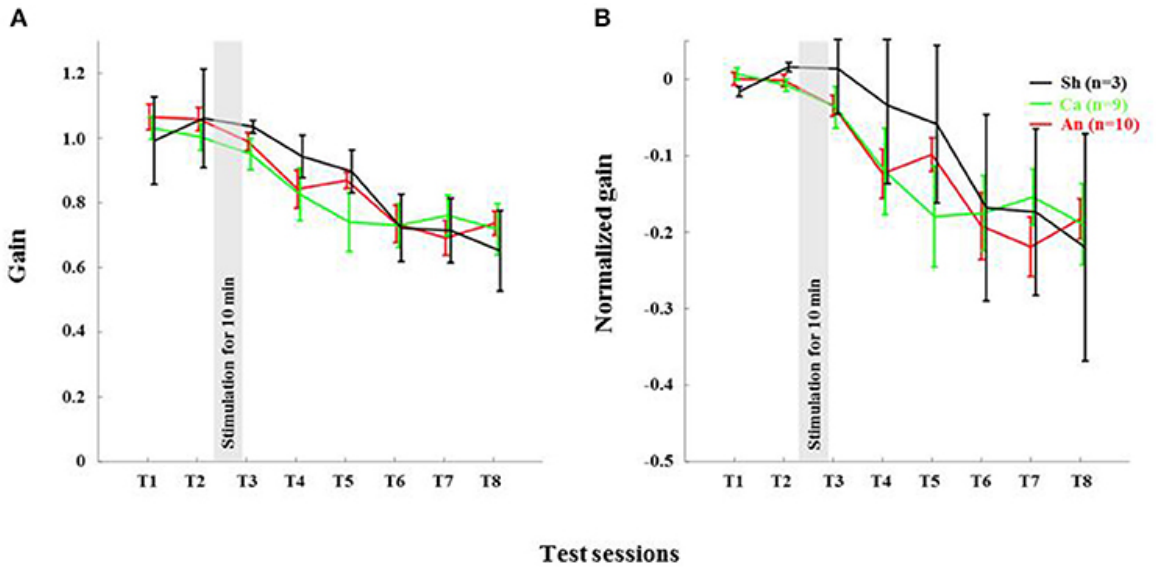

Figure 5.6. Genetic ablation of PC plasticity in L7-PP2B mice abolishes effects of anodal stimulation on gain-down adaptation. (A) Plot of gain during gain-down adaptation: Changes in VOR gain during VOR-decrease training in L7-PP2B mice. The VOR was tested pre- and post-training by measuring the eye movement response to the vestibular stimulus. (B) Plot of normalized gain throughout the course of the behavioural paradigm: Changes in VOR gain during VOR-decrease training. Black, Green and Red lines are for sham, cathodal and anodal stimulation conditions, respectively. The grey bar indicates the stimulation period. Error bars represent SEM, because of large SEM we do not find any significant difference between the groups.

the post-stimulation period. To discover the actual cause, similar experiments should be performed with a gain increase VOR adaptation paradigm (Z. Gao et al., 2012).

L7-PP2B mice often showed more than one gain during baseline measurements (Figure 5.6A). Possibly, the eye overshoots the head-position as we have used higher sinusoidal velocity (amplitude of 5° at 1 Hz frequency). We think that sensory signals coming from the parallel fibres fail to excite PC sharply, as there is no LTP in L7-PP2B mice. Therefore, when the high velocity head-movement stops, PCs could not generate sharp inhibition on the VN to stop the eye-movement. A sub-optimal PC inhibition may have caused facilitation of the eye movement in the absence of the head-movement.

We propose three, non-exclusive, possibilities that may explain reduced sensitivity to anodal stimulation in the L7-PP2B mutants: (i) PCs in the mutants may receive more background inhibition; (ii) plasticity at the PC-VN synapses may be essential for VOR gain-down adaptation (De Zeeuw & Ten Brinke, 2015); and/or (iii) plasticity of synapses on PCs in mutants may be saturated, preventing adaptation. The first point reflects the possibility that anodal stimulation may cause inhibition rather than excitation of PCs when there is no LTP or intrinsic plasticity at PCs. Anodal stimulation driven subthreshold depolarisation may augment GABA release from molecular layer interneurones (MLI)

(Christie, Chiu, & Jahr, 2011; Stagg & Nitsche, 2011) and thereby increase inhibition onto PCs. The second possibility is that anodal DCS has a direct impact on PC-VN plasticity and thereby directly regulates the adaptation process. Loss of PC LTP may retard the effects of anodal stimulation on these synapses. The third reason could be that loss of LTP makes the circuit unresponsive to the pairing of the sensory stimulus with the motor response, as intrinsic plasticity of PCs is also erratic in these mutants (M. Schonewille et al., 2010). The PP2B transgene may disrupt normal signalling through the PCs or the homeostasis of the network (Lamont & Weber, 2012). This can corrupt the instructive signals sent by PCs to downstream sites like the VN.

Cathodal stimulation induced inhibition of adaptation in L7-PP2B mutants is significantly stronger compared to C57BL/6 mice but similar to the sham group of L7-PP2B mice (Figures 5.5, 5.6B). It is evident that this cathodal suppression is a by-product of the mutation of potentiation at the PCs, as these mice fail to learn cerebellar tasks (M. Schonewille et al., 2010). In addition, we need to examine to what extent long-term depression (LTD) at PF-PC pathway plays a role following cathodal stimulation.

In conclusion, we have successfully developed a mouse model of cerebellar DCS, allowing us to present the first demonstration of cerebellar DCS driven behavioural changes in rodents. We used this model in combination with the popular paradigm of VOR adaptation to test the effect of current stimulation on motor adaptation. The results presented here provide evidence that anodal DCS reduces VOR gain acutely, an effect that is disrupted by ablation of PP2B in PCs. This study also finds support for recent claims that anodal and cathodal stimulation modulate cerebellar dependent adaptation acutely through distinct pathways. Future research must address the neuronal activity following cerebellar stimulation to understand the spatiotemporal aspects of DCS effects.

Chapter 6 - Influence of Environmental Enrichment on Visual and Vestibular Function and Learning [5]

Marcella Spoor, Jos N. van der Geest, Maarten A. Frens

Abstract

Research has shown that a larger cage and a more complex environment have positive effects on the welfare of i.e. laboratory mice. This is called environmental enrichment (EE). It has also been shown that environmental enrichment affects various behaviour and neuro-anatomical and molecular characteristics. In this study, the behavioural effects of environmental enrichment on contrast sensitivity, reflexive eye movements and on oculomotor learning were measured in mice that were housed in an enriched environment.

We found a clear effect on oculomotor learning, where animals that were housed in an enriched environment learned significantly faster than controls that were housed under standard conditions. In line with existing literature, the enriched group also outperformed the controls in behavioural tests for explorative behaviour. Meanwhile, both visual and reflexive oculomotor performance in response to visual and vestibular stimuli was unaffected. This points towards an underlying mechanism that is specific for motor learning, rather than overall motor performance.

Introduction

Behavioural, cellular and molecular studies have revealed significant effects of environmental enrichment on rodents. Rearing these animals in larger, more complex environments results in changes in brain structure and function, including increased brain weight, dendritic branching, neurogenesis, gene expression, and improved learning and memory (Bhagya, Srikumar, Veena, & Shankaranarayana Rao, 2017; Fan, Li, Zheng, Hua, & Zuo, 2016; Lewis, 2004; Sager, Kashon, & Krajnak, 2018). The classic definition of environmental enrichment is “a combination of complex inanimate and social stimulation” (Rosenzweig, Bennett, Hebert, & Morimoto, 1978). Leach, Ambrose, Bowell, & Morton (2000) suggested that any change to the housing system that increases the frequency and diversity of positive natural behaviours, decreases the occurrence of abnormal behaviour, maximizes the utilisation of the environment, or increase the animal’s ability to cope with challenges of captivity, qualifies the environment as being enriched. Classic behavioural tests, such as the Open Field test (Hall, 1934), the Hole Board test (File & Wardill, 1975a), and the Light/Dark test (Crawley & Goodwin, 1980), show that mice show less signs of anxiety and hyperactivity in

[5] In preparation

response to novelty, when housed in an enriched environment (Würbel, 2001). At the behavioural level, enrichment enhances learning and memory (Schrijver, Bahr, Weiss, & Würbel, 2002), reduces memory decline in aged animals (J. C. Bennett, McRae, Levy, & Frick, 2006), decreases anxiety, and increases exploratory activity (Chapillon, Manneché, Belzung, & Caston, 1999; Roy, Belzung, Delarue, & Chapillon, 2001).

Various studies have shown that enrichment increases dendritic branching and length, the number of dendritic spines and the size of synapses on some neuronal populations (Leggio et al., 2005; Sager et al., 2018). Many of these cellular changes are also consistent with enrichment-induced alterations in the expression of genes involved in synaptic function and cellular plasticity (Rampon et al., 2000). Enrichment can increase levels of neurotrophins, such as brain-derived neurotrophic factor (BDNF) and nerve growth factor (NGF), which play integral roles in neuronal signalling (Fan et al., 2016; Ickes et al., 2000; Novkovic, Mittmann, & Manahan-Vaughan, 2015; Pham et al., 1999). Furthermore, enrichment results in increased synaptic strength, including specific forms of synaptic plasticity such as long-term potentiation (Bhagya et al., 2017; Cortese, Olin, O'Riordan, Hullinger, & Burger, 2018; Foster & Dumas, 2001; Foster, Gagne, & Massicotte, 1996).

Improvements in motor coordination have been observed in mice housed in an enriched environment, as opposed to mice kept in regular housing system (Chapillon et al., 1999). An enriched environment causes specific alterations in the biophysical properties of cerebellar granule cells, allowing for higher firing frequencies. These alterations were accompanied by superior motor skills (Hallermann, Eshra, & Hirrlinger, 2019). The volume of the cerebellum, along with other brain areas, increases as a result of environmental enrichment (Scholz, Allemang-Grand, Dazai, & Lerch, 2015).

In the present study, the effects of environmental enrichment on visual and sensorimotor function, and cerebellum dependent learning were measured. Mice, being afoveate mammals, show robust cerebellum dependent gaze-stabilising eye movements like the optokinetic reflex (OKR), which prevents the image of the surroundings to slip across the retina during movement of the visual scene and the vestibulo-ocular reflex (VOR), which responds to vestibular stimulation (Collewijn, 1981). We use the OKR response to measure the animal's visuo-motor functioning. The VOR is induced to analyse the functioning of the vestibular system. Using the method described in Chapter 4, we determine the visual acuity of the mice at various contrast levels, to assess if putative differences in behaviour could be due to differences in visual capabilities. As a positive control we measured the mice in a number of standard behavioural tests (see above) that are known to be affected by environmental enrichment.

In the lab, paired visual and vestibular stimuli are used to evoke cerebellum-dependent learning. When moving visual and vestibular stimuli in phase, the vestibular stimulation drives the VOR, while the visual stimuli trigger the eyes not to move, since that creates a retinal slip. In order to reduce this mismatch, oculomotor learning takes place to reduce the magnitude of the VOR (Frens & Donchin, 2009). Learning is measured by comparing the post-training amplitude of the VOR with the pre-training amplitude.

Based on the previous findings of improved motor performance and cerebellar changes in mice housed in an enriched environment, we hypothesized that these mice showed normal visual, visuo-motor and vestibular function, but improved cerebellar-dependent motor learning.

Methods

Animals

In total eighteen male C57/Bl6 mice (Charles River Netherlands) were used in the present study. All efforts were made in order to minimize animal pain or discomfort. Two cohorts of mice were measured. Cohort I consisted of six animals at the age of ten weeks, cohort II of twelve mice at the age of sixteen weeks. Since we observed no significant differences between these groups, the data of both groups were pooled. Experiments were conducted with approval of the local ethics committee and in accordance with the European Communities Council Directive (2010/63/EU).

Housing conditions

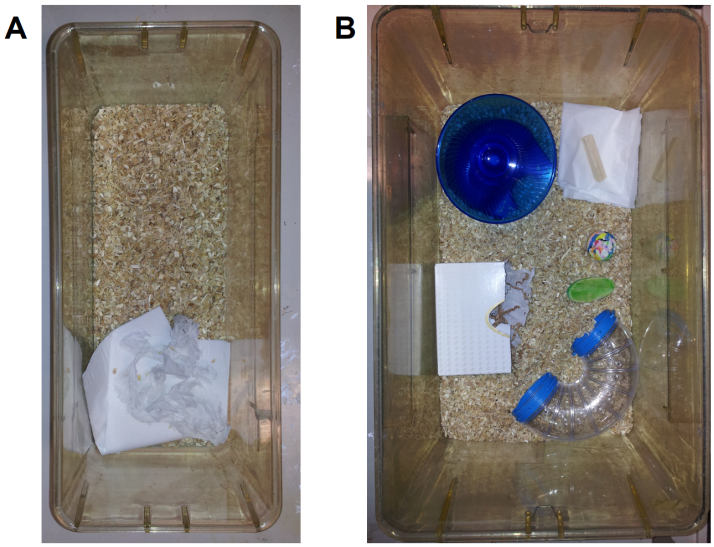

Figure 6.1: Housing used in this study. A: Standard housing B: Enriched housing. The pictures are not at the same scale (see text)

Littermates were randomly assigned to one of the two experimental groups, containing nine animals each. The first group was housed in standard conditions, the second group was housed in enriched conditions (Figure 6.1). The mice kept in standard housing conditions were housed with three littermates in a Makrolon 1L cage (33×15×13cm), containing one tissue for nest building. The enriched mice were housed with three littermates in a larger Makrolon type IV cage

(48×38× 210cm). Besides sawdust, this cage contained wood shavings, a running wheel, a shelter, plastic tunnel and coloured wooden blocks. Throughout the enrichment period, the objects were replaced once a week. Both groups of animals received the same type of food. Food and water were provided ad libitum until the end of experiment. All mice were housed on a 12-hour light/12- hour dark cycle.

Surgical preparation

After three weeks, all animals were prepared for behavioural experiments by attaching, under anaesthesia, a pedestal to their skull using a construct made of a micro glass composite. This pedestal was necessary for head fixation during the experiments. The full procedure is described in van Alphen, Winkelman, & Frens (2009). After the surgery, mice were placed back in their cage and had a week to recover.

Experimental Procedures

Behavioural Assessments

Environmental enrichment is a poorly defined condition, and therefore we subjected every mouse to a number of tests of explorative behaviour, whose outcomes have been well established to be affected by it (Wolfer et al., 2004; Würbel, 2001). These were the Open Field Test (Hall, 1934, 1936), the Hole Board test (File & Wardill, 1975b, 1975a), and the Light/Dark test (Crawley, 2007; Crawley & Goodwin, 1980).

In the Open Field environment, the mice were in a lighted environment of 72x72x40cm. They were released in one of the corners of the environment and filmed for 10 minutes. In the Hole Board test the mice were in an environment with identical dimensions. The bottom of this lighted environment had 6x6 holes (⌀ 2.5cm) at regular distances. Mice were released in one of the corners of the environment and filmed for 10 minutes. In the Light/Dark test the mice were in an environment with identical dimensions. Half of the environment was dark, and the other half was lighted with a single light source. There was one small opening between both compartments that was blocked at the onset of the experiments. Each mouse was released in the dark compartment and after 5 min of acclimatisation the small opening was opened. After that the mouse was filmed for 10 minutes.

The recorded videos were scored by hand. In the Open Field test, we scored how often the mice entered the central 18x18cm. In the Hole Board test, we scored the number of times that a mouse explored a hole by putting its head in it. Finally, for the Light/Dark test we recorded the total amount of time spent in the light compartment.

Eye Movement Measurements

Stimulus setup

Optokinetic stimuli were created using a modified Electrohome Marquee 9000 CRT projector (Christie Digital Systems, Cypress CA, USA), which projected stimuli via mirrors onto three transparent anthracite-coloured screens (156*125 cm) that were placed in a triangular formation around the recording setup (see van Alphen et al. (2009), for more details). This created a green monochrome panoramic stimulus, fully surrounding the animal. Each pixel subtended 4.5 x 4.5 arc minutes.

Visual stimuli were programmed in C++ and rendered in openGL. Depending on the experimental condition, they consisted of a virtual sphere with a dotted pattern or a virtual cylinder with vertically oriented sine grating on its wall.

Vestibular stimulation was provided via a motorized turntable Mavilor-DC motor 80 (Mavilor Motors S.A., Barcelona, Spain) on which the mouse and eye movement recording system were mounted. The driving signal of both the visual and vestibular stimulation, which specified the required position, was computed and delivered by a CED Power1401 data acquisition interface (Cambridge Electronic Design, Cambridge, UK) with a resolution of 0.1 º and 0.01s.

Eye movement recordings

Mice were immobilized by placing them in a plastic tube, with the head pedestal bolted to a restrainer that allowed placing the eye of the mouse in the centre of the visual stimulus, in front of the eye position recording apparatus. This mouse holder was mounted on the vestibular table.

Position of the left eye was recorded with an infrared video system (Iscan ETL-200). Images of the eye were captured at 120 Hz with an infrared sensitive CCD camera (see van Alphen et al. (2009) for more details). To keep the field of view as free from obstacles as possible, the camera and lens were mounted under the table surface, and recordings were made with a hot mirror that was transparent to visible light and reflective to infrared light. The eye was illuminated with two infrared LEDs at the base of the hot mirror. The camera, mirror and LEDs were all mounted on an arm that could rotate about the vertical axis over a range of 26.12˚ (peak to peak). Eye movement recordings and calibration procedures were similar to those described by Stahl, van Alphen, & De Zeeuw, (2000). During all oculomotor paradigms, position of the left eye was recorded and stored to be analysed offline.

For the oculomotor tests, data analysis was done in Matlab (version R2019a, the Mathworks, Natick, USA). Recorded eye positions were transformed offline into a velocity signal. Fast phases and

saccades were removed from the eye movement recordings using a velocity threshold of twice the stimulus velocity.

For every mouse we performed the same paradigms. We determined the properties of the Optokinetic and Vestibulo-Ocular reflex as a measure for oculomotor performance. We determined the contrast sensitivity function to probe the visual performance. Finally, we performed a VOR learning paradigm to assess the motor learning capabilities of the animals.

Contrast sensitivity

The method used in this study infers contrast sensitivity by measuring how the magnitude (gain) of the OKR varies with different combinations of contrast and spatial frequency.

Contrast sensitivity was tested by presenting moving vertically oriented visual sine gratings to the mice and recording eye movements evoked by those stimuli. The methods have been described fully in van Alphen et al. (2009). Each stimulus was made up of a combination of one of seven spatial frequencies (0.03, 0.05, 0.08, 0.17, 0.25, 0.33, or 0.42 c/˚) and one of six contrast values (100%, 75%, 50%, 25%, 10%, or 1%). The 42 stimulus combinations were presented in random order.

A stimulus was first projected and kept stationary for one minute, allowing the animal to adjust to changes in the stimulus. Subsequently, the stimulus started to move with a constant velocity of 1.5˚/s. After moving to one direction for two seconds, it changed direction and moved in the opposite direction for two seconds. This was repeated six times, yielding 11 changes in direction.

In analysing the responses, the first 200 ms after stimulus onset and after each change in direction were removed. Because the stimulus velocity was constant and eye data in the first 200 ms after the stimulus direction changes were ignored, average absolute eye velocity could be divided directly by the stimulus velocity to calculate a gain value for each combination of spatial frequency and contrast. An eye movement that perfectly follows the visual stimulus has a gain of 1 (Collewijn, 1981).

Optokinetic reflex (OKR)

The stimulus to induce an optokinetic reflex was consisted of 1592 green dots that were equally spaced on a virtual sphere that has its centre at the left eye of the mouse. The stimulus oscillated sinusoidally about the earth vertical axis with a constant amplitude of 5˚ at maximum contrast. By using different oscillation frequencies (0.1, 0.2, 0.4, 0.8, 1.6 Hz) the peak velocity of the stimulus was varied. To analyse the data, a sinusoid with the frequency of the stimulus was fitted through the eye velocity data. Gain was the determined by dividing the amplitude of this fit by the stimulus peak velocity.

Vestibulo-ocular reflex (VOR)

Mice were rotated in the dark by the turntable to measure the VOR. Vestibular stimuli were created by oscillating the mouse about the earth vertical axis at 3 different frequencies (0.2, 0.6, and 1 Hz) with a constant amplitude of 5˚. Data analysis was identical to what we did for OKR.

VOR learning

To induce motor learning, a VOR gain down training paradigm was used, where the presented sinusoidal visual and vestibular stimuli moved at the same speed and exactly in phase at a frequency of 1 Hz and an amplitude of 5°. The pattern of the visual stimulus used was the same as the one used to evoke the OKR. These training stimuli were presented in six blocks of twenty minutes. To probe the effects of training, VOR in the dark was measured before the training and after each training block. These test stimuli had the same amplitude and frequency as the training stimuli and were presented for two minutes each. Data analysis was identical to what we did for OKR.

Experimental Procedure

The standard behavioural tests were performed on the day before the surgery. The order of these tests was always the same: Open Field, Hole Board, Light/Dark test.

Prior to the start of the whole set of oculomotor experiments, each mouse was acclimatized to the experimental setup for 15-30 min. This means that they were placed in the setup, but that no experiments were performed. One day after acclimatisation, experiments were started. For each mouse the order of experiments was the same. Between the experiments, animals had at least one day rest and were housed in their assigned environment.

On day one, the OKR was tested to determine the effects of enrichment on visuomotor function. Additionally, the contrast sensitivity function was determined to assess differences in visual capabilities. On the last day, we measured the VOR at various frequencies. Finally, we measured VOR learning.

Data analysis

Group differences were statistically assessed using one-sided non-parametric tests (Mann-Whitney) in the behavioural experiments, and in the compensatory eye movement experiments using repeated measures ANOVA's with one between-subject factor Group (2 levels: standard vs. enriched) and one within-subject factor Frequency (5 levels for OKR, and 3 levels for VOR, being the stimulus frequencies). Group differences in the motor learning experiment on normalised VOR gains (being the ratios of the VOR gains in the adaptation blocks to the baseline VOR gain) were also

assessed using a repeated measure ANOVA with one between-subject factor Group (2 levels: standard vs. enriched) and one within-subject factor Block (6 levels: being the adaptation blocks).

Statistics were performed using JASP (v1.0) and statistical thresholds were set at an alpha level of 5%.

Results

We compared explorative behaviour, compensatory eye movements (OKR and VOR), and VOR learning between mice housed in an enriched environment (n=9) and mice housed in a standard environment (n=9).

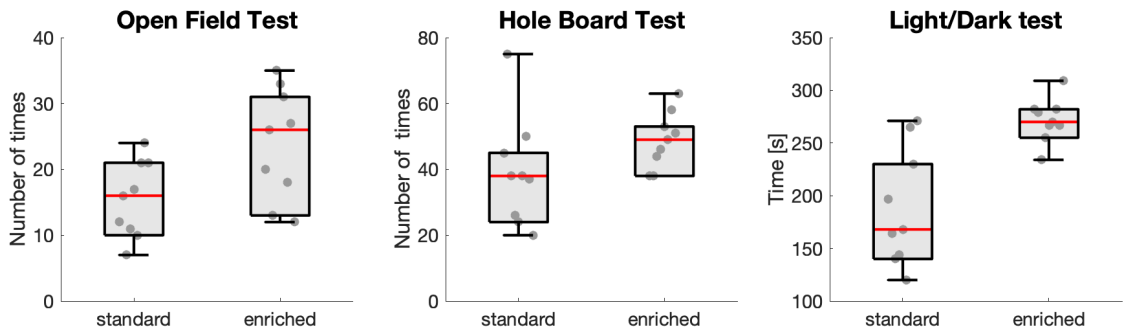

Figure 6.2. Box-and-whisker plots showing the results of the three behavioural tests for the two groups of mice (Barren and Enriched). Each dot is an individual mouse. The red line in the box is the median value of the group.

Explorative behaviour

Housing conditions did affect explorative behaviour: mice in the enriched group showed more explorative and less anxious behaviour than mice in the standard housing group (Figure 6.2). They visited the central part of the floor of the arena in the Open Field test more often (median ± IQR: 26 ± 17 vs. 16 ± 11, U = 16.5, p = .019), dipped their head more often into one of the holes in the Hole

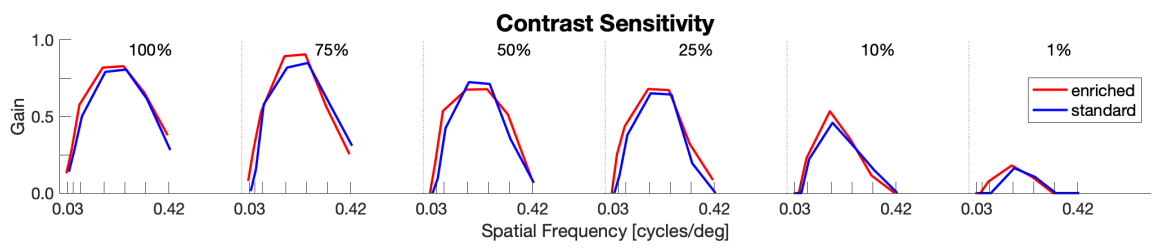

Figure 6.3. OKR gain as function of spatial frequency for different levels of contrast. No differences between the enriched (red) and standard (blue) housed groups could be observed.

Board test (49±15 vs. 38±23, U=19, p = .031), and spent more time in the light chamber of the Light/Dark test (270 ± 21 vs. 168 ±106, U = 7, p = .002).

Contrast sensitivity

No significant differences in visual functioning between the two groups were observed as reflected by similar optokinetic responses to moving gratings with combinations of different contrasts and spatial frequencies (Figure 6.3).

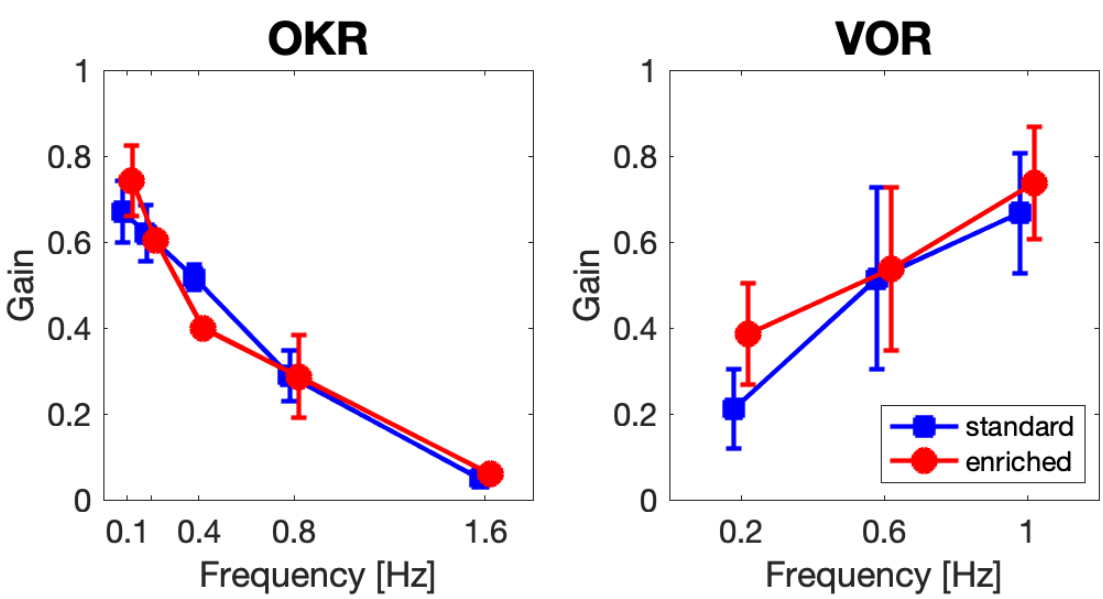

Figure 6.4. Optokinetic (OKR) and vestibulo-ocular (VOR) gain in response to different stimulation frequencies for the two groups of mice.

Compensatory Eye Movements

Housing conditions did not importantly affect optokinetic and vestibulo-ocular reflexes (Figure 6.4). As expected, the main effect of stimulus frequency was significant for both types of compensatory eye movements: OKR gain decreased ($F(4,64) = 722.8$, $p < .001$, $\omega^2 = .95$), and VOR gain increased ($F(2,32) = 114.0$, $p < .001$, $\omega^2 = .55$), with increasing stimulus frequencies. The overall differences in gain between the two groups were not significant (OKR: $F(1,16) = 0.28$, $p = .60$, $\omega^2 = .00$; VOR: $F(1,16) = 1.88$, $p = .189$, $\omega^2 = .05$). For both types of eye movements, the interactions between group and stimulus frequency were significant but small (OKR: $F(4,64) = 12.7$, $p<.001$, $\omega^2 = .24$; VOR: $F(2,32) = 4.20$, $p = .024$, $\omega^2 = .034$).

Motor learning

Housing conditions did however affect motor learning (Figure 6.5). Normalised VOR gains decreased during the adaptation blocks (effect of block on VOR gain: $F(5, 80) = 26.0$, $p < .001$, $\omega2 = .45$) in both groups, but the overall reduction in VOR gain was larger in the enriched group than in the standard

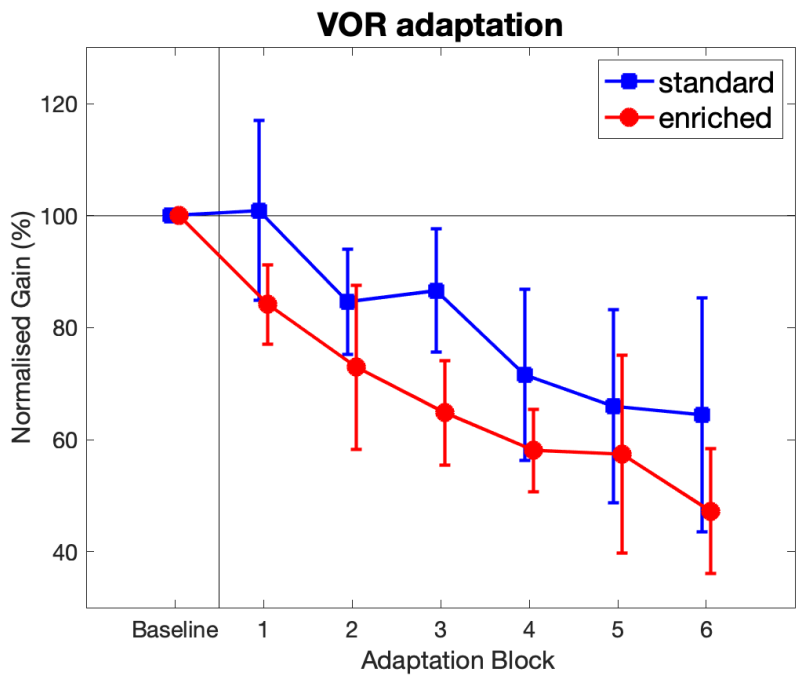

Figure 6.5. Normalised VOR gain during the six blocks of VOR adaptation.

housing group ($F(1,16) = 11.6$, $p = .004$, $\omega 2 = .37$). The interactions between Group and Block was not significant ($F(5,80) = 0.80$, $p = .56$, $\omega 2 = .00$). A post-hoc non-parametric analysis showed that the normalised VOR gain in the last block was smaller in the enriched group (median ± IQR: 0.51 ± .18) than in the standard housing group (0.55 ± .25, $U = 62$, $p = .031$).

Discussion

Environmental improvement has been a topic in rodent research for more than 60 years, inspired by Donald O. Hebb's finding that the rats he kept as pets, exposed to a more complex environment, showed better performance in learning and memory than his research animals (R. E. Brown, 2006). Experiments have shown that exposure to an enriched environment has been shown to induce robust neuronal plastic changes in both the cerebral as well as in the cerebellar cortex (Angelucci et al., 2009).

In this study we assessed whether differences in housing affect oculomotor and cerebellar motor learning behaviour. We also conducted standard behavioural protocols to ascertain that the enrichment protocol that we used had its effect.

Adding structuring to an enlarged cage provided the mice with shelter and increased opportunities for exploration and locomotion. From our results of the standard behavioural tests Open Field Test (OFT), Hole Board (HB) and Light Dark (LD) we can infer that such altered housing conditions indeed

did have an effect on measured behaviour. Enriched animals showed increased open field behaviour, more explorative behaviour and seemed to be less anxious (Figure 6.2). These results are in accordance with many other research findings where typical results were increased activity, or reduced signs of anxiety in the open field, exploration test (Chapillon, Manneché, Belzung, & Caston, 1999; Roy, Belzung, Delarue, & Chapillon, 2001; Würbel, 2001).

Vision: Contrast Sensitivity Function

By measuring how the gain of the OKR varies with different contrasts and spatial frequencies the contrast sensitivity function was inferred. In this study improved housing conditions did not improve the contrast sensitivity, which is in line with earlier findings of Greifzu, Kalogeraki, & Löwel (2016). However, it has been previously shown that environmental enrichment from birth does enhance visual acuity in mice (Cancedda et al., 2004; Prusky, Reidel, & Douglas, 2000; Sale et al., 2004).

Thus, different environmental conditions could act as indirect mediator for the earliest effects on visual system development. Our study deviates from these findings in that the mice were older (10-16 weeks), and in that (consequently) there was no role for maternal care.

Oculomotor Performance

Overall an enriched environment did not alter the OKR nor the VOR gain. Apparently, these reflexes are sufficiently robust in the C57Bl/6J mice that they do not vary with varying housing conditions. Earlier literature has reported on the effects of enrichment on motor behaviour, but this was either about locomotion in disease models (Jadavji, Kolb, & Metz, 2006; Knieling, Metz, Antonow-Schlorke, & Witte, 2009), or about higher level movement parameters, such as the amount of stereotypical behaviour (Marashi, Barnekow, Ossendorf, & Sachser, 2003; Powell, Newman, McDonald, Bugenhagen, & Lewis, 2000; Turner & Lewis, 2003). Our data seem to be the first to report that the compensatory eye movements are not affected, despite the fact that the animals can move around more in their cages, and therefore presumably also make more head movements.

VOR learning

In this study cerebellar dependent learning was assessed. This form of learning was assessed by means of a paradigm which induces a decrease in VOR response. Mice from the enriched group showed a more enhanced VOR decrease than the mice from the standard housing condition group (Figure 6.5). Because both the OKR and VOR are unaffected, it is likely that these differences are due to the learning mechanism itself.

This gain decrease test is a frequently used test in neuroscience to assess cerebellar learning (Das et al., 2017; Galliano et al., 2018; Gutierrez-Castellanos, Winkelman, Tolosa-Rodriguez, De Gruijl, & De

Zeeuw, 2013; Inagaki & Hirata, 2017; Martijn Schonewille et al., 2011; Shin, Zhao, & Raymond, 2014b; Voges, Wu, Post, Schonewille, & De Zeeuw, 2017). The results obtained in this study tell us to carefully interpret such data, especially because differences in brain anatomy and function due to housing condition instead of inherent to the animal model tested can be accounted for the obtained differences on behavioural level. The differences that we find between the standard and enhanced housed groups are in the same order of magnitude as the effects that are often reported in mouse mutants.

We can only speculate on the underlying mechanism that causes the differences in learning speed between the two groups. Previous studies showed that different housing conditions can cause differences in brain anatomy and function. Enriched rodents have been observed to have increased brain weight and size (E. Bennett & Rosenzweig, 1969). Also various studies have shown that enrichment increases dendritic branching and length, the number of dendritic spines and the size of synapses on some neuronal populations in the hippocampus and cerebral cortex (Faherty, Kerley, & Smeyne, 2003; Greenough & Volkmar, 1973; Greenough, Volkmar, & Juraska, 1973; Leggio et al., 2005; Sager et al., 2018). Electrophysiological data measured in the hippocampus has shown that differential experience results in increased synaptic strength, including specific forms of synaptic plasticity such as long-term potentiation (LTP; Artola et al., 2006; Foster & Dumas, 2001; Foster et al., 1996) and long- term depression (LTD; Artola et al., 2006). Morphological and electrophysiological data cerebellar data from rodents kept in complex housing conditions confirm these observations (Hallermann et al., 2019).

The molecular mechanism of a different brain anatomy and function caused by varying housing conditions has been partially attributed to the up-regulation of proteins involved in neuronal survival and activity-dependent plasticity, such as the neurotrophins nerve growth factor (NGF) and brain derived neurotrophic factor (BDNF), in the cerebral cortex and hippocampus of mice and rats (Bindu et al., 2007; Birch, McGarry, & Kelly, 2013; G. R. Brown & Nemes, 2008; Ickes et al., 2000; Pham et al., 1999; Zhu et al., 2006). Angelucci et al (2009) found a significant increase of both BDNF and NGF concentrations in the cerebellum of rats reared in an enriched environment, as compared to rats reared in standard conditions suggesting that the beneficial effects of a more complex environment on the cerebellum of adult animals could be mediated, at least in part, by neurotrophins. A similar mechanism has been suggested for the improvement of cerebellar learning due to direct current stimulation (Das et al., 2017).

From the results obtained in this study we can confirm that a more complex environment decreases anxious behaviour and increases exploratory behaviour. Additionally, we can conclude that more

environmental complexity improves learning measured by an often-used paradigm in neuroscientific studies to asses learning. These results provide food for thought regarding the potential effects of the conventional housing laboratory animals are usually kept in. Even though it is basic biology that the phenotype of an animal is the product of a complex and dynamic interplay between nature (genotype) and nurture (environment), the latter, a sterile small box, is far less considered into the interpretation of animal experiments.

Standardisation is an important concept in neuroscientific research. Environmental standardisation has become a sort of dogma. It is explicitly encouraged, because between-experiment standardisation is thought to increase reproducibility of results, whereas within experiment standardisation is thought to increase test sensitivity (van de Weerd, Baumans, Koolhaas, & van Zutphen, 1994). Ironically, despite rigorous standardisation poor between-laboratory replicability has been revealed (standardisation fallacy), which can be causing conflicting findings published (Würbel, 2000). The introduction of a more complex environment may change certain characteristics of animals, and as a consequence, experimental results may not be comparable with previously found results. This, however should not hamper the introduction of enrichment, as it may be questioned whether the maintenance of animals in unresponsive environments makes them adequate models for extrapolating results (Markowitz & Gavassi, 1995). A growing body of evidence indicates that current approaches to behavioural phenotyping might often produce results that are idiosyncratic to the study in which they were obtained, because the interactive nature of genotype-environment relationships underlying behavioural phenotypes was not taken into account (Olsson & Dahlborn, 2002; Simpson & Kelly, 2011; Würbel, 2001).

Because the effect of a mutation on behaviour might substantially differ depending on the animals' genetic or environmental background, and because idiosyncratic results are scientifically useless, it is absolutely crucial that variation of experimental conditions forms an integral part of behavioural phenotyping research (Würbel, 2000).

Acknowledgements

We would like to thank S. Souleki and S. Ernst for helping with part of the experiments. MS was funded by a Human Frontier grant.

Chapter 7 - General Discussion

In this thesis we were able to assess both visual function and motor learning capabilities based on a thorough assessment of compensatory eye movement behaviour. We did so in human participants (Chapter 2), as well as in mutant mice (Chapter 3, 4 and 5) and mice that were housed in different environments (Chapter 6).

Assessment of visual function in humans

In humans we observed that the gaze following response (GFR) is influenced by both the spatial frequency and the contrast of a sinusoidally moving sine grating. Reduced central visual acuity induced lower GFR gains. This suggests that the GFR response can be used to estimate human contrast-sensitivity function and to determine how well a stimulus is seen.

Conventional tests of acuity do not cover the whole visual spectrum but only the high spatial frequency and very high contrast ranges (Ginsburg, 2003), while we found that the largest differences between people were observed under low contrast situations. Therefore, such conventional test may overestimate one's visual function. While this is an important finding, further research is needed to assess whether this also has practical consequences. It would be interesting to investigate if measurements at low contrast lead to different, and more appropriate, prescriptions for visual correction.

Tests in low vision patients often depend on self-reported changes in visual function and acuity, which can be highly inaccurate (Skeel et al., 2003; Warrian et al., 2010). This becomes even worse if the patients are non-verbal, like in small children or patients with intellectual disability. Low vision is a prominent issue in children that were born prematurely (Hellström, Smith, & Dammann, 2013; Michael X. Repka, 2002; Wen, Smith, Yang, & Walker, 2004), with incidences reported in 10 – 35% of the preterm children. Although any test that requires self-reports is obviously useless in these groups, it must be noted that also measuring eye movements can be challenging. However, video recording techniques have steadily improved over the last decade (Dalrymple, Manner, Harmelink, Teska, & Elison, 2018; Hessels, Andersson, Hooge, Nyström, & Kemner, 2015; Hessels, Hooge, & Kemner, 2016; Nyström, Hooge, & Andersson, 2016; Pel, Manders, & van der Steen, 2010), which makes this approach increasingly feasible.

At present, measuring the GFR at all possible combinations of spatial frequencies and contrasts took about 40 minutes, whereas a regular visual acuity test takes only a few minutes to complete. This would also hamper the practical usability substantially. However, one could modify the test into an adaptive procedure, thereby reducing the total time of the test substantially. As already discussed in

Chapter 2, a simple modification could make it possible to test foveal and peripheral vision separately.

Assessment of visual function in mice

Our findings in Chapter 3 demonstrate that the DNA repair defect in Ercc1δ/− mouse results in accelerated age-related decline of both vision and hearing compared to wild type littermates. The overall decrease in contrast sensitivity occurring in the Ercc1δ/− during a period of only eight weeks followed a similar pattern as was reported for normal ageing in C57Bl/6J mice (van Alphen et al., 2009a), for which the ability to perceive low contrasts and high spatial frequencies disappeared first.

Likewise, we found abnormalities in the ocular motor phenotype among three albino mouse strains (Chapter 4). Pigmented strains had a robust optokinetic reflex (OKR) to a full visual field (fVF) stimulus, but the median OKR velocities of albino mice were significantly lower during fVF stimulation as compared with pigmented mice. This may point either to an afferent or efferent visual system dysfunction (Optican & Zee, 1984), or to a combination of both.

Visual performance is often required in common behavioural studies for mice, such as for example the Morris watermaze (Vorhees & Williams, 2006), and vestibulo-ocular reflex (VOR) learning tasks (e.g. Gutierrez-Castellanos et al., 2013; Schonewille et al., 2011). Although visual acuity in mice varies greatly with both gender and age (van Alphen, Winkelman, & Frens, 2009b), and is also affected by other mutations than those that we explicitly tested here, it has not become standard yet to test vision as a possible confounder when comparing between different groups. In Chapter 5 and 6, we engaged in the VOR learning task ourselves, and tested the visual acuity ourselves (Chapter 6), or relied on previous reports of unperturbed vision (van Alphen et al., 2009b) in that particular mouse strain.

Assessment of motor learning in mice

In Chapter 5 we show that anodal stimulation of cerebellar cortex decreases VOR gain acutely compared to the cathodal stimulation condition in C57BL/6 control mice, but that the final gain reduction is similar in the anodal and the cathodal stimulation groups of C57BL/6 control mice. However, in L7-PP2B mice, where potentiation of Purkinje cells (PCs) is genetically ablated, anodal stimulation no longer led to VOR gain reduction. Hence, our interpretation is that anodal stimulation driven VOR gain reduction depends on a PP2B-dependent PC potentiation pathway, either at the upstream dendritic level or at the downstream axonal level where PCs innervate VN neurones (Schonewille et al., 2010).

Several studies have suggested that *transcranial direct current stimulation* (tDCS) could facilitate (motor) learning and rehabilitation in humans (Hummel et al., 2005; Marquez, van Vliet, McElduff, Lagopoulos, & Parsons, 2015). Unlike DCS, tDCS stimulates via the scalp. There is considerable disagreement concerning the effect of tDCS in the current literature (Krause & Cohen Kadosh, 2014; Minarik et al., 2016), with some researchers even arguing that tDCS, as it is currently used, is not able to influence brain activity since most of the applied current is shunted by participants' skin and skull (Underwood, 2016). In recent work by our lab (Gaiser, 2019) using a within-subject, repeated-measurement and sham-controlled design, we found no evidence for any effect of tDCS on muscle evoked potentials (MEPs) when applied to the motor cortex in 80 healthy subjects. This is in contrast to other studies, with less well controlled conditions, that claimed to have observed effects of tDCSAlthough similar, DCS (as used in Chapter 5), and tDCS have quite different properties with the current density as the most obvious difference. It is noteworthy that the alleged mechanisms behind tDCS have mostly been determined using in-vivo or in vitro DCS (Fritsch et al., 2010). Hence, although tDCS may be a doubtful technique, this has little meaning for the interpretation of DCS results.

In Chapter 6 we show that differences in housing affect cerebellar motor learning behaviour in wild-type mice, without affecting the vision of the animals, or their oculomotor performance. Furthermore, we can confirm that a more complex environment decreases anxious behaviour and increases exploratory behaviour. These results combined provide food for thought regarding the potential effects of the conventional housing laboratory animals are usually kept in. The environment in which mice are kept is usually not taken in account into the interpretation of data despite the basic biology that the phenotype of an animal is the product of an interplay between nature (genotype) ànd nurture (environment). Results of experiments with animals kept in a more complex environment, changing the phenotype, may differ from previously found results. Moreover, it may be questioned whether keeping animals in barren environments makes them adequate models for extrapolating results (Markowitz & Gavassi, 1995). Since the effect of a mutation will differ depending on nature and nurture aspects, always differences in between labs,

Taken together, these four experimental chapters show how measuring compensatory eye movements can be applied to assess sensory and motor functions, which can change as a result of visual disturbances, age-related genetic defects and/or environmental circumstances.

References

Abraham, J., Balbo, S., Crabb, D., & Brooks, P. J. (2011). Alcohol Metabolism in Human Cells Causes DNA Damage and Activates the Fanconi Anemia-Breast Cancer Susceptibility (FA-BRCA) DNA Damage Response Network. *Alcoholism: Clinical and Experimental Research*, *35*(12), 2113–2120. https://doi.org/10.1111/j.1530-0277.2011.01563.x

Acland, G. M., Aguirre, G. D., Ray, J., Zhang, Q., Aleman, T. S., Cideciyan, A. V., … Bennett, J. (2001). Gene therapy restores vision in a canine model of childhood blindness. *Nature Genetics*, *28*(1), 92–95. https://doi.org/10.1038/88327

Aggarwal, P., Nag, T. C., & Wadhwa, S. (2007). Age-related decrease in rod bipolar cell density of the human retina: an immunohistochemical study. *Journal of Biosciences*, *32*(2), 293–298. https://doi.org/10.1007/s12038-007-0029-9

Ambrus, G. G., Antal, A., & Paulus, W. (2011). Comparing cutaneous perception induced by electrical stimulation using rectangular and round shaped electrodes. *Clinical Neurophysiology*, *122*(4), 803–807. https://doi.org/10.1016/j.clinph.2010.08.023

Anderson, J. R. (1953). Causes and Treatment of Congenital Eccentric Nystagmus. *British Journal of Ophthalmology*, *37*(5), 267–281. https://doi.org/10.1136/bjo.37.5.267

Anderson, M. G., Smith, R. S., Hawes, N. L., Zabaleta, A., Chang, B., Wiggs, J. L., & John, S. W. M. (2002). Mutations in genes encoding melanosomal proteins cause pigmentary glaucoma in DBA/2J mice. *Nature Genetics*, *30*(1), 81–85. https://doi.org/10.1038/ng794

Angelucci, F., De Bartolo, P., Gelfo, F., Foti, F., Cutuli, D., Bossù, P., … Petrosini, L. (2009). Increased Concentrations of Nerve Growth Factor and Brain-Derived Neurotrophic Factor in the Rat Cerebellum After Exposure to Environmental Enrichment. *The Cerebellum*, *8*(4), 499–506. https://doi.org/10.1007/s12311-009-0129-1

Armbrecht, A. M., Aspinall, P. A., & Dhillon, B. (2004). A prospective study of visual function and quality of life following PDT in patients with wet age related macular degeneration. *The British Journal of Ophthalmology*, *88*(10), 1270–1273. https://doi.org/10.1136/bjo.2003.038604

Artola, A., von Frijtag, J. C., Fermont, P. C. J., Gispen, W. H., Schrama, L. H., Kamal, A., & Spruijt, B. M. (2006). Long-lasting modulation of the induction of LTD and LTP in rat hippocampal CA1 by behavioural stress and environmental enrichment. *European Journal of Neuroscience*, *23*(1), 261–272. https://doi.org/10.1111/j.1460-9568.2005.04552.x

Arundale, K. (1978). An investigation into the variation of human contrast sensitivity with age and ocular pathology. *The British Journal of Ophthalmology*, *62*(4), 213–215. https://doi.org/10.1136/bjo.62.4.213

Avila, E., van der Geest, J. N., Kengne Kamga, S., Verhage, M. C., Donchin, O., & Frens, M. A. (2015). Cerebellar Transcranial Direct Current Stimulation Effects on Saccade Adaptation. *Neural Plasticity*, *2015*, 1–9. https://doi.org/10.1155/2015/968970

Bahill, A., Bahill, K., Clark, M., & Stark, L. (1975). Closely spaced saccades. *Investigative Ophthalmology & Visual Science*, *14*(4), 317–321. Retrieved from https://iovs.arvojournals.org/article.aspx?articleid=2158541

Balkema, G W, Mangini, N. J., Pinto, L. H., & Vanable, J. W. (1984). Visually evoked eye movements in mouse mutants and inbred strains. A screening report. *Investigative Ophthalmology & Visual Science*, *25*(7), 795–800. Retrieved from http://www.ncbi.nlm.nih.gov/pubmed/6735643

Balkema, G W, Pinto, L. H., Dräger, U. C., & Vanable, J. W. (1981). Characterization of abnormalities in the visual system of the mutant mouse pearl. *The Journal of Neuroscience : The Official Journal of the Society for Neuroscience*, *1*(11), 1320–1329. Retrieved from http://www.ncbi.nlm.nih.gov/pubmed/7310489

Balkema, Grant W., & Dräger, U. C. (1990). Origins of uncrossed retinofugal projections in normal and hypopigmented mice. *Visual Neuroscience*, *4*(6), 595–604. https://doi.org/10.1017/S0952523800005794

Barabas, P., Huang, W., Chen, H., Koehler, C. L., Howell, G., John, S. W. M., … Križaj, D. (2011). Missing Optomotor Head-Turning Reflex in the DBA/2J Mouse. *Investigative Opthalmology & Visual Science*, *52*(9), 6766. https://doi.org/10.1167/iovs.10-7147

Bastian, A. J. (2011). Moving, sensing and learning with cerebellar damage. *Current Opinion in Neurobiology*, *21*(4), 596–601. https://doi.org/10.1016/j.conb.2011.06.007

Bennett, E., & Rosenzweig, M. (1969). Rat brain: effects of environmental enrichment on wet and dry weights. *Science*, *163*(3896), 825–826. Retrieved from https://science.sciencemag.org/content/163/3869/825.short

Bennett, J. C., McRae, P. A., Levy, L. J., & Frick, K. M. (2006). Long-term continuous, but not daily, environmental enrichment reduces spatial memory decline in aged male mice. *Neurobiology of Learning and Memory*, *85*(2), 139–152. https://doi.org/10.1016/J.NLM.2005.09.003

Benussi, A., Koch, G., Cotelli, M., Padovani, A., & Borroni, B. (2015). Cerebellar transcranial direct

current stimulation in patients with ataxia: A double-blind, randomized, sham-controlled study. *Movement Disorders*, *30*(12), 1701–1705. https://doi.org/10.1002/mds.26356

Betts-Henderson, J., Bartesaghi, S., Crosier, M., Lindsay, S., Chen, H.-L., Salomoni, P., … Nicotera, P. (2010). The nystagmus-associated FRMD7 gene regulates neuronal outgrowth and development. *Human Molecular Genetics*, *19*(2), 342–351. https://doi.org/10.1093/hmg/ddp500

Bhagya, V. R., Srikumar, B. N., Veena, J., & Shankaranarayana Rao, B. S. (2017). Short-term exposure to enriched environment rescues chronic stress-induced impaired hippocampal synaptic plasticity, anxiety, and memory deficits. *Journal of Neuroscience Research*, *95*(8), 1602–1610. https://doi.org/10.1002/jnr.23992

Bindman, L. J., Lippold, O. C. J., & Redfearn, J. W. T. (1964). The action of brief polarizing currents on the cerebral cortex of the rat (1) during current flow and (2) in the production of long-lasting after-effects. *The Journal of Physiology*, *172*(3), 369–382. https://doi.org/10.1113/jphysiol.1964.sp007425

Bindu, B., Alladi, P. A., Mansooralikhan, B. M., Srikumar, B. N., Raju, T. R., & Kutty, B. M. (2007). Short-term exposure to an enriched environment enhances dendritic branching but not brain-derived neurotrophic factor expression in the hippocampus of rats with ventral subicular lesions. *Neuroscience*, *144*(2), 412–423. https://doi.org/10.1016/J.NEUROSCIENCE.2006.09.057

Birch, A. M., McGarry, N. B., & Kelly, Á. M. (2013). Short-term environmental enrichment, in the absence of exercise, improves memory, and increases NGF concentration, early neuronal survival, and synaptogenesis in the dentate gyrus in a time-dependent manner. *Hippocampus*, *23*(6), 437–450. https://doi.org/10.1002/hipo.22103

Bismuth, M., Funakoshi, N., Cadranel, J.-F., & Blanc, P. (2011). Hepatic encephalopathy. *European Journal of Gastroenterology & Hepatology*, *23*(1), 8–22. https://doi.org/10.1097/MEG.0b013e3283417567

Borgesius, N. Z., de Waard, M. C., van der Pluijm, I., Omrani, A., Zondag, G. C. M., van der Horst, G. T. J., … Elgersma, Y. (2011). Accelerated Age-Related Cognitive Decline and Neurodegeneration, Caused by Deficient DNA Repair. *Journal of Neuroscience*, *31*(35), 12543–12553. https://doi.org/10.1523/JNEUROSCI.1589-11.2011

Braddick, O., Campbell, F. W., & Atkinson, J. (1978). Channels in Vision: Basic Aspects. In *Perception* (pp. 3–38). Berlin, Heidelberg: Springer Berlin Heidelberg. https://doi.org/10.1007/978-3-642-

46354-9_1

Bravo-Nuevo, A., Walsh, N., & Stone, J. (2004). Photoreceptor Degeneration and Loss of Retinal Function in the C57BL/6-C ^{2J} Mouse. *Investigative Opthalmology & Visual Science*, *45*(6), 2005. https://doi.org/10.1167/iovs.03-0842

Brooks, P. J. (2008). The 8,5′-cyclopurine-2′-deoxynucleosides: Candidate neurodegenerative DNA lesions in xeroderma pigmentosum, and unique probes of transcription and nucleotide excision repair. *DNA Repair*, *7*(7), 1168–1179. https://doi.org/10.1016/j.dnarep.2008.03.016

Brown, G. R., & Nemes, C. (2008). The exploratory behaviour of rats in the hole-board apparatus: Is head-dipping a valid measure of neophilia? *Behavioural Processes*, *78*(3), 442. https://doi.org/10.1016/J.BEPROC.2008.02.019

Brown, R. E. (2006). The life and work of Donald Olding Hebb. *Acta Neurologica Taiwanica*, *15*(2), 127–142. Retrieved from http://www.ncbi.nlm.nih.gov/pubmed/16871901

Cahill, H., & Nathans, J. (2008). The Optokinetic Reflex as a Tool for Quantitative Analyses of Nervous System Function in Mice: Application to Genetic and Drug-Induced Variation. *PLoS ONE*, *3*(4), e2055. https://doi.org/10.1371/journal.pone.0002055

Campbell, F. W., Cooper, G. F., Robson, J. G., & Sachs, M. B. (1969). The spatial selectivity of visual cells of the cat and the squirrel monkey. *The Journal of Physiology*, *204*(2), 120P+. Retrieved from http://www.ncbi.nlm.nih.gov/pubmed/4980964

Cancedda, L., Putignano, E., Sale, A., Viegi, A., Berardi, N., & Maffei, L. (2004). Acceleration of visual system development by environmental enrichment. *Journal of Neuroscience*, *24*(20), 4840–4848. Retrieved from http://www.jneurosci.org/content/24/20/4840.short

Chalupa, L. M., & Williams, R. W. (2008). *Eye, retina, and visual system of the mouse*. MIT Press. Retrieved from https://mitpress.mit.edu/books/eye-retina-and-visual-system-mouse

Chan, C. Y., Hounsgaard, J., & Nicholson, C. (1988). Effects of electric fields on transmembrane potential and excitability of turtle cerebellar Purkinje cells in vitro. *The Journal of Physiology*, *402*(1), 751–771. https://doi.org/10.1113/jphysiol.1988.sp017232

Chan, C. Y., & Nicholson, C. (1986). Modulation by applied electric fields of Purkinje and stellate cell activity in the isolated turtle cerebellum. *The Journal of Physiology*, *371*(1), 89–114. https://doi.org/10.1113/jphysiol.1986.sp015963

Chapillon, P., Manneché, C., Belzung, C., & Caston, J. (1999). Rearing environmental enrichment in

two inbred strains of mice: 1. Effects on emotional reactivity. *Behavior Genetics*, *29*(1), 41–46. Retrieved from http://www.ncbi.nlm.nih.gov/pubmed/10371757

Chapman, B. B., & Corneil, B. D. (2008). Properties of human eye-head gaze shifts in an anti-gaze shift task. *Vision Research*, *48*(4), 538–548. https://doi.org/10.1016/J.VISRES.2007.11.014

Christie, J. M., Chiu, D. N., & Jahr, C. E. (2011). Ca2+-dependent enhancement of release by subthreshold somatic depolarization. *Nature Neuroscience*, *14*(1), 62–68. https://doi.org/10.1038/nn.2718

Collewijn, H. (1969). Optokinetic eye movements in the rabbit: Input-output relations. *Vision Research*, *9*(1), 117–132. https://doi.org/10.1016/0042-6989(69)90035-2

Collewijn, H. (1981). *The Oculomotor System of the Rabbit and Its Plasticity (Hardcover): H Collewijn: 9780387106786 | Books | Buy online in South Africa from Loot.co.za*. (V. Braitenberg, Ed.). Berlin: Springer Verlag . Retrieved from https://www.loot.co.za/product/h-collewijn-the-oculomotor-system-of-the-rabbit-and-its/tcgx-366-g360

Collewijn, H., Apkarian, P., & Spekreijse, H. (1985). The oculomotor behaviour of human albinos. *Brain*, *108*(1), 1–28. https://doi.org/10.1093/brain/108.1.1

Collewijn, H., Winterson, B., & Dubois, M. (1978). Optokinetic eye movements in albino rabbits: inversion in anterior visual field. *Science*, *199*(4335), 1351–1353. https://doi.org/10.1126/science.628845

Compston, A., & Coles, A. (2008). Multiple Sclerosis. *The Lancet*, *372*(9648), 1502–1517.

Cortese, G. P., Olin, A., O'Riordan, K., Hullinger, R., & Burger, C. (2018). Environmental enrichment improves hippocampal function in aged rats by enhancing learning and memory, LTP, and mGluR5-Homer1c activity. *Neurobiology of Aging*, *63*, 1–11. https://doi.org/10.1016/J.NEUROBIOLAGING.2017.11.004

Crawley, J. (2007). *What's wrong with my mouse? : behavioral phenotyping of transgenic and knockout mice*. Wiley-Interscience. Retrieved from https://books.google.nl/books?hl=en&lr=&id=CTES09IWtm0C&oi=fnd&pg=PR7&ots=HQ6atvgu6l&sig=BG_l_q5wt0XhI-B7E896UTJ2VG0&redir_esc=y#v=onepage&q&f=false

Crawley, J., & Goodwin, F. (1980). Preliminary report of a simple animal behavior model for the anxiolytic effects of benzodiazepines. *Pharmacology Biochemistry and Behavior*, *13*(2), 167–170. https://doi.org/10.1016/0091-3057(80)90067-2

Creel, D., Witkop, C. J., & King, R. A. (1974). Asymmetric visually evoked potentials in human albinos: evidence for visual system anomalies. *Investigative Ophthalmology*, *13*(6), 430–440. Retrieved from http://www.ncbi.nlm.nih.gov/pubmed/4831697

Creutzfeldt, O. D., Fromm, G. H., & Kapp, H. (1962). Influence of transcortical d-c currents on cortical neuronal activity. *Experimental Neurology*, *5*(6), 436–452. https://doi.org/10.1016/0014-4886(62)90056-0

Cucchiaro, J., & Guillery, R. (1984). The development of the retinogeniculate pathways in normal and albino ferrets. *Proceedings of the Royal Society of London. Series B. Biological Sciences*, *223*(1231), 141–164. https://doi.org/10.1098/rspb.1984.0087

Curcio, C., Millican, C., Allen KA, & Kalina, R. (1993). Aging of the human photoreceptor mosaic: evidence for selective vulnerability of rods in central retina. *Investigative Ophthalmology & Visual Science*, *34*(12), 3278–3296. Retrieved from https://iovs.arvojournals.org/article.aspx?articleid=2160884

Dalrymple, K. A., Manner, M. D., Harmelink, K. A., Teska, E. P., & Elison, J. T. (2018). An Examination of Recording Accuracy and Precision From Eye Tracking Data From Toddlerhood to Adulthood. *Frontiers in Psychology*, *9*, 803. https://doi.org/10.3389/fpsyg.2018.00803

Darrat, I., Ahmad, N., Seidman, K., & Seidman, M. D. (2007). Auditory research involving antioxidants. *Current Opinion in Otolaryngology & Head and Neck Surgery*, *15*(5), 358–363. https://doi.org/10.1097/MOO.0b013e3282efa641

Das, S., Holland, P., Frens, M. A., & Donchin, O. (2016). Impact of Transcranial Direct Current Stimulation (tDCS) on Neuronal Functions. *Frontiers in Neuroscience*, *10*. https://doi.org/10.3389/fnins.2016.00550

Das, S., Spoor, M., Sibindi, T. M., Holland, P., Schonewille, M., De Zeeuw, C. I., … Donchin, O. (2017). Impairment of Long-Term Plasticity of Cerebellar Purkinje Cells Eliminates the Effect of Anodal Direct Current Stimulation on Vestibulo-Ocular Reflex Habituation. *Frontiers in Neuroscience*, *11*, 444. https://doi.org/10.3389/fnins.2017.00444

Davis, R. R., Kuo, M.-W., Stanton, S. G., Krieg, E., & Alagramam, K. N. (2007). N-Acetyl l-cysteine does not protect against premature age-related hearing loss in C57BL/6J mice: A pilot study. *Hearing Research*, *226*(1), 203–208. https://doi.org/10.1016/j.heares.2006.07.003

de Jong, P. T. V. M. (2006). Age-Related Macular Degeneration. *New England Journal of Medicine*, *355*(14), 1474–1485. https://doi.org/10.1056/NEJMra062326

de Waard, M. C., van der Pluijm, I., Zuiderveen Borgesius, N., Comley, L. H., Haasdijk, E. D., Rijksen, Y., … Jaarsma, D. (2010). Age-related motor neuron degeneration in DNA repair-deficient Ercc1 mice. *Acta Neuropathologica*, *120*(4), 461–475. https://doi.org/10.1007/s00401-010-0715-9

De Zeeuw, C. I., Hoebeek, F. E., Bosman, L. W. J., Schonewille, M., Witter, L., & Koekkoek, S. K. (2011). Spatiotemporal firing patterns in the cerebellum. *Nature Reviews Neuroscience*, *12*(6), 327–344. https://doi.org/10.1038/nrn3011

De Zeeuw, C. I., & Ten Brinke, M. M. (2015). Motor Learning and the Cerebellum. *Cold Spring Harbor Perspectives in Biology*, *7*(9), a021683. https://doi.org/10.1101/cshperspect.a021683

Dell'Osso, L. F. (2006). Biologically Relevant Models of Infantile Nystagmus Syndrome: The Requirement for Behavioral Ocular Motor System Models. *Seminars in Ophthalmology*, *21*(2), 71–77. https://doi.org/10.1080/08820530600613795

Dell'osso, L. F., & Daroff, R. B. (1975). Congenital nystagmus waveforms and foveation strategy. *Documenta Ophthalmologica*, *39*(1), 155–182. https://doi.org/10.1007/BF00578761

Dell'Osso, L. F., & Williams, R. W. (1995). Ocular motor abnormalities in achiasmatic mutant Belgian sheepdogs: Unyoked eye movements in a mammal. *Vision Research*, *35*(1), 109–116. https://doi.org/10.1016/0042-6989(94)E0045-M

Dell'Osso, L. F., Williams, R. W., Jacobs, J. B., & Erchul, D. M. (1998). The congenital and see-saw nystagmus in the prototypical achiasma of canines: comparison to the human achiasmatic prototype. *Vision Research*, *38*(11), 1629–1641. Retrieved from http://www.ncbi.nlm.nih.gov/pubmed/9747500

Derefeldt, G., Lennerstrandt, G., & Lundh, B. (2009). Age Variations in Normal Human Contrast Sensitivity. *Acta Ophthalmologica*, *57*(4), 679–690. https://doi.org/10.1111/j.1755-3768.1979.tb00517.x

Derin, A., Agirdir, B., Derin, N., Dinc, O., Guney, K., Ozcaglar, H., & Kilincarslan, S. (2004). The effects of l-carnitine on presbyacusis in the rat model. *Clinical Otolaryngology and Allied Sciences*, *29*(3), 238–241. https://doi.org/10.1111/j.1365-2273.2004.00790.x

Donatien, P., Aigner, B., & Jeffery, G. (2002). Variations in cell density in the ganglion cell layer of the retina as a function of ocular pigmentation. *European Journal of Neuroscience*, *15*(10), 1597–1602. https://doi.org/10.1046/j.1460-9568.2002.02022.x

Dorn, P. A., Piskorski, P., Keefe, D. H., Neely, S. T., & Gorga, M. P. (1998). On the existence of an age/threshold/frequency interaction in distortion product otoacoustic emissions. *The Journal*

of the Acoustical Society of America, *104*(2), 964–971. https://doi.org/10.1121/1.423339

Dräger, U. C. (1974). Autoradiography of tritiated proline and fucose transported transneuronally from the eye to the visual cortex in pigmented and albino mice. *Brain Research*, *82*(2), 284–292. https://doi.org/10.1016/0006-8993(74)90607-6

Dräger, U. C., & Olsen, J. F. (1980). Origins of crossed and uncrossed retinal projections in pigmented and albino mice. *Journal of Comparative Neurology*, *191*(3), 383–412. https://doi.org/10.1002/cne.901910306

Drover, J. R., Wyatt, L. M., Stager, D. R., & Birch, E. E. (2009). The Teller Acuity Cards Are Effective in Detecting Amblyopia. *Optometry and Vision Science : Official Publication of the American Academy of Optometry*, *86*(6), 755. https://doi.org/10.1097/OPX.0B013E3181A523A3

Durga, J., Verhoef, P., Anteunis, L. J. C., Schouten, E., & Kok, F. J. (2007). Effects of Folic Acid Supplementation on Hearing in Older Adults. *Annals of Internal Medicine*, *146*(1), 1. https://doi.org/10.7326/0003-4819-146-1-200701020-00003

Elschnig, A. (1913). Zur Anatomie des menschlichen Albinoauges. *Albrecht von Graefes Archiv Für Ophthalmologie*, *84*(3), 401–419. https://doi.org/10.1007/BF02080368

Faherty, C., Kerley, D., & Smeyne, R. (2003). A Golgi-Cox morphological analysis of neuronal changes induced by environmental enrichment. *Developmental Brain Research*, *141*(1–2), 55–61. Retrieved from https://www.sciencedirect.com/science/article/pii/S0165380602006429

Fan, D., Li, J., Zheng, B., Hua, L., & Zuo, Z. (2016). Enriched Environment Attenuates Surgery-Induced Impairment of Learning, Memory, and Neurogenesis Possibly by Preserving BDNF Expression. *Molecular Neurobiology*, *53*(1), 344–354. https://doi.org/10.1007/s12035-014-9013-1

File, S., & Wardill, A. (1975a). The reliability of the hole-board apparatus. *Psychopharmacologia*, *44*(1), 47–51. https://doi.org/10.1007/BF00421183

File, S., & Wardill, A. (1975b). Validity of head-dipping as a measure of exploration in a modified hole-board. *Psychopharmacologia*, *44*, 53–59. Retrieved from https://link.springer.com/article/10.1007/BF00421184

Fletcher, A. E. (2010). Free Radicals, Antioxidants and Eye Diseases: Evidence from Epidemiological Studies on Cataract and Age-Related Macular Degeneration. *Ophthalmic Research*, *44*(3), 191–198. https://doi.org/10.1159/000316476

Forssman, B., & Ringnér, B. (1971). Prevalence and inheritance of congenital nystagmus in a Swedish

population. *Annals of Human Genetics*, *35*(2), 139–147. Retrieved from http://www.ncbi.nlm.nih.gov/pubmed/5159530

Foster, T. C., & Dumas, T. C. (2001). Mechanism for Increased Hippocampal Synaptic Strength Following Differential Experience. *Journal of Neurophysiology*, *85*(4), 1377–1383. https://doi.org/10.1152/jn.2001.85.4.1377

Foster, T. C., Gagne, J., & Massicotte, G. (1996). Mechanism of altered synaptic strength due to experience: relation to long-term potentiation. *Brain Research*, *736*(1–2), 243–250. https://doi.org/10.1016/0006-8993(96)00707-X

Frens, M. A., & Donchin, O. (2009). Forward models and state estimation in compensatory eye movements. *Frontiers in Cellular Neuroscience*, *3*, 13. https://doi.org/10.3389/neuro.03.013.2009

Fritsch, B., Reis, J., Martinowich, K., Schambra, H. M., Ji, Y., Cohen, L. G., & Lu, B. (2010). Direct Current Stimulation Promotes BDNF-Dependent Synaptic Plasticity: Potential Implications for Motor Learning. *Neuron*, *66*(2), 198–204. https://doi.org/10.1016/j.neuron.2010.03.035

Gaiser, C. (2019). *No Effect of Transcranial Direct Current Stimulation on Cortical Excitability: A pre-registered, randomized, repeated-meausres, placebo-controlled, double-blind Study.* Erasmus Univeristy.

Galea, J. M., Jayaram, G., Ajagbe, L., & Celnik, P. (2009). Modulation of Cerebellar Excitability by Polarity-Specific Noninvasive Direct Current Stimulation. *Journal of Neuroscience*, *29*(28), 9115–9122. https://doi.org/10.1523/JNEUROSCI.2184-09.2009

Galliano, E., Schonewille, M., Peter, S., Rutteman, M., Houtman, S., Jaarsma, D., … De Zeeuw, C. I. (2018). Impact of NMDA Receptor Overexpression on Cerebellar Purkinje Cell Activity and Motor Learning. *Eneuro*, *5*(1), ENEURO.0270-17.2018. https://doi.org/10.1523/ENEURO.0270-17.2018

Gao, H., & Hollyfield, J. (1992). Aging of the human retina. Differential loss of neurons and retinal pigment epithelial cells. *Investigative Ophthalmology & Visual Science*, *33*(1), 1–17. Retrieved from https://iovs.arvojournals.org/article.aspx?articleid=2160563

Gao, Z., van Beugen, B. J., & De Zeeuw, C. I. (2012). Distributed synergistic plasticity and cerebellar learning. *Nature Reviews Neuroscience*, *13*(9), 619–635. https://doi.org/10.1038/nrn3312

Gates, G. A., & Mills, J. H. (2005). Presbycusis. *The Lancet*, *366*(9491), 1111–1120. https://doi.org/10.1016/S0140-6736(05)67423-5

Gibson, R. A., & Sanderson, H. F. (1980). Observer variation in ophthalmology. *The British Journal of Ophthalmology*, *64*(6), 457–460. https://doi.org/10.1136/bjo.64.6.457

Gillet, L. C. J., & Schärer, O. D. (2006). Molecular Mechanisms of Mammalian Global Genome Nucleotide Excision Repair. *Chemical Reviews*, *106*(2), 253–276. https://doi.org/10.1021/cr040483f

Ginsburg, A. P. (2003). Contrast sensitivity and functional vision. *International Ophthalmology Clinics*, *43*(2), 5–15. Retrieved from http://www.ncbi.nlm.nih.gov/pubmed/12711899

Giolli, R. A., & Creel, D. J. (1974). Inheritance and variability of the organization of the retinogeniculate projections in pigmented and albino rats. *Brain Research*, *78*(2), 335–339. https://doi.org/10.1016/0006-8993(74)90559-9

Gorgels, T. G. M. F., van der Pluijm, I., Brandt, R. M. C., Garinis, G. A., van Steeg, H., van den Aardweg, G., … van der Horst, G. T. J. (2007). Retinal Degeneration and Ionizing Radiation Hypersensitivity in a Mouse Model for Cockayne Syndrome. *Molecular and Cellular Biology*, *27*(4), 1433–1441. https://doi.org/10.1128/MCB.01037-06

Greene, H. A., & Madden, D. J. (1987). Adult age differences in visual acuity, stereopsis, and contrast sensitivity. *American Journal of Optometry and Physiological Optics*, *64*(10), 749–753. Retrieved from http://www.ncbi.nlm.nih.gov/pubmed/3688177

Greenough, W. T., & Volkmar, F. R. (1973). Pattern of dendritic branching in occipital cortex of rats reared in complex environments. *Experimental Neurology*, *40*(2), 491–504. https://doi.org/10.1016/0014-4886(73)90090-3

Greenough, W. T., Volkmar, F. R., & Juraska, J. M. (1973). Effects of rearing complexity on dendritic branching in frontolateral and temporal cortex of the rat. *Experimental Neurology*, *41*(2), 371–378. https://doi.org/10.1016/0014-4886(73)90278-1

Greifzu, F., Kalogeraki, E., & Löwel, S. (2016). Environmental enrichment preserved lifelong ocular dominance plasticity, but did not improve visual abilities. *Neurobiology of Aging*, *41*, 130–137. https://doi.org/10.1016/J.NEUROBIOLAGING.2016.02.014

Gresty, M., Page, N., & Barratt, H. (1984). The differential diagnosis of congenital nystagmus. *Journal of Neurology, Neurosurgery & Psychiatry*, *47*(9), 936–942. https://doi.org/10.1136/jnnp.47.9.936

Guillery, R. W. (1969). An abnormal retinogeniculate projection in Siamese cats. *Brain Research*, *14*(3), 739–741. https://doi.org/10.1016/0006-8993(69)90213-3

Guillery, R. W. (1971). An abnormal retinogeniculate projection in the albino ferret (Mustela furo). *Brain Research*, *33*(2), 482–485. https://doi.org/10.1016/0006-8993(71)90121-1

Guillery, R. W., Hickey, T. L., Kaas, J. H., Felleman, D. J., Debruyn, E. J., & Sparks, D. L. (1984). Abnormal central visual pathways in the brain of an albino green monkey (Cercopithecus aethiops). *The Journal of Comparative Neurology*, *226*(2), 165–183. https://doi.org/10.1002/cne.902260203

Guillery, R. W., & Kaas, J. H. (1973). Genetic Abnormality of the Visual Pathways in a "White" Tiger. *Science*, *180*(4092), 1287–1289. https://doi.org/10.1126/science.180.4092.1287

Guillery, R. W., Okoro, A. N., & Witkop, C. J. (1975). Abnormal visual pathways in the brain of a human albino. *Brain Research*, *96*(2), 373–377. https://doi.org/10.1016/0006-8993(75)90750-7

Guillery, R. W., Scott, G. L., Cattanach, B. M., & Deol, M. S. (1973). Genetic Mechanisms Determining the Central Visual Pathways of Mice. *Science*, *179*(4077), 1014–1016. https://doi.org/10.1126/science.179.4077.1014

Gutierrez-Castellanos, N., Winkelman, B. H. J., Tolosa-Rodriguez, L., De Gruijl, J. R., & De Zeeuw, C. I. (2013). Impact of aging on long-term ocular reflex adaptation. *Neurobiology of Aging*, *34*(12), 2784–2792. https://doi.org/10.1016/j.neurobiolaging.2013.06.012

Hall, C. (1934). Emotional behavior in the rat. I. Defecation and urination as measures of individual differences in emotionality. *Journal of Comparative Psychology*, *18*(3), 385–403. Retrieved from https://insights.ovid.com/comparative-psychology/jopsy/1934/12/000/emotional-behavior-rat-defecation-urination/7/01437424

Hall, C. (1936). Emotional behavior in the rat. III. The relationship between emotionality and ambulatory activity. *Journal of Comparative Psychology*, *22*(3), 345–352. Retrieved from https://insights.ovid.com/comparative-psychology/jopsy/1936/12/000/emotional-behavior-rat-iii-relationship/3/01437424

Hallermann, S., Eshra, A., & Hirrlinger, P. (2019). Enriched environment shortens the duration of action potentials in cerebellar granule cells. *Frontiers in Cellular Neuroscience*, *13*, 289. https://doi.org/10.3389/FNCEL.2019.00289

Halmagyi, G. M., Gresty, M. A., & Leech, J. (1980). Reversed Optokinetic Nystagmus (OKN): Mechanism and Clinical Significance. *Annals of Neurology*, *7*(5), 429–435. https://doi.org/10.1002/ana.410070507

Hansel, C. (2005). When the B-team runs plasticity: GluR2 receptor trafficking in cerebellar long-term potentiation. *Proceedings of the National Academy of Sciences*, *102*(51), 18245–18246. https://doi.org/10.1073/pnas.0509686102

Hardwick, R. M., & Celnik, P. A. (2014). Cerebellar direct current stimulation enhances motor learning in older adults. *Neurobiology of Aging*, *35*(10), 2217–2221. https://doi.org/10.1016/j.neurobiolaging.2014.03.030

Harris, C., & Berry, D. (2006). A Developmental Model of Infantile Nystagmus. *Seminars in Ophthalmology*, *21*(2), 63–69. https://doi.org/10.1080/08820530600613746

Hellström, A., Smith, L. E., & Dammann, O. (2013). Retinopathy of prematurity. *The Lancet*, *382*(9902), 1445–1457. https://doi.org/10.1016/S0140-6736(13)60178-6

Heman-Ackah, S. E., Juhn, S. K., Huang, T. C., & Wiedmann, T. S. (2010). A combination antioxidant therapy prevents age-related hearing loss in C57BL/6 mice. *Otolaryngology - Head and Neck Surgery*, *143*(3), 429–434. https://doi.org/10.1016/j.otohns.2010.04.266

Herzfeld, D. J., Pastor, D., Haith, A. M., Rossetti, Y., Shadmehr, R., & O'Shea, J. (2014). Contributions of the cerebellum and the motor cortex to acquisition and retention of motor memories. *NeuroImage*, *98*, 147–158. https://doi.org/10.1016/j.neuroimage.2014.04.076

Hessels, R. S., Andersson, R., Hooge, I. T. C., Nyström, M., & Kemner, C. (2015). Consequences of Eye Color, Positioning, and Head Movement for Eye-Tracking Data Quality in Infant Research. *Infancy*, *20*(6), 601–633. https://doi.org/10.1111/infa.12093

Hessels, R. S., Hooge, I. T. C., & Kemner, C. (2016). An in-depth look at saccadic search in infancy. *Journal of Vision*, *16*(8), 10. https://doi.org/10.1167/16.8.10

Hoffmann, M. B., Lorenz, B., Morland, A. B., & Schmidtborn, L. C. (2005). Misrouting of the Optic Nerves in Albinism: Estimation of the Extent with Visual Evoked Potentials. *Investigative Opthalmology & Visual Science*, *46*(10), 3892. https://doi.org/10.1167/iovs.05-0491

Howarth, A. (2006). Ageing and the auditory system. *Postgraduate Medical Journal*, *82*(965), 166–171. https://doi.org/10.1136/pgmj.2005.039388

Huang, Y.-Y., Rinner, O., Hedinger, P., Liu, S.-C., & Neuhauss, S. C. F. (2006). Oculomotor Instabilities in Zebrafish Mutant belladonna: A Behavioral Model for Congenital Nystagmus Caused by Axonal Misrouting. *Journal of Neuroscience*, *26*(39), 9873–9880. https://doi.org/10.1523/JNEUROSCI.2886-06.2006

Huberman, A. D., & Niell, C. M. (2011). What can mice tell us about how vision works? *Trends in Neurosciences*, *34*(9), 464–473. https://doi.org/10.1016/j.tins.2011.07.002

Hummel, F., Celnik, P., Giraux, P., Floel, A., Wu, W.-H., Gerloff, C., & Cohen, L. G. (2005). Effects of non-invasive cortical stimulation on skilled motor function in chronic stroke. *Brain*, *128*(3), 490–499. https://doi.org/10.1093/brain/awh369

Ickes, B. R., Pham, T. M., Sanders, L. A., Albeck, D. S., Mohammed, A. H., & Granholm, A.-C. (2000). Long-Term Environmental Enrichment Leads to Regional Increases in Neurotrophin Levels in Rat Brain. *Experimental Neurology*, *164*(1), 45–52. https://doi.org/10.1006/EXNR.2000.7415

Ilia, M., & Jeffery, G. (1996). Delayed neurogenesis in the albino retina: evidence of a role for melanin in regulating the pace of cell generation. *Developmental Brain Research*, *95*(2), 176–183. https://doi.org/10.1016/0165-3806(96)00075-2

Inagaki, K., & Hirata, Y. (2017). Computational Theory Underlying Acute Vestibulo-ocular Reflex Motor Learning with Cerebellar Long-Term Depression and Long-Term Potentiation. *Cerebellum (London, England)*, *16*(4), 827–839. https://doi.org/10.1007/s12311-017-0857-6

Ito, M. (1982). Cerebellar Control of the Vestibulo-Ocular Reflex--Around the Flocculus Hypothesis. *Annual Review of Neuroscience*, *5*(1), 275–297. https://doi.org/10.1146/annurev.ne.05.030182.001423

Ivry, R. B., & Spencer, R. M. (2004). The neural representation of time. *Current Opinion in Neurobiology*, *14*(2), 225–232. https://doi.org/10.1016/j.conb.2004.03.013

Iwasaki, S., & Kaga, K. (1994). *Chronological changes of auditory brainstem responses in Cockayne's syndrome*. *International Journal of Pediatric Otorhinolaryngology* (Vol. 30). https://doi.org/10.1016/0165-5876(94)90062-0

Jacobs, J. B., & Dell'Osso, L. F. (2004). Congenital nystagmus: Hypotheses for its genesis and complex waveforms within a behavioral ocular motor system model. *Journal of Vision*, *4*(7), 7. https://doi.org/10.1167/4.7.7

Jadavji, N. M., Kolb, B., & Metz, G. A. (2006). Enriched environment improves motor function in intact and unilateral dopamine-depleted rats. *Neuroscience*, *140*(4), 1127–1138. https://doi.org/10.1016/J.NEUROSCIENCE.2006.03.027

Jayaram, G., Tang, B., Pallegadda, R., Vasudevan, E. V. L., Celnik, P., & Bastian, A. (2012). Modulating locomotor adaptation with cerebellar stimulation. *Journal of Neurophysiology*, *107*(11), 2950–2957. https://doi.org/10.1152/jn.00645.2011

Jeffery, G., Brem, G., & Montoliu, L. (1997). Correction of retinal abnormalities found in albinism by introduction of a functional tyrosinase gene in transgenic mice and rabbits. *Developmental Brain Research*, *99*(1), 95–102. https://doi.org/10.1016/S0165-3806(96)00211-8

Jeffery, G., & Kinsella, B. (1992). Translaminar deficits in the retinae of albinos. *The Journal of Comparative Neurology*, *326*(4), 637–644. https://doi.org/10.1002/cne.903260410

Jeffery, G., Schütz, G., & Montoliu, L. (1994). Correction of Abnormal Retinal Pathways Found with Albinism by Introduction of a Functional Tyrosinase Gene in Transgenic Mice. *Developmental Biology*, *166*(2), 460–464. https://doi.org/10.1006/dbio.1994.1329

Jiang, H., Talaska, A. E., Schacht, J., & Sha, S.-H. (2007). Oxidative imbalance in the aging inner ear. *Neurobiology of Aging*, *28*(10), 1605–1612. https://doi.org/10.1016/j.neurobiolaging.2006.06.025

Jiménez-Cervantes, C., Solano, F., Kobayashi, T., Urabe, K., Hearing, V. J., Lozano, J. A., & García-Borrón, J. C. (1994). A new enzymatic function in the melanogenic pathway. The 5,6-dihydroxyindole-2-carboxylic acid oxidase activity of tyrosinase-related protein-1 (TRP1). *The Journal of Biological Chemistry*, *269*(27), 17993–18000. Retrieved from http://www.ncbi.nlm.nih.gov/pubmed/8027058

Kara-Junior, N., Espindola, R. F., Gomes, B. A. F., Ventura, B., Smadja, D., & Santhiago, M. R. (2011). Effects of blue light–filtering intraocular lenses on the macula, contrast sensitivity, and color vision after a long-term follow-up. *Journal of Cataract & Refractive Surgery*, *37*(12), 2115–2119. https://doi.org/10.1016/J.JCRS.2011.06.024

Kawato, M., & Gomi, H. (1992). The cerebellum and VOR/OKR learning models. *Trends in Neurosciences*, *15*(11), 445–453. https://doi.org/10.1016/0166-2236(92)90008-V

Kelly, J. P., & Weiss, A. H. (2006). Topographical Retinal Function in Oculocutaneous Albinism. *American Journal of Ophthalmology*, *141*(6), 1156–1158. https://doi.org/10.1016/j.ajo.2006.01.045

Kenyon, G. S., Booth, J. B., Prasher, D. K., & Rudge, P. (1985). Neuro-otological Abnormalities in Xeroderma Pigmentosum with Particular Reference to Deafness. *Brain*, *108*(3), 771–784. https://doi.org/10.1093/brain/108.3.771

Kline, L., Arnold, A., & Eggenberger, E. (2008). No Title. In *Basic and Clinical Science Course: Section 5: Neuro-Ophthalmology* (p. 27). San Francisco, CA: American Academy of Opthalmology.

Knieling, M., Metz, G. A., Antonow-Schlorke, I., & Witte, O. W. (2009). Enriched environment

promotes efficiency of compensatory movements after cerebral ischemia in rats. *Neuroscience*, *163*(3), 759–769. https://doi.org/10.1016/J.NEUROSCIENCE.2009.07.004

Kobayashi, T., Urabe, K., Winder, A., Jiménez-Cervantes, C., Imokawa, G., Brewington, T., … Hearing, V. J. (1994). Tyrosinase related protein 1 (TRP1) functions as a DHICA oxidase in melanin biosynthesis. *The EMBO Journal*, *13*(24), 5818–5825. Retrieved from http://www.ncbi.nlm.nih.gov/pubmed/7813420

Kolpakov, V. G., Alekhina, T. A., Barykina, N. N., Chugui, V. F., & Popova, N. K. (2001). Some physiological manifestations of the activity of the gene controlling the predisposition to pendulum-like movements in rats. *Neuroscience and Behavioral Physiology*, *31*(3), 311–316. Retrieved from http://www.ncbi.nlm.nih.gov/pubmed/11430576

Kraemer, K. H., Patronas, N. J., Schiffmann, R., Brooks, B. P., Tamura, D., & DiGiovanna, J. J. (2007). Xeroderma pigmentosum, trichothiodystrophy and Cockayne syndrome: A complex genotype–phenotype relationship. *Neuroscience*, *145*(4), 1388–1396. https://doi.org/10.1016/j.neuroscience.2006.12.020

Krause, B., & Cohen Kadosh, R. (2014). Not all brains are created equal: the relevance of individual differences in responsiveness to transcranial electrical stimulation. *Frontiers in Systems Neuroscience*, *8*, 25. https://doi.org/10.3389/fnsys.2014.00025

Lamont, M. G., & Weber, J. T. (2012). The role of calcium in synaptic plasticity and motor learning in the cerebellar cortex. *Neuroscience & Biobehavioral Reviews*, *36*(4), 1153–1162. https://doi.org/10.1016/j.neubiorev.2012.01.005

Langevin, F., Crossan, G. P., Rosado, I. V., Arends, M. J., & Patel, K. J. (2011). Fancd2 counteracts the toxic effects of naturally produced aldehydes in mice. *Nature*, *475*(7354), 53–58. https://doi.org/10.1038/nature10192

Lavado, A., Jeffery, G., Tovar, V., Villa, P., & Montoliu, L. (2006). Ectopic expression of tyrosine hydroxylase in the pigmented epithelium rescues the retinal abnormalities and visual function common in albinos in the absence of melanin. *Journal of Neurochemistry*, *96*(4), 1201–1211. https://doi.org/10.1111/j.1471-4159.2006.03657.x

Lavail, J. H., Nixon, R. A., & Sidman, R. L. (1978). Genetic control of retinal ganglion cell projections. *The Journal of Comparative Neurology*, *182*(3), 399–421. https://doi.org/10.1002/cne.901820304

Lawrence, N. J., Sacco, J. J., Brownstein, D. G., Gillingwater, T. H., & Melton, D. W. (2008). A

neurological phenotype in mice with DNA repair gene Ercc1 deficiency. *DNA Repair*, *7*(2), 281–291. https://doi.org/10.1016/j.dnarep.2007.10.005

Le, T., & Keithley, E. M. (2007). Effects of antioxidants on the aging inner ear. *Hearing Research*, *226*(1), 194–202. https://doi.org/10.1016/j.heares.2006.04.003

Leach, M. C., Ambrose, N., Bowell, V. J., & Morton, D. B. (2000). The Development of a Novel Form of Mouse Cage Enrichment. *Journal of Applied Animal Welfare Science*, *3*(2), 81–91. https://doi.org/10.1207/S15327604JAWS0302_1

Leggio, M. G., Mandolesi, L., Federico, F., Spirito, F., Ricci, B., Gelfo, F., & Petrosini, L. (2005). Environmental enrichment promotes improved spatial abilities and enhanced dendritic growth in the rat. *Behavioural Brain Research*, *163*(1), 78–90. https://doi.org/10.1016/J.BBR.2005.04.009

Leguire, L. E., Zaff, B. S., Freeman, S., Rogers, G. L., Bremer, D. L., & Wali, N. (1991). Contrast sensitivity of optokinetic nystagmus. *Vision Research*, *31*(1), 89–97. https://doi.org/10.1016/0042-6989(91)90076-H

Leigh, R., & Zee, D. (2015). *The neurology of eye movements*. USA: OUP. Retrieved from https://books.google.nl/books?hl=nl&lr=&id=v2s0BwAAQBAJ&oi=fnd&pg=PP1&dq=leigh+zee&ots=4qvkTaEPyM&sig=B-2y90uVA4umHdshOqE9t4nunsE

Lewis, M. H. (2004). Environmental complexity and central nervous system development and function. *Mental Retardation and Developmental Disabilities Research Reviews*, *10*(2), 91–95. https://doi.org/10.1002/mrdd.20017

Liebetanz, D., Fregni, F., Monte-Silva, K. K., Oliveira, M. B., Amâncio-dos-Santos, Â., Nitsche, M. A., & Guedes, R. C. A. (2006). After-effects of transcranial direct current stimulation (tDCS) on cortical spreading depression. *Neuroscience Letters*, *398*(1–2), 85–90. https://doi.org/10.1016/j.neulet.2005.12.058

Liebetanz, D., Klinker, F., Hering, D., Koch, R., Nitsche, M. A., Potschka, H., … Tergau, F. (2006). Anticonvulsant Effects of Transcranial Direct-current Stimulation (tDCS) in the Rat Cortical Ramp Model of Focal Epilepsy. *Epilepsia*, *47*(7), 1216–1224. https://doi.org/10.1111/j.1528-1167.2006.00539.x

Liebetanz, D., Koch, R., Mayenfels, S., König, F., Paulus, W., & Nitsche, M. A. (2009). Safety limits of cathodal transcranial direct current stimulation in rats. *Clinical Neurophysiology*, *120*(6), 1161–1167. https://doi.org/10.1016/j.clinph.2009.01.022

Lisberger, S. G., & Fuchs, A. F. (1974). Response of flocculus Purkinje cells to adequate vestibular stimulation in the alert monkey: fixation vs. compensatory eye movements. *Brain Research*, *69*(2), 347–353. https://doi.org/10.1016/0006-8993(74)90013-4

Lorenz, B., & Gampe, E. (2001). Analyse von 180 Patienten mit sensorischem Defektnystagmus (SDN) und kongenitalem idiopathischen Nystagmus (CIN)12. *Klinische Monatsblätter Für Augenheilkunde*, *218*(1), 3–12. https://doi.org/10.1055/s-2001-11254

Lu, H., Li, L., Watson, E. R., Williams, R. W., Geisert, E. E., Jablonski, M. M., & Lu, L. (2011). Complex interactions of Tyrp1 in the eye. *Molecular Vision*, *17*, 2455–2468. Retrieved from http://www.ncbi.nlm.nih.gov/pubmed/21976956

Lund, R. D. (1965). Uncrossed Visual Pathways of Hooded and Albino Rats. *Science*, *149*(3691), 1506–1507. https://doi.org/10.1126/science.149.3691.1506

Lütcke, H., Murayama, M., Hahn, T., Margolis, D. J., Astori, S., Zum Alten Borgloh, S. M., … Hasan, M. T. (2010). Optical recording of neuronal activity with a genetically-encoded calcium indicator in anesthetized and freely moving mice. *Frontiers in Neural Circuits*, *4*, 9. https://doi.org/10.3389/fncir.2010.00009

Maffei, L., & Fiorentini, A. (1973). The visual cortex as a spatial frequency analyser. *Vision Research*, *13*(7), 1255–1267. https://doi.org/10.1016/0042-6989(73)90201-0

Mangini, N. J., Vanable, J. W., Williams, M. A., & Pinto, L. H. (1985). The optokinetic nystagmus and ocular pigmentation of hypopigmented mouse mutants. *The Journal of Comparative Neurology*, *241*(2), 191–209. https://doi.org/10.1002/cne.902410207

Marashi, V., Barnekow, A., Ossendorf, E., & Sachser, N. (2003). Effects of different forms of environmental enrichment on behavioral, endocrinological, and immunological parameters in male mice. *Hormones and Behavior*, *43*(2), 281–292. https://doi.org/10.1016/S0018-506X(03)00002-3

Markowitz, H., & Gavassi, A. (1995). Eleven principles for improving the quality of captive animal life. *Lab Animal*, *24*, 30–33. Retrieved from https://books.google.nl/books?id=xCFeAgAAQBAJ&pg=PA157&lpg=PA157&dq=%22Eleven+principles+for+improving+the+quality+of+captive+animal+life%22&source=bl&ots=Vv0nmCb9nw&sig=ACfU3U271qJzDOi97c5Cr36bsngP1XsJkQ&hl=nl&sa=X&ved=2ahUKEwicmf319KzjAhVHaVAKHYd4Dt4Q6A

Marquez-Ruiz, J., Leal-Campanario, R., Sanchez-Campusano, R., Molaee-Ardekani, B., Wendling, F.,

Miranda, P. C., … Delgado-Garcia, J. M. (2012). Transcranial direct-current stimulation modulates synaptic mechanisms involved in associative learning in behaving rabbits. *Proceedings of the National Academy of Sciences*, *109*(17), 6710–6715. https://doi.org/10.1073/pnas.1121147109

Marquez, J., van Vliet, P., McElduff, P., Lagopoulos, J., & Parsons, M. (2015). Transcranial Direct Current Stimulation (tDCS): Does it Have Merit in Stroke Rehabilitation? A Systematic Review. *International Journal of Stroke*, *10*(3), 306–316. https://doi.org/10.1111/ijs.12169

Maybodi, M. (2003). Infantile-onset nystagmus. *Current Opinion in Ophthalmology*, *14*(5), 276–285. https://doi.org/10.1097/00055735-200310000-00008

McFadden, S. L., Ding, D., Burkard, R. F., Jiang, H., Reaume, A. G., Flood, D. G., & Salvi, R. J. (1999). Cu/Zn SOD deficiency potentiates hearing loss and cochlear pathology in aged 129,CD-1 mice. *The Journal of Comparative Neurology*, *413*(1), 101–112. https://doi.org/10.1002/(SICI)1096-9861(19991011)413:1<101::AID-CNE7>3.0.CO;2-L

McFadden, S. L., Ding, D., Reaume, A. G., Flood, D. G., & Salvi, R. J. (1999). Age-related cochlear hair cell loss is enhanced in mice lacking copper/zinc superoxide dismutase. *Neurobiology of Aging*, *20*(1), 1–8. https://doi.org/10.1016/S0197-4580(99)00018-4

McGrath, C., & Morrison, J. D. (1981). THE EFFECTS OF AGE ON SPATIAL FREQUENCY PERCEPTION IN HUMAN SUBJECTS. *Quarterly Journal of Experimental Physiology*, *66*(3), 253–261. https://doi.org/10.1113/expphysiol.1981.sp002554

McMullen, C. A., Andrade, F. H., & Stahl, J. S. (2004). Functional and Genomic Changes in the Mouse Ocular Motor System in Response to Light Deprivation from Birth. *Journal of Neuroscience*, *24*(1), 161–169. https://doi.org/10.1523/JNEUROSCI.3234-03.2004

McWhir, J., Selfridge, J., Harrison, D. J., Squires, S., & Melton, D. W. (1993). Mice with DNA repair gene (ERCC-1) deficiency have elevated levels of p53, liver nuclear abnormalities and die before weaning. *Nature Genetics*, *5*(3), 217–224. https://doi.org/10.1038/ng1193-217

Mehdorn, E., & Schade, K. (1988). Mechanism of "inversion; of optokinetic nystagmus and pursuit movement in congenital nystagmus. *Fortschritte Der Ophthalmologie : Zeitschrift Der Deutschen Ophthalmologischen Gesellschaft*, *85*(3), 285–288. Retrieved from http://www.ncbi.nlm.nih.gov/pubmed/3209158

Mimaki, T., Itoh, N., Abe, J., Tagawa, T., Sato, K., Yabuuchi, H., & Takebe, H. (1986). Neurological manifestations in xeroderma pigmentosum. *Annals of Neurology*, *20*(1), 70–75.

https://doi.org/10.1002/ana.410200112

Minarik, T., Berger, B., Althaus, L., Bader, V., Biebl, B., Brotzeller, F., … Sauseng, P. (2016). The Importance of Sample Size for Reproducibility of tDCS Effects. *Frontiers in Human Neuroscience*, *10*, 453. https://doi.org/10.3389/fnhum.2016.00453

Morland, A., Hoffmann, M., Neveu, M., & Holder, G. (2002). Abnormal visual projection in a human albino studied with functional magnetic resonance imaging and visual evoked potentials. *J Neurol Neurosurg Psychiatry*, *72*, 523–526.

Nameda, N., Kawara, T., & Ohzu, H. (1989). Human Visual Spatio-Temporal Frequency Performance as a Function of Age. *Optometry and Vision Science*, *66*(11), 760–765. https://doi.org/10.1097/00006324-198911000-00007

Naumann, G. O. H., Lerche, W., & Schroeder, W. (1976). Foveola-Aplasie bei Tyrosinase-positivem oculocutanen Albinismus. *Albrecht von Graefes Archiv F*[illegible]*r Klinische Und Experimentelle Ophthalmologie*, *200*(1), 39–50. https://doi.org/10.1007/BF00411431

Nguyen-Vu, T. D. B., Kimpo, R. R., Rinaldi, J. M., Kohli, A., Zeng, H., Deisseroth, K., & Raymond, J. L. (2013). Cerebellar Purkinje cell activity drives motor learning. *Nature Neuroscience*, *16*(12), 1734–1736. https://doi.org/10.1038/nn.3576

Niedernhofer, L. J., Garinis, G. A., Raams, A., Lalai, A. S., Robinson, A. R., Appeldoorn, E., … Hoeijmakers, J. H. J. (2006). A new progeroid syndrome reveals that genotoxic stress suppresses the somatotroph axis. *Nature*, *444*(7122), 1038–1043. https://doi.org/10.1038/nature05456

Nomura, H., Ando, F., Niino, N., Shimokata, H., & Miyake, Y. (2003). Age-related Change in Contrast Sensitivity Among Japanese Adults. *Japanese Journal of Ophthalmology*, *47*(3), 299–303. https://doi.org/10.1016/S0021-5155(03)00011-X

Novkovic, T., Mittmann, T., & Manahan-Vaughan, D. (2015). BDNF contributes to the facilitation of hippocampal synaptic plasticity and learning enabled by environmental enrichment. *Hippocampus*, *25*(1), 1–15. https://doi.org/10.1002/hipo.22342

Nyström, M., Hooge, I., & Andersson, R. (2016). Pupil size influences the eye-tracker signal during saccades. *Vision Research*, *121*, 95–103. https://doi.org/10.1016/J.VISRES.2016.01.009

Oeken, J., Lenk, F. A., & Bootz, F. (2000). Influence of Age and Presbyacusis on DPOAE. *Acta Oto-Laryngologica*, *120*(3), 396–403. https://doi.org/10.1080/000164800750000630

Oetting, W. S., & King, R. A. (1999). Molecular basis of albinism: Mutations and polymorphisms of pigmentation genes associated with albinism. *Human Mutation*, *13*(2), 99–115. https://doi.org/10.1002/(SICI)1098-1004(1999)13:2<99::AID-HUMU2>3.0.CO;2-C

Ohlemiller, K. K. (2006). Contributions of mouse models to understanding of age- and noise-related hearing loss. *Brain Research*, *1091*(1), 89–102. https://doi.org/10.1016/j.brainres.2006.03.017

Olsson, I. A. S., & Dahlborn, K. (2002). Improving housing conditions for laboratory mice: a review of "environmental enrichment." *Laboratory Animals*, *36*(3), 243–270. https://doi.org/10.1258/002367702320162379

Olzak, L. A., & Thomas, J. P. (1981). Gratings: why frequency discrimination is sometimes better than detection. *Journal of the Optical Society of America*, *71*(1), 64. https://doi.org/10.1364/JOSA.71.000064

Optican, L. M., & Zee, D. S. (1984). A hypothetical explanation of congenital nystagmus. *Biological Cybernetics*, *50*(2), 119–134. https://doi.org/10.1007/BF00337159

Owsley, C., Sekuler, R., & Siemsen, D. (1983). Contrast sensitivity throughout adulthood. *Vision Research*, *23*(7), 689–699. https://doi.org/10.1016/0042-6989(83)90210-9

Paige, G. (1994). Senescence of human visual-vestibular interactions: smooth pursuit, optokinetic, and vestibular control of eye movements with aging. *Experimental Brain Research*, *98*(2), 355–372. https://doi.org/10.1007/BF00228423

Pak, M. W., Pinto, L. H., Mangini, N. J., Vanable, J. W., Giolli, R. A., & Gregory, K. M. (1987). Retinopretectal and accessory optic projections of normal mice and the OKN-defective mutant mice beige, beige-J, and pearl. *The Journal of Comparative Neurology*, *258*(3), 435–446. https://doi.org/10.1002/cne.902580311

Panda-Jonas, S., Jonas, J. B., & Jakobczyk-Zmija, M. (1995). Retinal Photoreceptor Density Decreases with Age. *Ophthalmology*, *102*(12), 1853–1859. https://doi.org/10.1016/S0161-6420(95)30784-1

Pandit, J. C. (1994). Testing acuity of vision in general practice: reaching recommended standard. *BMJ (Clinical Research Ed.)*, *309*(6966), 1408. https://doi.org/10.1136/bmj.309.6966.1408

Pel, J. J. M., Manders, J. C. W., & van der Steen, J. (2010). Assessment of visual orienting behaviour in young children using remote eye tracking: Methodology and reliability. *Journal of Neuroscience Methods*, *189*(2), 252–256. https://doi.org/10.1016/J.JNEUMETH.2010.04.005

Perry, V. H., & Cowey, A. (1985). The ganglion cell and cone distributions in the monkey's retina: Implications for central magnification factors. *Vision Research*, *25*(12), 1795–1810. https://doi.org/10.1016/0042-6989(85)90004-5

Pham, T. ., Ickes, B., Albeck, D., Söderström, S., Granholm, A.-C., & Mohammed, A. . (1999). Changes in brain nerve growth factor levels and nerve growth factor receptors in rats exposed to environmental enrichment for one year. *Neuroscience*, *94*(1), 279–286. https://doi.org/10.1016/S0306-4522(99)00316-4

Pickles, J. O. (2004). Mutation in Mitochondrial DNA as a Cause of Presbyacusis. *Audiology and Neurotology*, *9*(1), 23–33. https://doi.org/10.1159/000074184

Pinto, L. H., & Enroth-Cugell, C. (2000). Tests of the mouse visual system. *Mammalian Genome*, *11*(7), 531–536. https://doi.org/10.1007/s003350010102

Pott, J. W. R., Jansonius, N. M., & Kooijman, A. C. (2003). Chiasmal coefficient of flash and pattern visual evoked potentials for detection of chiasmal misrouting in albinism. *Documenta Ophthalmologica. Advances in Ophthalmology*, *106*(2), 137–143. Retrieved from http://www.ncbi.nlm.nih.gov/pubmed/12678278

Powell, S. B., Newman, H. A., McDonald, T. A., Bugenhagen, P., & Lewis, M. H. (2000). Development of spontaneous stereotyped behavior in deer mice: Effects of early and late exposure to a more complex environment. *Developmental Psychobiology*, *37*(2), 100–108. https://doi.org/10.1002/1098-2302(200009)37:2<100::AID-DEV5>3.0.CO;2-6

Probst, T., Brandt, T., & Degner, D. (1986). Object-motion detection affected by concurrent self-motion perception: Psychophysics of a new phenomenon. *Behavioural Brain Research*, *22*(1), 1–11. https://doi.org/10.1016/0166-4328(86)90076-8

Prusky, G. T., Reidel, C., & Douglas, R. M. (2000). Environmental enrichment from birth enhances visual acuity but not place learning in mice. *Behavioural Brain Research*, *114*(1–2), 11–15. https://doi.org/10.1016/S0166-4328(00)00186-8

Puk, O., Dalke, C., Hrabé de Angelis, M., & Graw, J. (2008). Variation of the response to the optokinetic drum among various strains of mice. *Frontiers in Bioscience : A Journal and Virtual Library*, *13*, 6269–6275. Retrieved from http://www.ncbi.nlm.nih.gov/pubmed/18508659

Purpura, D. P., & McMurtry, J. G. (1965). Intracellular activities and evoked potential changes during polarization of motor cortex. *Journal of Neurophysiology*, *28*, 166–185. https://doi.org/10.1152/jn.1965.28.1.166

Rampon, C., Jiang, C. H., Dong, H., Tang, Y. P., Lockhart, D. J., Schultz, P. G., … Hu, Y. (2000). Effects of environmental enrichment on gene expression in the brain. *Proceedings of the National Academy of Sciences of the United States of America*, *97*(23), 12880–12884. https://doi.org/10.1073/pnas.97.23.12880

Rangarajan, K. V., Lawhn-Heath, C., Feng, L., Kim, T. S., Cang, J., & Liu, X. (2011). Detection of Visual Deficits in Aging DBA/2J Mice by Two Behavioral Assays. *Current Eye Research*, *36*(5), 481–491. https://doi.org/10.3109/02713683.2010.549600

Rapin, I., Weidenheim, K., Lindenbaum, Y., Rosenbaum, P., Merchant, S. N., Krishna, S., & Dickson, D. W. (2006). Cockayne Syndrome in Adults: Review With Clinical and Pathologic Study of a New Case. *Journal of Child Neurology*, *21*(11), 991–1006. https://doi.org/10.1177/08830738060210110101

Ray, K., Chaki, M., & Sengupta, M. (2007). Tyrosinase and ocular diseases: Some novel thoughts on the molecular basis of oculocutaneous albinism type 1. *Progress in Retinal and Eye Research*, *26*(4), 323–358. https://doi.org/10.1016/j.preteyeres.2007.01.001

Redfern, W. S., Storey, S., Tse, K., Hussain, Q., Maung, K. P., Valentin, J.-P., … McKay, J. S. (2011). Evaluation of a convenient method of assessing rodent visual function in safety pharmacology studies: Effects of sodium iodate on visual acuity and retinal morphology in albino and pigmented rats and mice. *Journal of Pharmacological and Toxicological Methods*, *63*(1), 102–114. https://doi.org/10.1016/j.vascn.2010.06.008

Remtulla, S., & Hallett, P. E. (1985). A schematic eye for the mouse, and comparisons with the rat. *Vision Research*, *25*(1), 21–31. https://doi.org/10.1016/0042-6989(85)90076-8

Repka, M X, & Tusa, R. J. (1995). Refractive error and axial length in a primate model of strabismus and congenital nystagmus. *Investigative Ophthalmology & Visual Science*, *36*(13), 2672–2677. Retrieved from http://www.ncbi.nlm.nih.gov/pubmed/7499089

Repka, Michael X. (2002). Ophthalmological problems of the premature infant. *Mental Retardation and Developmental Disabilities Research Reviews*, *8*(4), 249–257. https://doi.org/10.1002/mrdd.10045

Rice, D. S., Williams, R. W., & Goldowitz, D. (1995). Genetic control of retinal projections in inbred strains of albino mice. *The Journal of Comparative Neurology*, *354*(3), 459–469. https://doi.org/10.1002/cne.903540312

Rick, J. M., Horschke, I., & Neuhauss, S. C. F. (2000). Optokinetic behavior is reversed in achiasmatic

mutant zebrafish larvae. *Current Biology*, *10*(10), 595–598. https://doi.org/10.1016/S0960-9822(00)00495-4

Robbins, J. H., Brumback, R. A., Mendiones, M., Barrett, S. F., Carl, J. R., Cho, S., … Tarone, R. E. (1991). Neurological Disease in Xeroderma Pigmentosum: Documentation of a Late Onset Type of the Juvenile Onset Form. *Brain*, *114*(3), 1335–1361. https://doi.org/10.1093/brain/114.3.1335

Rosenzweig, M. R., Bennett, E. L., Hebert, M., & Morimoto, H. (1978). Social grouping cannot account for cerebral effects of enriched environments. *Brain Research*, *153*(3), 563–576. https://doi.org/10.1016/0006-8993(78)90340-2

Roy, V., Belzung, C., Delarue, C., & Chapillon, P. (2001). Environmental enrichment in BALB/c mice: Effects in classical tests of anxiety and exposure to a predatory odor. *Physiology & Behavior*, *74*(3), 313–320. https://doi.org/10.1016/S0031-9384(01)00561-3

Sager, T., Kashon, M. L., & Krajnak, K. (2018). Estrogen and Environmental Enrichment Differentially Affect Neurogenesis, Dendritic Spine Immunolabeling and Synaptogenesis in the Hippocampus of Young and Reproductively Senescent Female Rats. *Neuroendocrinology*, *106*(3), 252–263. https://doi.org/10.1159/000479699

Sale, A., Putignano, E., Cancedda, L., Landi, S., Cirulli, F., Berardi, N., & Maffei, L. (2004). Enriched environment and acceleration of visual system development. *Neuropharmacology*, *47*(5), 649–660. https://doi.org/10.1016/J.NEUROPHARM.2004.07.008

Samardzija, M., Wenzel, A., Thiersch, M., Frigg, R., Reme´, C., & Grimm, C. (2006). Caspase-1 Ablation Protects Photoreceptors in a Model of Autosomal Dominant Retinitis Pigmentosa. *Investigative Opthalmology & Visual Science*, *47*(12), 5181. https://doi.org/10.1167/iovs.06-0556

Samuel, M. A., Zhang, Y., Meister, M., & Sanes, J. R. (2011). Age-Related Alterations in Neurons of the Mouse Retina. *Journal of Neuroscience*, *31*(44), 16033–16044. https://doi.org/10.1523/JNEUROSCI.3580-11.2011

Sanderson, K. J. (1975). Retinogeniculate projections in the rabbits of the albino allelomorphic series. *The Journal of Comparative Neurology*, *159*(1), 15–27. https://doi.org/10.1002/cne.901590103

Sanyal, S., & Hawkins, R. K. (1986). Development and degeneration of retina inrds mutant mice: Effects of light on the rate of degeneration in albino and pigmented homozygous and heterozygous mutant and normal mice. *Vision Research*, *26*(8), 1177–1185. https://doi.org/10.1016/0042-6989(86)90099-4

Sarvananthan, N., Surendran, M., Roberts, E. O., Jain, S., Thomas, S., Shah, N., … Gottlob, I. (2009). The Prevalence of Nystagmus: The Leicestershire Nystagmus Survey. *Investigative Opthalmology & Visual Science*, *50*(11), 5201. https://doi.org/10.1167/iovs.09-3486

Scaioli, V., D'Arrigo, S., & Pantaleoni, C. (2004). *Unusual neurophysiological features in Cockayne's syndrome: a report of two cases as a contribution to diagnosis and classification*. *Brain and Development* (Vol. 26). https://doi.org/10.1016/S0387-7604(03)00130-X

Schefrin, B. E., Tregear, S. J., Harvey, L. O., & Werner, J. S. (1999). Senescent changes in scotopic contrast sensitivity. *Vision Research*, *39*(22), 3728–3736. https://doi.org/10.1016/S0042-6989(99)00072-3

Schmitz, B., Krick, C., & Käsmann-Kellner, B. (2007). Morphologie des Chiasma opticum bei Albinismus. *Der Ophthalmologe*, *104*(8), 662–665. https://doi.org/10.1007/s00347-007-1572-3

Schmucker, C., & Schaeffel, F. (2004). A paraxial schematic eye model for the growing C57BL/6 mouse. *Vision Research*, *44*(16), 1857–1867. https://doi.org/10.1016/j.visres.2004.03.011

Scholz, J., Allemang-Grand, R., Dazai, J., & Lerch, J. P. (2015). Environmental enrichment is associated with rapid volumetric brain changes in adult mice. *NeuroImage*, *109*, 190–198. https://doi.org/10.1016/j.neuroimage.2015.01.027

Schonewille, M., Belmeguenai, A., Koekkoek, S. K., Houtman, S. H., Boele, H. J., van Beugen, B. J., … De Zeeuw, C. I. (2010). Purkinje Cell-Specific Knockout of the Protein Phosphatase PP2B Impairs Potentiation and Cerebellar Motor Learning. *Neuron*, *67*(4), 618–628. https://doi.org/10.1016/j.neuron.2010.07.009

Schonewille, Martijn, Gao, Z., Boele, H.-J., Veloz, M. F. V., Amerika, W. E., Simek, A. A. M., … De Zeeuw, C. I. (2011). Reevaluating the role of LTD in cerebellar motor learning. *Neuron*, *70*(1), 43–50. https://doi.org/10.1016/j.neuron.2011.02.044

Schor, C., & Levi, D. (1980). Disturbances of small-field horizontal and vertical optokinetic nystagmus in amblyopia. *Investigative Ophthalmology & Visual Science*, *19*(6), 668–683. Retrieved from https://iovs.arvojournals.org/article.aspx?articleid=2176119

Schrijver, N. C. ., Bahr, N. I., Weiss, I. C., & Würbel, H. (2002). Dissociable effects of isolation rearing and environmental enrichment on exploration, spatial learning and HPA activity in adult rats. *Pharmacology Biochemistry and Behavior*, *73*(1), 209–224. https://doi.org/10.1016/S0091-3057(02)00790-6

Seidman, M. D., Ahmad, N., & Bai, U. (2002). Molecular mechanisms of age-related hearing loss.

Ageing Research Reviews, *1*(3), 331–343. https://doi.org/10.1016/S1568-1637(02)00004-1

Seidman, M. D., Khan, M. J., Tang, W. X., & Quirk, W. S. (2002). Influence of lecithin on mitochondrial DNA and age-related hearing loss. *Otolaryngology - Head and Neck Surgery*, *127*(3), 138–144. https://doi.org/10.1067/mhn.2002.127627

Seifter, J., & Samuels, M. (2011). Uremic Encephalopathy and Other Brain Disorders Associated with Renal Failure. *Seminars in Neurology*, *31*(02), 139–143. https://doi.org/10.1055/s-0031-1277984

Sekuler, R., Hutman, L., & Owsley, C. (1980). Human aging and spatial vision. *Science*, *209*(4462), 1255–1256. Retrieved from https://science.sciencemag.org/content/209/4462/1255.short

Selfridge, J. (2001). Correction of liver dysfunction in DNA repair-deficient mice with an ERCC1 transgene. *Nucleic Acids Research*, *29*(22), 4541–4550. https://doi.org/10.1093/nar/29.22.4541

Selfridge, J., Song, L., Brownstein, D. G., & Melton, D. W. (2010). Mice with DNA repair gene Ercc1 deficiency in a neural crest lineage are a model for late-onset Hirschsprung disease. *DNA Repair*, *9*(6), 653–660. https://doi.org/10.1016/j.dnarep.2010.02.018

Serfilippi, L. M., Pallman, D. R. S., Gruebbel, M. M., Kern, T. J., & Spainhour, C. B. (2004). Assessment of retinal degeneration in outbred albino mice. *Comparative Medicine*, *54*(1), 69–76. Retrieved from http://www.ncbi.nlm.nih.gov/pubmed/15027621

Shaia, W. T., Shapiro, S. M., & Spencer, R. F. (2005). The Jaundiced Gunn Rat Model of Auditory Neuropathy/Dyssynchrony. *The Laryngoscope*, *115*(12), 2167–2173. https://doi.org/10.1097/01.MLG.0000181501.80291.05

Shapiro, S. M. (2003). Bilirubin toxicity in the developing nervous system. *Pediatric Neurology*, *29*(5), 410–421. https://doi.org/10.1016/j.pediatrneurol.2003.09.011

Shimizu, N., Tabata, H., Wada, Y., Sugita, Y., Yamanaka, T., Hosoi, H., & Kawano, K. (2010). Distribution of optokinetic sensitivity across the retina of mice in relation to eye orientation. *Neuroscience*, *168*(1), 200–208. https://doi.org/10.1016/j.neuroscience.2010.03.025

Shin, S.-L., Zhao, G. Q., & Raymond, J. L. (2014a). Signals and learning rules guiding oculomotor plasticity. *The Journal of Neuroscience : The Official Journal of the Society for Neuroscience*, *34*(32), 10635–10644. https://doi.org/10.1523/JNEUROSCI.4510-12.2014

Shin, S.-L., Zhao, G. Q., & Raymond, J. L. (2014b). Signals and learning rules guiding oculomotor plasticity. *The Journal of Neuroscience : The Official Journal of the Society for Neuroscience*,

34(32), 10635–10644. https://doi.org/10.1523/JNEUROSCI.4510-12.2014

Shoji, M., Okada, M., Ohta, A., Higuchi, K., Hosokawa, M., & Honda, Y. (1998). A Morphological and Morphometrical Study of the Retina in Aging SAM Mice. *Ophthalmic Research*, *30*(3), 172–179. https://doi.org/10.1159/000055471

Shupe, J. M., Kristan, D. M., Austad, S. N., & Stenkamp, D. L. (2006). The Eye of the Laboratory Mouse Remains Anatomically Adapted for Natural Conditions. *Brain, Behavior and Evolution*, *67*(1), 39–52. https://doi.org/10.1159/000088857

Simpson, J., & Kelly, J. P. (2011). The impact of environmental enrichment in laboratory rats—Behavioural and neurochemical aspects. *Behavioural Brain Research*, *222*(1), 246–264. https://doi.org/10.1016/J.BBR.2011.04.002

Sirkin, D. W., Hess, B. J. M., & Precht, W. (1985). Optokinetic nystagmus in albino rats depends on stimulus pattern. *Experimental Brain Research*, *61*(1). https://doi.org/10.1007/BF00235639

Skeel, R. L., Nagra, A., VanVoorst, W., & Olson, E. (2003). The Relationship Between Performance-based Visual Acuity Screening, Self-reported Visual Acuity, and Neuropsychological Performance. *The Clinical Neuropsychologist*, *17*(2), 129–136. https://doi.org/10.1076/clin.17.2.129.16509

Snellen, H. (1868). *Test-types for the determination of the acuteness of vision*. London: Williams and Norgate. Retrieved from https://dspace.library.uu.nl/handle/1874/328593

Spear, P. D. (1993). Neural bases of visual deficits during aging. *Vision Research*, *33*(18), 2589–2609. https://doi.org/10.1016/0042-6989(93)90218-L

St John, R., Fisk, J. D., Timney, B., & Goodale, M. A. (1984). Eye movements of human albinos. *American Journal of Optometry and Physiological Optics*, *61*(6), 377–385. Retrieved from http://www.ncbi.nlm.nih.gov/pubmed/6742098

Stagg, C. J., & Nitsche, M. A. (2011). Physiological Basis of Transcranial Direct Current Stimulation. *The Neuroscientist*, *17*(1), 37–53. https://doi.org/10.1177/1073858410386614

Stahl, J.S, van Alphen, A. ., & De Zeeuw, C. . (2000). A comparison of video and magnetic search coil recordings of mouse eye movements. *Journal of Neuroscience Methods*, *99*(1–2), 101–110. https://doi.org/10.1016/S0165-0270(00)00218-1

Stahl, John S. (2004). Eye Movements of the Murine P/Q Calcium Channel Mutant *Rocker* , and the Impact of Aging. *Journal of Neurophysiology*, *91*(5), 2066–2078.

https://doi.org/10.1152/jn.01068.2003

Stahl, John S., James, R. A., Oommen, B. S., Hoebeek, F. E., & De Zeeuw, C. I. (2006). Eye Movements of the Murine P/Q Calcium Channel Mutant *Tottering* , and the Impact of Aging. *Journal of Neurophysiology*, *95*(3), 1588–1607. https://doi.org/10.1152/jn.00318.2005

Stone, J., Rowe, M. H., & Campion, J. E. (1978). Retinal abnormalities in the Siamese cat. *The Journal of Comparative Neurology*, *180*(4), 773–782. https://doi.org/10.1002/cne.901800408

Takano, Y., Yokawa, T., Masuda, A., Niimi, J., Tanaka, S., & Hironaka, N. (2011). A rat model for measuring the effectiveness of transcranial direct current stimulation using fMRI. *Neuroscience Letters*, *491*(1), 40–43. https://doi.org/10.1016/j.neulet.2011.01.004

Takumida, M., & Anniko, M. (2009). Radical scavengers for elderly patients with age-related hearing loss. *Acta Oto-Laryngologica*, *129*(1), 36–44. https://doi.org/10.1080/00016480802008215

Tarpey, P., Thomas, S., Sarvananthan, N., Mallya, U., Lisgo, S., Talbot, C. J., … Gottlob, I. (2006). Mutations in FRMD7, a newly identified member of the FERM family, cause X-linked idiopathic congenital nystagmus. *Nature Genetics*, *38*(11), 1242–1244. https://doi.org/10.1038/ng1893

Tempia, F., Dieringer, N., & Strata, P. (1991). Adaptation and habituation of the vestibulo-ocular reflex in intact and inferior olive-lesioned rats. *Experimental Brain Research*, *86*(3). https://doi.org/10.1007/BF00230530

Thurtell, M. J., & Leigh, R. J. (2011). Nystagmus and saccadic intrusions. In *Handbook of clinical neurology* (Vol. 102, pp. 333–378). https://doi.org/10.1016/B978-0-444-52903-9.00019-4

Tiliket, C., Shelhamer, M., Tan, H. S., & Zee, D. S. (1993). Adaptation of the vestibulo-ocular reflex with the head in different orientations and positions relative to the axis of body rotation. *Journal of Vestibular Research : Equilibrium & Orientation*, *3*(2), 181–195. Retrieved from http://www.ncbi.nlm.nih.gov/pubmed/8275253

Turano, K., Rubin, G. S., Herdman, S. J., Chee, E., & Fried, L. P. (1994). Visual stabilization of posture in the elderly: fallers vs. nonfallers. *Optometry and Vision Science : Official Publication of the American Academy of Optometry*, *71*(12), 761–769. Retrieved from http://www.ncbi.nlm.nih.gov/pubmed/7898883

Turner, C. A., & Lewis, M. H. (2003). Environmental enrichment: effects on stereotyped behavior and neurotrophin levels. *Physiology & Behavior*, *80*(2–3), 259–266. https://doi.org/10.1016/J.PHYSBEH.2003.07.008

Tusa, R. J., Mustari, M. J., Das, V. E., & Boothe, R. G. (2002). Animal Models for Visual Deprivation-Induced Strabismus and Nystagmus. *Annals of the New York Academy of Sciences*, *956*(1), 346–360. https://doi.org/10.1111/j.1749-6632.2002.tb02833.x

Uchida, Y., Ando, F., Shimokata, H., Sugiura, S., Ueda, H., & Nakashima, T. (2008). The Effects of Aging on Distortion-Product Otoacoustic Emissions in Adults with Normal Hearing. *Ear and Hearing*, *29*(2), 176–184. https://doi.org/10.1097/AUD.0b013e3181634eb8

Underwood, E. (2016). Cadaver study challenges brain stimulation methods. *Science* , *352*(6284), 397. https://doi.org/10.1126/science.352.6284.397

van Alphen, B., Winkelman, B. H. J., & Frens, M. A. (2009a). Age- and Sex-Related Differences in Contrast Sensitivity in C57Bl/6 Mice. *Investigative Opthalmology & Visual Science*, *50*(5), 2451. https://doi.org/10.1167/iovs.08-2594

van Alphen, B., Winkelman, B. H. J., & Frens, M. A. (2009b). Age- and Sex-Related Differences in Contrast Sensitivity in C57Bl/6 Mice. *Investigative Opthalmology & Visual Science*, *50*(5), 2451. https://doi.org/10.1167/iovs.08-2594

van Alphen, B., Winkelman, B. H. J., & Frens, M. A. (2010). Three-Dimensional Optokinetic Eye Movements in the C57BL/6J Mouse. *Investigative Opthalmology & Visual Science*, *51*(1), 623. https://doi.org/10.1167/iovs.09-4072

van de Weerd, H. A., Baumans, V., Koolhaas, J. M., & van Zutphen, L. F. (1994). Strain specific behavioural response to environmental enrichment in the mouse. *Journal of Experimental Animal Science*, *36*(4–5), 117–127. Retrieved from http://www.ncbi.nlm.nih.gov/pubmed/7948063

van der Geest, J. N., & Frens, M. A. (2002a). Recording eye movements with video-oculography and scleral search coils: a direct comparison of two methods. *Journal of Neuroscience Methods*, *114*(2), 185–195. https://doi.org/10.1016/S0165-0270(01)00527-1

van der Geest, J. N., & Frens, M. A. (2002b). Recording eye movements with video-oculography and scleral search coils: a direct comparison of two methods. *Journal of Neuroscience Methods*, *114*(2), 185–195. https://doi.org/10.1016/S0165-0270(01)00527-1

van der Horst, G. T. ., van Steeg, H., Berg, R. J. ., van Gool, A. J., de Wit, J., Weeda, G., … Hoeijmakers, J. H. . (1997). Defective Transcription-Coupled Repair in Cockayne Syndrome B Mice Is Associated with Skin Cancer Predisposition. *Cell*, *89*(3), 425–435. https://doi.org/10.1016/S0092-8674(00)80223-8

van der Pluijm, I., Garinis, G. A., Brandt, R. M. C., Gorgels, T. G. M. F., Wijnhoven, S. W., Diderich, K. E. M., … van der Horst, G. T. J. (2006). Impaired Genome Maintenance Suppresses the Growth Hormone–Insulin-Like Growth Factor 1 Axis in Mice with Cockayne Syndrome. *PLoS Biology*, *5*(1), e2. https://doi.org/10.1371/journal.pbio.0050002

van Looij, M. A. ., Liem, S.-S., van der Burg, H., van der Wees, J., De Zeeuw, C. I., & van Zanten, B. G. . (2004). Impact of conventional anesthesia on auditory brainstem responses in mice. *Hearing Research*, *193*(1), 75–82. https://doi.org/10.1016/j.heares.2004.02.009

Voges, K., Wu, B., Post, L., Schonewille, M., & De Zeeuw, C. I. (2017). Mechanisms underlying vestibulo-cerebellar motor learning in mice depend on movement direction. *The Journal of Physiology*, *595*(15), 5301–5326. https://doi.org/10.1113/JP274346

von dem Hagen, E. A. H., Hoffmann, M. B., & Morland, A. B. (2008). Identifying Human Albinism: A Comparison of VEP and fMRI. *Investigative Opthalmology & Visual Science*, *49*(1), 238. https://doi.org/10.1167/iovs.07-0458

von dem Hagen, E. A. H., Houston, G. C., Hoffmann, M. B., & Morland, A. B. (2007). Pigmentation predicts the shift in the line of decussation in humans with albinism. *European Journal of Neuroscience*, *25*(2), 503–511. https://doi.org/10.1111/j.1460-9568.2007.05303.x

Voogd, J., & Barmack, N. H. (2006). Oculomotor cerebellum. *Progress in Brain Research*, *151*, 231–268. https://doi.org/10.1016/S0079-6123(05)51008-2

Vorhees, C. V, & Williams, M. T. (2006). Morris water maze: procedures for assessing spatial and related forms of learning and memory. *Nature Protocols*, *1*(2), 848–858. https://doi.org/10.1038/nprot.2006.116

Waespe, W., Cohen, B., & Raphan, T. (1985). Dynamic modification of the vestibulo-ocular reflex by the nodulus and uvula. *Science*, *228*(4696), 199–202. https://doi.org/10.1126/science.3871968

Walton, J. P. (2010). Timing is everything: Temporal processing deficits in the aged auditory brainstem. *Hearing Research*, *264*(1), 63–69. https://doi.org/10.1016/j.heares.2010.03.002

Wang, Y. (2001). Effects of Aging on Shape Discrimination. *Optometry and Vision Science*, *78*(6), 447–454. https://doi.org/10.1097/00006324-200106000-00019

Warrian, K. J., Altangerel, U., & Spaeth, G. L. (2010). Performance-based Measures of Visual Function. *Survey of Ophthalmology*, *55*(2), 146–161. https://doi.org/10.1016/J.SURVOPHTHAL.2009.06.006

Watkins, R. J., Thomas, M. G., Talbot, C. J., Gottlob, I., & Shackleton, S. (2012). The Role of FRMD7 in Idiopathic Infantile Nystagmus. *Journal of Ophthalmology*, *2012*, 1–7. https://doi.org/10.1155/2012/460956

Watson, A. B., & Robson, J. G. (1981). Discrimination at threshold: Labelled detectors in human vision. *Vision Research*, *21*(7), 1115–1122. https://doi.org/10.1016/0042-6989(81)90014-6

Weeda, G., Donker, I., de Wit, J., Morreau, H., Janssens, R., Vissers, C. J., … Hoeijmakers, J. H. J. (1997). Disruption of mouse ERCC1 results in a novel repair syndrome with growth failure, nuclear abnormalities and senescence. *Current Biology*. https://doi.org/10.1016/S0960-9822(06)00190-4

Weiss, A. H., & Biersdorf, W. R. (1989). Visual Sensory Disorders in Congenital Nystagmus. *Ophthalmology*, *96*(4), 517–523. https://doi.org/10.1016/S0161-6420(89)32864-8

Wen, S. W., Smith, G., Yang, Q., & Walker, M. (2004). Epidemiology of preterm birth and neonatal outcome. *Seminars in Fetal and Neonatal Medicine*, *9*(6), 429–435. https://doi.org/10.1016/J.SINY.2004.04.002

Wester, S. T., Rizzo, J. F., Balkwill, M. D., & Wall, C. (2007). Optokinetic Nystagmus as a Measure of Visual Function in Severely Visually Impaired Patients. *Investigative Ophthalmology & Visual Science*, *48*(10), 4542–4548. https://doi.org/10.1167/iovs.06-1206

Wikler, K. C., & Rakic, P. (1990). Distribution of photoreceptor subtypes in the retina of diurnal and nocturnal primates. *The Journal of Neuroscience : The Official Journal of the Society for Neuroscience*, *10*(10), 3390–3401. https://doi.org/10.1523/JNEUROSCI.10-10-03390.1990

Williams, D. R. (1985). Aliasing in human foveal vision. *Vision Research*, *25*(2), 195–205. https://doi.org/10.1016/0042-6989(85)90113-0

Willott, J. F., Hnath Chisolm, T., & Lister, J. J. (2001). Modulation of Presbycusis: Current Status and Future Directions. *Audiology and Neurotology*, *6*(5), 231–249. https://doi.org/10.1159/000046129

Winkelman, B., & Frens, M. (2006). Motor Coding in Floccular Climbing Fibers. *Journal of Neurophysiology*, *95*(4), 2342–2351. https://doi.org/10.1152/jn.01191.2005

Wolfer, D. P., Litvin, O., Morf, S., Nitsch, R. M., Lipp, H.-P., & Würbel, H. (2004). Cage enrichment and mouse behaviour. *Nature*, *432*(7019), 821–822. https://doi.org/10.1038/432821a

Wong, A. A., & Brown, R. E. (2006). Visual detection, pattern discrimination and visual acuity in 14

strains of mice. *Genes, Brain and Behavior*, *5*(5), 389–403. https://doi.org/10.1111/j.1601-183X.2005.00173.x

Wright, C. E., & Drasdo, N. (1985). The influence of age on the spatial and temporal contrast sensitivity function. *Documenta Ophthalmologica*, *59*(4), 385–395. https://doi.org/10.1007/BF00159172

Würbel, H. (2000). Behaviour and the standardization fallacy. *Nature Genetics*, *26*(3), 263–263. https://doi.org/10.1038/81541

Würbel, H. (2001). Ideal homes? Housing effects on rodent brain and behaviour. *Trends in Neurosciences*, *24*(4), 207–211. https://doi.org/10.1016/S0166-2236(00)01718-5

Xu-Wilson, M., Chen-Harris, H., Zee, D. S., & Shadmehr, R. (2009). Cerebellar Contributions to Adaptive Control of Saccades in Humans. *Journal of Neuroscience*, *29*(41), 12930–12939. https://doi.org/10.1523/JNEUROSCI.3115-09.2009

Ying-Yu Huang, M., Chen, C.-C., Huber-Reggi, S. P., Neuhauss, S. C. F., & Straumann, D. (2011). Comparison of infantile nystagmus syndrome in achiasmatic zebrafish and humans. *Annals of the New York Academy of Sciences*, *1233*(1), 285–291. https://doi.org/10.1111/j.1749-6632.2011.06150.x

Yokoyama, T., Silversides, D. W., Waymire, K. G., Kwon, B. S., Takeuchi, T., & Overbeek, P. A. (1990). Conserved cysteine to serine mutation in tyrosinase is responsible for the classical albino mutation in laboratory mice. *Nucleic Acids Research*, *18*(24), 7293–7298. https://doi.org/10.1093/nar/18.24.7293

Zhu, S.-W., Yee, B. K., Nyffeler, M., Winblad, B., Feldon, J., & Mohammed, A. H. (2006). Influence of differential housing on emotional behaviour and neurotrophin levels in mice. *Behavioural Brain Research*, *169*(1), 10–20. https://doi.org/10.1016/J.BBR.2005.11.024

Zuchowski, M. L., Timmann, D., & Gerwig, M. (2014). Acquisition of Conditioned Eyeblink Responses is Modulated by Cerebellar tDCS. *Brain Stimulation*, *7*(4), 525–531. https://doi.org/10.1016/j.brs.2014.03.010

Summary

This thesis deals with measuring compensatory eye movements to assess sensory and learning properties of humans and mice. In **Chapter 1**, a number of the key elements of vision and learning, which underlie the thesis are introduced, and an outline of the rest of the thesis is given.

In **Chapter 2**, we investigated how human gaze following eye movements (i.e. compensatory and smooth pursuit eye movements) are affected by stimulus contrast and spatial frequency and by aberrations in central visual acuity due to refractive errors. We measured 30 healthy subjects with a range of visual acuities but without any refractive correction. Visual acuity was tested using a Landolt-C chart. Subjects were divided into three groups with low, intermediate, or good visual acuity. Gaze following responses (GFR) to moving Gabor patches were recorded by video-oculography. In each trial, the subjects were presented with a single Gabor patch with a specific spatial frequency and luminance contrast that moved sinusoidally in the horizontal plane.

We observed that GFR gain decreased with increasing spatial frequency and decreasing contrast and was correlated with visual acuity. GFR gain was lower and decreased more for subjects with lower visual acuity; this was especially so for lower stimulus contrasts that are not tested in standard acuity tests. The largest differences between the groups were observed at spatial frequencies around 4 cpd and at contrasts up to 10%. Aberrations in central visual acuity due to refractive errors affect the GFR response depending on the contrast and spatial frequency of the moving stimulus. Measuring this effect may contribute to a better estimate of changes in visual function as a result of aging, disease, or treatments meant to improve vision.

In **Chapter 3**, we investigated hearing and vision in Ercc1δ/− mutant mice, which are deficient in DNA repair of helix-distorting DNA lesions and interstrand DNA crosslinks, in order to investigate whether DNA damage can contribute to age-related hearing and vision loss. Age-related loss of hearing and vision are two very common disabling conditions, but the underlying mechanisms are still poorly understood. Damage by reactive oxygen species and other reactive cellular metabolites, which in turn may damage macromolecules such as DNA, has been implicated in both processes. Ercc1δ/− mice showed a progressive, accelerated increase of hearing level thresholds over time, most likely arising from deteriorating cochlear function. Ercc1δ/− mutants also displayed a progressive decrease in contrast sensitivity followed by thinning of the outer nuclear layer of the eyeball. The strong parallels with normal ageing suggest that unrepaired DNA damage can induce age-related decline of the auditory and visual system.

In **Chapter 4**, we screened wild-type mice of varying pigmentation for ocular motor abnormalities in order to identify a possible mouse model for Infantile Nystagmus Syndrome (INS). Individuals with oculocutaneous albinism are predisposed to visual system abnormalities affecting the retina and retinofugal projections, which may lead to reduced visual acuity and INS. Due to absence of an established mammalian animal model, mechanisms underlying INS remain elusive.

Three albino mouse strains (CD1, BALB/c, DBA/1), and two normally pigmented strains (129S6, C57BL/6) were screened using infrared oculography. Varying visual stimuli (black or white background, stationary pattern, optokinetic, i.e., horizontally rotating pattern) were displayed to the full (fVF) or anterior visual field (aVF) of the restrained mouse. We found spontaneous nystagmus, specifically jerks and oscillations, in albino mice under all experimental conditions. Median eye velocity was between 0.8 and 3.4 ˚/s, depending on the strain. In contrast, the eyes in pigmented mice were nearly stable with a median absolute eye velocity of below 0.4 ˚/s. In albino mice, fVF optokinetic stimuli elicited an optokinetic response (OKR) in the correct direction, albeit with superimposed oscillations. However, aVF optokinetic stimuli evoked reversed OKR in these strains, a well-known feature of INS. Based on our results, we endorse the investigated albino mouse strains as new animal models for INS.

In **Chapter 5**, we studied anodal direct current stimulation (DCS) of the cerebellum. DCS facilitates adaptation tasks, but the mechanism underlying this effect is poorly understood. We have evaluated whether the effects of DCS effects depend on plasticity of cerebellar Purkinje cells (PCs). We have successfully developed a mouse model of cerebellar DCS, allowing us to present the first demonstration of cerebellar DCS driven behavioural changes in rodents. We have utilized a simple gain down vestibulo-ocular reflex (VOR) adaptation paradigm that stabilizes a visual image on the retina during brief head movements, as behavioural tool. Our results provide evidence that anodal stimulation has an acute post-stimulation effect on baseline gain reduction of VOR (VOR gain in sham, anodal and cathodal groups are 0.75 ± 0.12, 0.68 ± 0.1, and 0.78 ± 0.05, respectively). Moreover, this anodal induced decrease in VOR gain is directly dependent on the PP2B medicated synaptic long-term potentiation (LTP) and intrinsic plasticity pathways of PCs.

In **Chapter 6**, the behavioural effects of environmental enrichment on contrast sensitivity, reflexive eye movements and on oculomotor learning were measured in mice that were housed in an enriched environment for a period of 3 weeks. Research has shown that a larger cage and a more complex environment have positive effects on the welfare of laboratory mice and other animals held in captivity. This is called environmental enrichment (EE). It has also been shown that environmental enrichment affects various behaviour and neuro-anatomical and molecular characteristics.

We found a clear effect on oculomotor learning, where animals that were housed in an enriched environment learned significantly faster than controls that were housed under standard conditions. In line with existing literature, the enriched group also outperformed the controls in behavioural tests for explorative behaviour. Meanwhile, both visual and reflexive oculomotor performance in response to visual and vestibular stimuli was unaffected. This points towards an underlying mechanism that is specific for motor learning, rather than overall motor performance.

Samenvatting

Dit proefschrift gaat over het meten van compensatoire oogbewegingen om de sensorische en leer eigenschappen van mens en muis te beoordelen. In Hoofdstuk 1 wordt een aantal van de sleutelelementen van zien en van leren, die ten grondslag liggen aan het proefschrift geïntroduceerd en wordt een overzicht van de rest van het proefschrift gegeven.

In **Hoofdstuk 2** hebben we onderzocht hoe menselijke compensatoire oogbewegingen worden beïnvloed door stimuluscontrast en spatiële frequentie en door aberraties in centrale gezichtsscherpte als gevolg van refractiefouten. We hebben 30 gezonde proefpersonen gemeten met een heel bereik aan gezichtsscherptes, zonder dat ze een bril op hadden. De gezichtsscherpte werd getest met behulp van een Landolt-C-kaart. De proefpersonen werden verdeeld in drie groepen met een lage, gemiddelde of goede gezichtsscherpte. We maten oogbewegingen (Gaze Following Responses [GFR]), die opgewekt werden door bewegende Gabor-patches door middel van video-oculografie. In elke proef kregen de proefpersonen een enkele Gabor-patch met een specifieke spatiële frequentie en luminantiecontrast aangeboden, die sinusvormig in het horizontale vlak bewoog.

De GFR-respons nam af met toenemende spatiële frequentie en met afnemend contrast. Dit was gecorreleerd met de gezichtsscherpte. De GFR-respons was kleiner en nam meer af voor personen met een lagere gezichtsscherpte. Dit was vooral het geval voor lagere stimuluscontrasten, die niet worden getest in standaard visustesten. De grootste verschillen tussen de groepen werden waargenomen bij spatiële frequenties rond 4 cpd en bij contrasten tot 10%. Afwijkingen in de centrale gezichtsscherpte als gevolg van refractiefouten beïnvloeden de GFR-respons, afhankelijk van het contrast en de ruimtelijke frequentie van de bewegende stimulus. Het meten van dit effect kan bijdragen aan een betere schatting van veranderingen in de visuele functie als gevolg van veroudering, ziekte of behandelingen die bedoeld zijn om het gezichtsvermogen te verbeteren.

In **Hoofdstuk 3** hebben we het gehoor en het gezichtsvermogen onderzocht in Ercc1δ / - mutant muizen, die deficiënt zijn in DNA-herstel van *helix-distorting* DNA-laesies en interstrand DNA *crosslinks*, om te onderzoeken of DNA-beschadiging kan bijdragen aan leeftijdsgebonden gehoor- en gezichtsverlies. Leeftijd gerelateerd verlies van gehoor en gezichtsvermogen zijn twee zeer algemene invaliderende omstandigheden, maar de onderliggende mechanismen worden nog steeds slecht begrepen. Schade door reactieve zuurstofsoorten en andere reactieve cellulaire metabolieten, die op hun beurt macromoleculen zoals DNA kunnen beschadigen, is bij beide processen betrokken. Ercc1δ / - muizen toonden een progressieve, versnelde toename van de drempels van het

gehoorniveau in de loop van de tijd, hoogstwaarschijnlijk als gevolg van de verslechterde cochleaire functie. Erccol / - mutanten vertoonden ook een progressieve afname in contrastgevoeligheid, als gevolg van het dunner worden van de buitenste nucleaire laag van de oogbol. De sterke parallellen met normale veroudering suggereren dat niet-gerepareerde DNA-schade leeftijd gerelateerde achteruitgang van het auditieve en visuele systeem kan veroorzaken.

In **Hoofdstuk 4** screenden we wildtype muizen met diverse pigmentatie op oculomotor afwijkingen om zo een mogelijk muismodel voor Infantile Nystagmus Syndrome (INS) te identificeren. Personen met oculocutaan albinisme hebben aanleg voor afwijkingen in het visuele systeem die de retina- en retinofugale projecties beïnvloeden, wat kan leiden tot verminderde gezichtsscherpte en INS. Door het ontbreken van een zoogdiermodel blijven mechanismen die ten grondslag liggen aan INS ongrijpbaar.
Drie albinomuisstammen (CD1, BALB / c, DBA / 1) en twee normaal gepigmenteerde stammen (129S6, C57BL / 6) werden gescreend met behulp van infrarood-oculografie. Verschillende visuele stimuli (zwarte of witte achtergrond, stationair patroon, optokinetisch, d.w.z. horizontaal roterend patroon) werden getoond aan het volledige (fVF) of anterior visuele veld (aVF) van de muis.
We vonden spontane nystagmus, specifiek *jerks* en oscillaties, in albinomuizen onder alle experimentele omstandigheden. De mediane oogsnelheid lag tussen 0,8 en 3,4 ˚/s, afhankelijk van de stam. Daarentegen waren de ogen bij gepigmenteerde muizen vrijwel stabiel met een mediane absolute oogsnelheid van minder dan 0,4 ˚/s. Bij albino-muizen wekten visuele stimuli van fVF een optokinetische respons (OKR) op in de juiste richting, zij het met gesuperponeerde oscillaties. AVF-optokinetische stimuli wekten echter omgekeerde OKR op bij deze stammen, een bekend kenmerk van INS. Op basis van onze resultaten bevestigen we de onderzochte albinomuisstammen als geschikte diermodellen voor INS.

In **Hoofdstuk 5** onderzochten we de effecten van anodale gelijkstroomstimulatie (*Direct Current Stimulation*, DCS) van het cerebellum. DCS versnelt motorisch leren, maar het onderliggende mechanisme van dit effect is slecht begrepen. Wij hebben onderzocht of de effecten van DCS-effecten afhankelijk zijn van de plasticiteit van Purkinje-cellen in de kleine hersenen (pc's). We hebben met succes een muismodel ontwikkeld voor cerebellaire DCS, waarmee we voor het eerst cerebellaire DCS-gestuurde gedragsveranderingen bij knaagdieren kunnen aantonen. We hebben gebruik gemaakt van een eenvoudig VOR-leerparadigma. De vestibulo-oculaire reflex (VOR) stabiliseert een visueel beeld op het netvlies tijdens hoofdbewegingen. Onze resultaten laten zien dat anodale stimulatie een acuut post-stimulatie-effect heeft op de sterkte van de VOR (0,75 ± 0,12, 0,68 ± 0,1 en 0,78 ± 0,05 voor, respectievelijk, de placebo, anodale en kathodale). Bovendien laten

we zien dat deze door anodale geïnduceerde afname in VOR sterkte direct afhankelijk van de PP2B-medicinale synaptische langetermijnpotentiatie (LTP) en intrinsieke plasticiteitspaden van pc's.

In **Hoofdstuk 6** hebben we de gedragseffecten van omgevingsverrijking op contrastgevoeligheid, reflexieve oogbewegingen en oculomotorisch leren gemeten bij muizen die gedurende 3 weken in een verrijkte omgeving werden gehuisvest. Onderzoek heeft laten zien dat een grotere kooi en een meer complexe omgeving positieve effecten hebben op het welzijn van laboratoriummuizen en andere (proef)dieren. Dit wordt omgevingsverrijking (Environmental Enrichment; EE) genoemd. Er is ook eerder aangetoond dat omgevingsverrijking verschillende vormen van gedrag, neuro-anatomische en moleculaire kenmerken beïnvloedt.
We vonden een duidelijk effect op oculomotorisch leren, waarbij dieren die zich in een verrijkte omgeving bevonden significant sneller leerden dan controles die onder standaardomstandigheden werden gehuisvest. In overeenstemming met de bestaande literatuur presteerde de verrijkte groep ook beter dan de controles bij gedragstests voor exploratief gedrag. Ondertussen werden zowel visuele als compensatoire oculomotorische prestaties als reactie op visuele en vestibulaire stimuli niet beïnvloed. Dit wijst op een onderliggend mechanisme dat specifiek is voor motorisch leren, in plaats van algemene motorprestaties.

Curriculum Vitae

Professional experience

2014 -	Process Manager at ScriptieMaster, Rotterdam, the Netherlands
2013 - 2014	Freelance thesis supervisor at ScriptieMaster, Rotterdam, the Netherlands
2008 - 2013	PhD neuroscience Erasmus MC, Rotterdam, the Netherlands

Education

2016 - 2020	Bachelor Behavioral therapy for horses, Tinley Academy, the Netherlands
2007 - 2009	Master Biological and Cognitive Psychology, Erasmus University Rotterdam, the Netherlands
2003 - 2006	Bachelor Psychology, Erasmus University Rotterdam, the Netherlands
2002 - 2003	Bachelor Maatschappelijk werk en dienstverlening (Social work and services), Ichthus Hogeschool Rotterdam, the Netherlands

Courses and additional education

2015 - 2016	Behavioral Biology, Open University, the Netherlands
2013	Module 2 animal training expert; General Ethology, Tinley Academy, the Netherlands
2012	Animal Behavior Field course, South west research station, Arizona, USA
2011 - 2012	Module 1 animal training expert: Stress and Welfare, Tinley Academy, the Netherlands
2011	Training as educator, Blijdorp the Rotterdam Zoo, the Netherlands
2010	Module Vision in Men and Mice, Masters Neuroscience, Erasmus MC Rotterdam, the Netherlands
2009	Module Linear Systems, Masters Neuroscience, Erasmus MC Rotterdam, the Netherlands
2009	Module Sensory Systems for promovendi, Utrecht University, the Netherlands
2009	Course on Laboratory Animal Science (Article 9 qualified), Erasmus MC Rotterdam, the Netherlands
2009	Exam Biology – animal anatomy, Faculty veterinary medicine, Utrecht University, the Netherlands

Other activities

2017-	Behavioral therapy for horses
2014 - 2016	Volunteer at Stichting SPOTS, a foundation to protect endangered wild felines
2013 - 2017	Research assistant cognitive research (object permanence) in dolphins Dolfinarium Harderwijk, the Netherlands in collaboration with Rebecca Singer, assistant professor of Psychology, Georgetown College, USA and Sabrina Brando of Animal Concept, the Netherlands.
2011 - 2013	Volunteer education at Blijdorp the Rotterdam Zoo, the Netherlands
2011 - 2014	Member editorial board Erasmus Magazine, Erasmus University, Rotterdam, The Netherlands

Dankwoord

Dit proefschrift heeft op zich laten wachten maar is er nu toch gekomen en dat betekent dat ik iedereen die mij geholpen en gesteund heeft eindelijk enorm kan bedanken. Een aantal van deze mensen wil ik hier in het bijzonder noemen. Prof. dr. M.A. Frens, Maarten, toen ik als student naar je toe kwam om te informeren voor een stage, kreeg ik enthousiast een rondleiding. Jouw enthousiasme was aanstekelijk en ik wist het meteen, het werd het muizenonderzoek. Door het vertrouwen en die ruimte en die jij gaf heb ik van a tot z zelfstandig onderzoek leren doen. Het onderzoek, vooral de aanvragen, het labmanagement en het onderzoek gingen voortvarend maar het afronden van dit proefschrift was een langdurig proces dat gepaard ging met ups en downs, zowel professioneel als persoonlijk. Je gaf me de ruimte toen ik die nodig had en je was er toen ik de motivatie weer teruggevonden had of je slingerde mij weer aan. Hoewel ik mij schuldig voelde heb je mij mij nooit schuldig laten voelen. Dit heb ik enorm gewaardeerd. Ook de leuke gesprekken en de roadtrip zullen mij altijd bijblijven. Naast een enthousiaste wetenschapper en fijne vent ben je een enorm bevlogen docent en staat goed onderwijs hoog bij jou in het vaandel. Hier ben ik mee besmet geraakt en ben de passie voor het onderwijzen en begeleiden van studenten gaan delen. Maarten, bedankt voor alles.

De leden van de kleine promotiecommissie, prof. dr. J.G. Borst, prof. dr. L.H.M. Sterck en A. Maassen van de Brink dank ik voor het beoordelen van mijn proefschrift en het plaatsnemen in de commissie. De overige leden van de promotiecommissie, prof. dr. Y. Elgersma, dr. J.N. van der Geest, dr. A. Badura, en dr. C. Muller wil ik bedanken voor het plaatsnemen in de commissie.

Van deze commissie wil ik graag in het speciaal dr. J.N. van der Geest bedanken. Lieve Jos, ik waardeer het zeer dat ik met jou van gedachten heb mogen wisselen over mijn proefschrift, het leven en het gedrag, de cognitie en emotie van dieren. Dit alles het liefst onder genot van een bakje koffie of een biertje. Zijn we er al uit, zijn wij slim genoeg om te begrijpen hoe slim dieren zijn? Op mijn bureau stonden dierminiaturen en bij jou op kantoor hersenmodellen van dieren. Daar was ik altijd wel jaloers op en het was dan ook erg leuk dat ik ze mocht lenen voor het vrijwilligerswerk educatie in Blijdorp en sindsdien bekend stond als het hersenmeisje en dat ik dankzij jou heb mogen dineren met Frans van der Waal. Ook bedankt voor de gezelligheid tijdens de seminars. Door jou zijn de buitenlandse seminars altijd ook een cultureel en ontspannen uitje geweest. Je bent altijd mijn steun en toeverlaat geweest op de Erasmus MC en mede dankzij jou hield ik de moed erin.

Beste Bart, met mijn keuze voor het muizenonderzoek kwam ik onder jouw hoede terecht. Met leuke gesprekken konden we de tijd prima doorkomen tijdens het staren naar een muis zijn oog. Dank voor je begeleiding, je aanstekelijk enthousiasme, jouw onderzoekende persoonlijkheid en de introductie van Surinaamse broodjes.

Stefan, jij gaat letterlijk fluitend door het leven. Ik vond jouw fluitje altijd bemoedigend en positief klinken en dat konden we zeker in het In het begin van onze samenwerking waarin wij vele uren samen hutjemutje in het lab gewerkt hebben, goed gebruiken. We hebben elkaar goed leren kennen en ik ben je dankbaar voor alle technische uitleg en je onuitputtelijke vertrouwen in mij en positieve woorden. Ontzettend leuk dat je leraar bent geworden. Je leerlingen boffen maar met jou.

Lieve Jeanine, wat een aanwinst was jij. We hebben hard gewerkt maar ook heel veel gelachen. Met jouw vaardigheden, humor en liefde voor sushi heb jij mijn tijd op het Erasmus MC verrijkt.

Alle Junior Med school studenten die ik heb mogen begeleiden, bedankt voor jullie enthousiasme, altijd kritische vragen en enorme inzet.

Het leven als onderzoeker op de afdeling is mij een stukje makkelijker gemaakt door mensen als Rogério de Avila Friere, Hans van der Burgh, Elise Haasdijk en Loes Nijs. Bedankt voor jullie hulp! Ook wil ik hierbij Hans van der Steen en Martijn Schonewille bedanken voor hun hulp als ik vragen had over het visuele en/of vestibulaire systeem en de praktische aspecten va het onderzoeken hiervan.

Met plezier heb ik veel onderwijs gegeven aan de geneeskunde studenten. Vaak mocht ik samen met Marcel van Riel het practicum leiden. Marcel je bent een groot voorbeeld geweest voor mij en een hele fijne collega. Je nam het onderwijs heel serieus en was bereid het uitvoerig uit te leggen mits de studenten het ook wilden leren. Ik heb altijd enorm jouw mentaliteit van streng maar rechtvaardig gewaardeerd.

Niet te vergeten zijn de mensen achter de schermen die het onderzoek mogelijk maken. Bij deze wil ik dan ook eenieder die zich met de verzorging van de muizen bedanken voor hun zorg voor de dieren.

Alle coauteurs wil ik bedanken voor hun intellectuele bijdrage. In de samenwerking betreffende het muismodel voor veroudering wil ik in het speciaal Nils Zuiderveen Borgesius en Ingrid van der Pluijm bedanken voor alle kennis en het van gedachte wisselen over het muismodel en de onderzoeken. Jan Hoeimakers en Yanto Ridwan wil ik bedanken voor het muismodel en de muizen.

In de samenwerking voor het onderzoek naar directe stimulatie van het muizencerebellum wil ik Opher Donchin, Suman Das en Shlomi Haar bedanken. In deze samenwerking wil ik Duco speciaal bedanken voor ons verblijf bij hem thuis en de dagen van samenwerking op de Vanderbilt University.

I would like to thank Melody (Ying-Yu Huang), Dominik Straumann and Christian Grimm for collaboration at the nystagmus project. Special thanks to Ghislaine Traber for working together in Rotterdam and for your follow up in your own lab.

Lieve vrienden, dank voor jullie interesse en fijn ook dat jullie op bepaalde momenten ook maar juist niet naar vroegen.

Beste Dave, je bent de meest awesome collega die ik mij wensen kan. Naast werk bespreken is er ook altijd ruimte voor persoonlijke onderwerpen en zodoende kon ik je nog wel eens lastigvallen met meestal mijn stress en frustratie rondom mijn promotie. Jouw enthousiasme en positieve instelling hebben mij geholpen de moed erin te houden. Klasse!
Jou en ook mijn andere harde kern collega's Sepaand, Richard en Jaap ben ik dankbaar voor de goede sfeer op werk en de humor die we delen waardoor werken op kantoor ook leuk is en het een goede tegenhanger was van hoe ik thuis voor mijn promotie achter de laptop of boven de papers zat.

Lieve paarden, Bento en Rossini, en kat Diesel bedankt dat jullie mij zoveel afleiding gegeven hebben. Jullie zijn mijn therapie geweest.

Lieve Hans, de liefste man die ik mij wensen kan, dank je wel voor jouw steun en vertrouwen in mij. Door jouw bemoedigende woorden en knuffels als ik het even niet meer zag zitten kreeg ik het vertrouwen en de energie weer terug om verder te gaan.

Lieve papa, je hebt mij altijd de ruimte gegeven om mijn eigen weg te gaan en ik weet dat je altijd achter mij staat. Juist deze vrijheid en onvoorwaardelijke steun hebben mij de mogelijkheid geboden mijn eigen weg in te slaan en uiteindelijk stap voor stap uiteindelijk toch mijn proefschrift af te ronden.